Effective Scheduling Algorithms for Cross-Interference Mitigation in Heterogeneous Wireless Networks

Xiao Wang

School of Computer Science and Electronic Engineering

University of Essex

This thesis is submitted for the degree of

Doctor of Philosophy

July 2021

Abstract

Wireless networks are making life easier, smarter and more convenient. However, the well-known Carrier-sense multiple access with collision avoidance (CSMA/CA) mechanism is powerless when dealing with Cross-Technology Interference (CTI) between Wi-Fi and Low-Rate Wireless Personal Area Network (LR-WPAN), because of asymmetric transmission power, incompatible Clear Channel Assessment (CCA) and different timing parameters. Plenty of studies have shown that WiFi always has a higher priority to access the wireless medium and even block LR-WPAN transmission in the worst case. Our experiments confirm this point and conclude that Wi-Fi can interrupt LR-WPAN severely even block LR-WPAN traffic, while the interference from LR-WPAN to Wi-Fi is negligible. Different from other studies, this thesis presents a novel centralized scheduling mechanism in the time domain to harmonize coexistence of Wi-Fi and LR-WPAN, also refer to as time-slot based scheduling mechanism. The mechanism is achieved by introducing a new command frame, named Access Notification (AN), into the IEEE802.15.4 Medium Access Control (MAC) layer. Based on this mechanism, a static time-slot based scheduling algorithm is designed and evaluated on both real hardware-based system and NS-3 simulator. The result shows the algorithm improves LR-WPAN Packet Loss Rate (PLR) significantly but at the cost of reducing Wi-Fi throughput. In order to maximize performance, based on slot-based congestion indicator (CI) that is proposed and defined to tell whether an allocated time slot is adequate for data transmission or not, we further design an adaptive time-slot based scheduling algorithm. The

evaluation shows that the adaptive algorithm covers the shortage of the static algorithm and offers a distinct improvement on LR-WPAN Packet Transmission Rate (PTR).

Key words: WiFi, IEEE802.15.4, cross-technology interference, coordination mechanism, time-slot, heterogeneous wireless network, wireless sensor network, scheduling algorithm

Table of contents

List of figures

List of tables

Symbols and Abbreviations

Greek Symbols

α The coefficient of EMA, a constant smoothing factor between 0 and 1

β The threshold of congestion indicator to categorize network as light traffic or high traffic

Acronyms / Abbreviations

ACI Adjacent-channel interference

AEDP Adaptive Energy Detection Detection

AN Access Notification

AP Access Point

ASN Access Suppression Notification

BI Beacon Interval

CAP Content-Access Period

CAP Contention Access period

CCI Co-channel interference

CFP Content-Free period

CFP Contention Free Period

CIM-HetNet Cross-Interference Mitigation Heterogeneous Network

CSMA/CA Carrier Sense Multiple Access with Collision Avoidance

CSMA/CD Carrier Sense Multiple Access with Collision Detection

CSMA/CA Carrier Sense Multiple Access With Collision Avoidance

CSMA Carrier-sense multiple access

CTI Cross-Technology Interference

CTS Clear To Send

DCF Distributed Coordination Function

DSSS direct sequence spread spectrum

EDCF Enhanced Distributed Coordination Function

ED Energy Detection

EMA Exponential Moving Average

EWLAN Enterprise Wireless Local Area Network

FCF Frame Control Field

FDMA Frequency-division multiple access

FFD Full-Function Device

FIFO First In First Out

GTS Guaranteed Time Slot

HetNet Heterogeneous network

HMM Hidden Markov Model

HWN Heterogeneous Wireless Network

IC Integrated Circuit

IIoT Industrial Internet of Things

IP Internet Protocol

IPv6 Internet Protocol version 6

ISI Intersymbol interference

ISM Industrial Scientific Medical

LBT Listen Before Talk

LR-WPAN Low-Rate Wireless Personal Area Network

MAC Medium Access Control

MHR MAC Header

MSCU MAC Layer SDU

NAV Network Allocation Vector

OFDM Orthogonal frequency-division multiplexing

OQPSK offset quadrature phase shift keying

OR_S Scheduling Overhead Ratio Estimation

OS Operating System

PAN Personal Area Network

PCF Point Coordination Function

PDU Protocol Data Unit

PER Packet Error Rate

PLR Packet Loss Rate

PSD Power Spectral Density

RFD Reduced-Function Device

RF Radio Frequency

RTS Request To Send

RX Transceiver receiving mode

SD Superframe Duration

SDU Service Data Unit

TDMA Time-division multiple access

TPC Transmission Power Control

TX Transceiver transmitting mode

VoIP Voice over IP

WLAN Wireless Local Area Network

WSN Wireless Sensor Network

Chapter 1

Introduction

Wireless technologies are ubiquitous today. Especially in a smart building environment, various wireless devices are deployed everywhere. For instance, high throughput wireless devices are used for web surfing, video streaming and Voice over IP (VoIP) services. With the advent of "smart working environment", low-power and low-speed wireless technologies are employed for battery-powered sensors collecting environment information. Generally, we need at least two kinds of networks in a smart building environment – (1) Low-power Wireless Sensor Networks (WSNs) and (2) High throughput Wireless Local Area Networks (WLANs). IEEE specifies various standardized technologies to meet the requirements. One popular wireless communication technology for WSNs is Low-Rate Wireless Personal Area Network (LR-WPAN), also known as IEEE 802.15.4 [34]. Thanks to its multiple benefits such as low power consumption, high receiver sensitivity, and flexible topology, many wireless protocol stacks have been developed on top of it, e.g. ZigBee [5], Contiki-6LoWPAN [87], Rime [25], Thread [35] and so on. Wi-Fi (IEEE 802.11) [8] is a widely adopted WLAN technology that is a universal and straightforward way to connect wireless devices, e.g. smartphones, laptops, TVs and digital camera to the internet for various online services. However, it is power-hungry, result in battery problems in small sensors [11, 24]. Kim and He [59] conclude that the standards for individual technologies are specialized; hence possess strengths in

different areas that are often the weaknesses of the others. Thus, it is necessary to have both LR-WPAN and Wi-Fi available in IoT. However, most of those wireless networks are working in the license-free Industrial Scientific Medical (ISM) frequency band and share the same wireless medium, where neither resource rescheduling nor allocation is available to guarantee communications, unavoidably leading to severe wireless coexistence problems [31, 97, 112, 146, 148]. In some extreme case, LR-WPAN communication can be blocked when Wi-Fi is in heavy load, e.g. downloading or sending large file through Wi-Fi, resulting in LR-WPAN to be unreliable.

In a smart indoor environment, the LR-WPAN coordinator and Wi-Fi Access Point (AP) tend to be integrated into one heterogeneous gateway to provide both high throughput Wireless Local Area Network (WLAN) and low-power Wireless Sensor Network (WSN). For example, there are popular smart home hubs that have both LR-WPAN and Wi-Fi available in one box, e.g. Samsung SmartThings Hub, Amazon Alexa smart home hub and Linkind Zigbee Smart Mini Hub. In consideration of the small size of a gateway and the fact that LR-WPAN and Wi-Fi antennas are at an extremely short distance, the interference became even severe because of out-of-band emission. Although many Cross-Technology Interference (CTI) studies have been carried out, most of them do not consider this particular case. Different from other research, in this thesis, we design and evaluate scheduling algorithms between Wi-Fi and IEEE 802.15.4, on a proposed system architecture named CIM-HetNet (Cross-Interference Mitigation Heterogeneous Network). CIM-HetNet system employs a network gateway, called CIM-HetNet gateway, to integrate two wireless technologies – Wi-Fi and LR-WPAN. In detail, the basic experiment is conducted to reveal CTI problems. Then, the mechanism of the time slot is designed and static time-slot based scheduling algorithm is proposed and evaluated. Finally, further research is carried out by developing and evaluating adaptive time-slot based scheduling algorithm.

1.1 Background

Typically, Heterogeneous Wireless Networks can be found in universities, companies and airports, which consist of large-scale WLANs and WSNs, including more than hundreds of Access Points (APs) and thousands of sensors.

1.1.1 WLAN

The rapidly increasing usage of mobile devices, including smartphones, laptops and tablets has been accelerating the development of wireless technology. One of the most popular WLAN technology is Wi-Fi, based on the IEEE 802.11 standard, which has become one of the most prolific technologies around the world. According to ABI research on 2012, surpass 5 billion Wi-Fi enabled devices had been shipped in the technologies lifetime [1], while this number was more than doubled three years later [4]. It was expected to continue the growth of nearly 4 billion annual device shipments by 2024 [2].

Over the past decade, WLAN capabilities have extensively expanded with the demands of higher capacity, improved power management, higher throughput and lower latency. Wireless networking specifications have upgraded from low rate IEEE 802.11b/a/g standard to much fast IEEE 802.11n standard, and recently IEEE 802.11ac boosts the performance to gigabit per send speed. Meantime, the progressive system improvement has been made due to the emerging of novel techniques such as multiple-input multiple-output (MIMO) antenna techniques, space-time coding, and the massive improvement in hardware as well as processing power. Regarding radio carrier frequency, IEEE 802.11b/g/n/ac standard introduced 2.4 GHz and 5 GHz frequency bands. Moreover, Au et al. [10] indicates that upcoming IEEE 802.11ad products will utilize the 60 GHz frequency band. Although Wi-Fi in 5Ghz provides faster speeds, 2.4Ghz is still widely used because of excellent coverage for a large area.

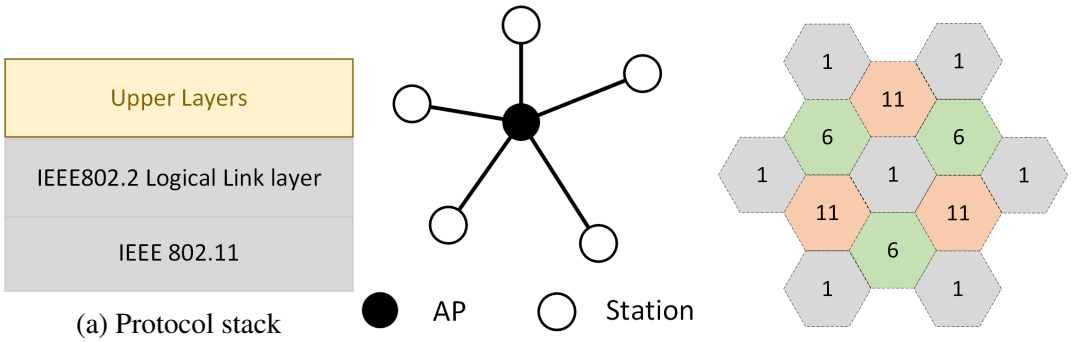

(a) Protocol stack

(b) Typical topology

(c) Three-channel plan

Fig. 1.1 WLAN basics

As shown in Fig. 1.1a, IEEE802.11 Specifies MAC layers. Upper layers can access services by the logical link layer, e.g. TCP/IP that is the most popular and widely adopted upper layers. Wi-Fi delivers network in star topology as illustrated in Fig. 1.1b. The central node is an Access Point (AP) that allows multiple stations to connect. The well-known stations include mobile phones, tablet PCs and laptops. In the case of small families or offices, one AP is able to cover the whole area. However, in public areas such as large airports, universities and major corporations, the WLANs may include hundreds even thousands of APs to deliver network service. Such a large-scale WLAN in an enterprise environment is an Enterprise WLAN (EWLAN). Because there is three non-overlapping channel 1, 6 and 11 available, each AP channel needs to be well planed. A typical deploy plan is as in Fig. 1.1c to reuse channels and reduce interference.

1.1.2 LR-WPAN

Modern technology has enabled distributed data and information gathering from different regions by a wireless sensor network (WSN), which is typically a collection of tiny wireless devices with a microprocessor and various embedded sensors [27]. The IEEE 802.15.4 standard, also known as LR-WPAN, profiles a framework for low power consumption, flexible topology, and low rate communications systems, which is ideal for WSN [22].

Based on this transport mechanism, many low-power and low-rate wireless technology are developed, including ZigBee, Contiki-6loWPAN, Thread, Rime and so on. IEEE 802.15.4 can operate in many frequency bands, e.g. 314-316 MHz, 430-434 MHz, 779-787 MHz, 868 MHz, 902 – 928 MHz, 2.4 GHz. Among them, only 2.4 GHz is global wide as well as the most widely adopted.

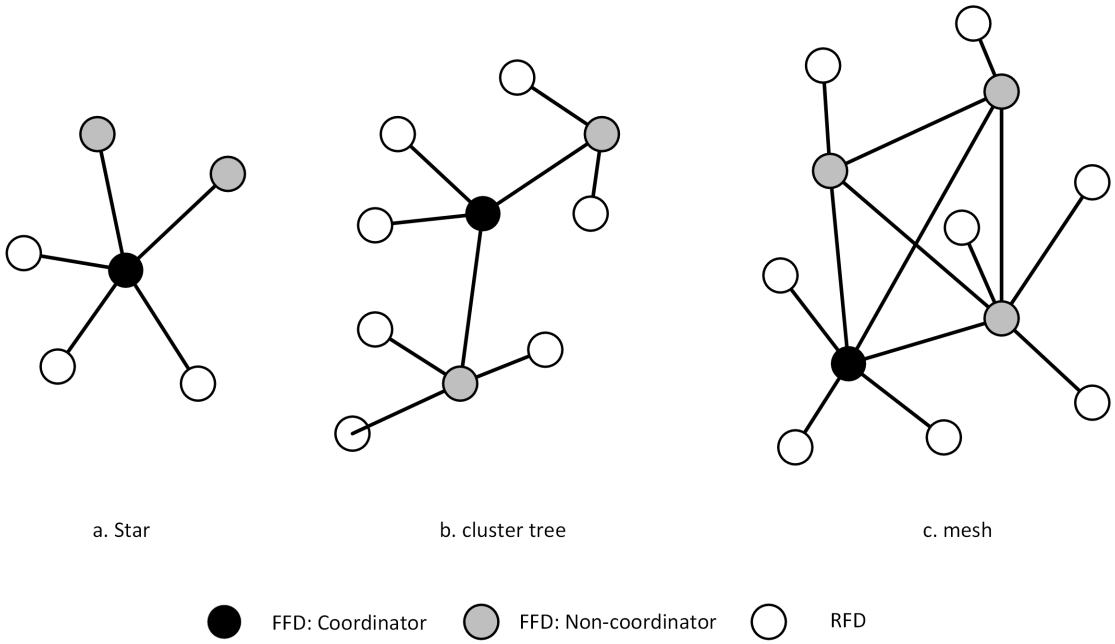

Fig. 1.2 LR-WPAN Topologies

LR-WPAN defines two node types: full-function device (FFD) and reduced-function device (RFD). An FFD serves as the coordinator of a personal area network. It may relay messages to other nodes when two nodes cannot directly talk to each other. RFDs are extremely simple devices with a very modest resource, which can only communicate with an FFD. It consumes significantly less energy than an FFD. Each device has a unique 64-bit identifier, while a short 16-bit identifier can be used within a personal area network (PAN) to make the frame short, which can reduce frame conflict chance and save energy. Fig. 1.3 depicts three typical topologies for LR-WPAN.

- Star: One FFD acts as network coordinator while multiple FFDs and RFDs act as end nodes.
- Cluster tree: Each cluster is a star topology composed by FFDs and RFDs. FFDs communicate and forward/relay packets to/form a tree topology.
- Mesh: FFDs form a mesh topology while RFDs connects to one FFD only.

As shown in Fig. 1.3, LR-WPAN doesn't define higher layers in the standards. Nevertheless, based on LR-WPAN, many upper-layer protocols and specifications are standardized with various features. For example, ZigBee Alliance carries out the ZigBee protocol that specifies application standard for diverse scenarios, such as ZigBee Building Automation, ZigBee Health Care, ZigBee Home Automation, ZigBee Smart Energy and so on [5]. It forms a mesh network and is one of the WSNs that play a dominant role in information collection by various sensors, such as temperature, humidity, brightness, motion detector and body sensors. The 6LoWPAN group has defined encapsulation and header compression mechanisms that allow IPv6 packets to be sent and received over LR-WPAN. Both Contiki-6loWPAN and Thread are 6loWPAN based network stack, but with different implementations and features. Thread aims to provide a reliable wireless network without a single point of failure in its system, while Contiki-6loWPAN emphasizes a much lower resource requirement in term of RAM and flash, and flexible power-saving algorithms in MAC layer, such as ContikiMAC [26] and X-MAC [114]. Furthermore, Rime is designed to be a lightweight layered communication stack for IoT [25]. Different from Wi-Fi that runs IP-based protocol in most case, the upper layers for LR-WPAN normally adopt special defined formats to reduce packet size.

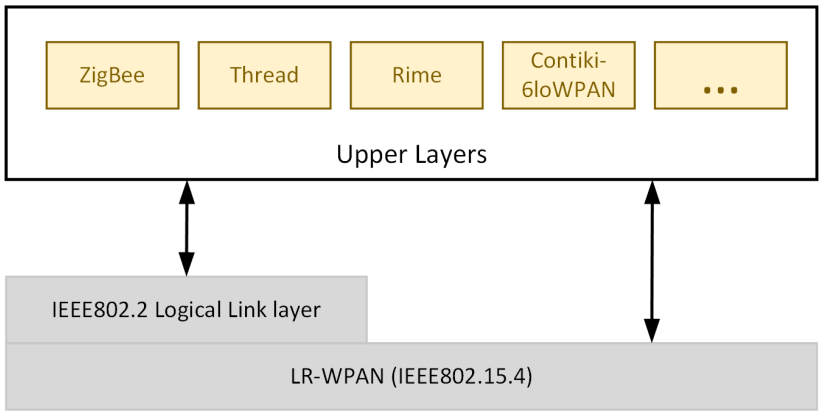

Fig. 1.3 LR-WPAN protocol stack

1.1.3 Coexistence

Interference Mitigation

The Wireless networks are built on the shared medium that potentially causes the interference and performance degradation, because different wireless nodes may occupy the same spatial area and compete for the same wireless spectrum resource [146, 115]. Especially in a smart building environment, the cross-technology interference caused by frequency overlaps across different wireless technologies [29, 66], e.g., Wi-Fi and ZigBee, largely degrades performance in terms of throughput, stability and reliability. In worse situation, some adversaries may conduct a denial of service attack that can be easily accomplished by either bypassing MAC-layer protocols or emitting a radio signal all the time [134]. It is possible to detect the interference and retreat from the interference by dynamic channel switching or adaptive power management. For example, the IEEE 802.11 specification defines 14 partial-overlapping channels, and there are three non-overlapping channels: 1, 6, and 11. Based on these channels, there are many studies about channel allocation strategies in wireless scenarios to improve WLAN performance [65, 73, 72]. Moreover, [92] claims that dynamically adjusting radio transmission power and minimize power consumption will help to maximize the spectrum utilization and mitigate interference. However, statistics from all the APs and perform dynamic real-time channel and power management are challengeable.

Compared with Wi-Fi, IEEE 802.15.4 has slower channel access speed and lower power, resulting in being victim of CTI. [45] notes that LR-WPAN communication can be pre-empted by Wi-Fi at any time and this will block IEEE 802.15.4 Communication in the worst case.

Resource scheduling over heterogeneous network

Wi-Fi and LR-WPAN share the same radio spectrum. They both use (Carrier sense multiple access with collision avoidance) CSMA/CA mechanism for collision avoidance by transmitting only when the channel is sensed to be clear. According to Bulhões et al. [17], Vu and Sakurai [122], packets collision probability increase with the increasing number of wireless nodes. Moreover, Hidden nodes, which are a well-known problem of CSMA/CA networks, may fail to sense an ongoing transmission and destroy the message. The huge differences in frame length and transmission power of Wi-Fi and LR-WPAN further degrade network performance. Therefore, extra resource scheduling is needed to reduce packet loss, improve spectrum efficiency and keep the fairness of medium access.

1.2 Wireless Interference

In the wireless world, interference occurs in many ways, such as Intersymbol interference (ISI), Co-channel interference (CCI), Adjacent-channel interference (ACI), and so on. ISI is a form of signal distortion caused by two neighbour symbols when transmitting wireless data [37]. The multipath propagation is the primary reason, in which the signal sent by a transmitter is reflected and reaches a receiver in different paths. Usually, this type of interference can be resolved by introducing a guard period between symbols and prolonging the system duration. Thus long-distance wireless technologies often have longer symbol duration such as LTE (500 us symbol duration), while short-distance technologies have shorter symbol duration such as Wi-Fi (3.2 us symbol duration in 2.4 GHz) and 802.15.4

(4 us symbol duration in 2.4GHz). CCI can be caused by two transmitters using the same wireless channel same. One of the popular mechanism in ISM frequency band communication is Carrier Sense Multiple Access/Collision Avoidance (CSMA/CA), in which transmitters sense whether the medium is busy or not before sending any data to avoid accessing channel at the same time, in other words, mitigating CCI. Both Wi-Fi and IEEE 802.15.4 have a Medium Access Control (MAC) in CSMA mechanism. ACI is the phenomenon that the adjacent non-overlapping channel may interfere with each other [79], which is mainly caused by out-of-band emission. One wireless channel is allocated a frequency band. If the radio transmitter restricts all the signal within the frequency band, there would not be any ACI. In real life, however, out-of-band emission always exists, which is inevitable from the modulation process. These unwanted emissions are weaker than in-band emissions, but they still affect communication in adjacent channels if they are close to each other.

1.2.1 Radio Frequency Spectrum and Channels

The most common wireless technologies use radio waves that carry information across space. To prevent interference and allow efficient use of the radio, wireless communication needs to be limited into a small section of the Radio Frequency (RF) Spectrum. Thus, the RF spectrum is vital for wireless communication. If more than one node broadcasts information by using the same RF frequencies at the same time, they interfere with each other, and the information transmission may fail. RF spectrum is allocated into small frequency band for various application purpose. Most of the radio band is allocated for commercial and military use, which is illegal to use without permission. However, there are ISM radio bands that reserved for industrial, scientific and medical purposes. In other words, they are free to use without the licence required. One of internally available the ISM radio band is well-known 2.4Ghz band that runs from 2.4 to 2.5 GHz. It is used by different wireless technologies including, Wi-Fi, LR-WPAN, Bluetooth and so on.

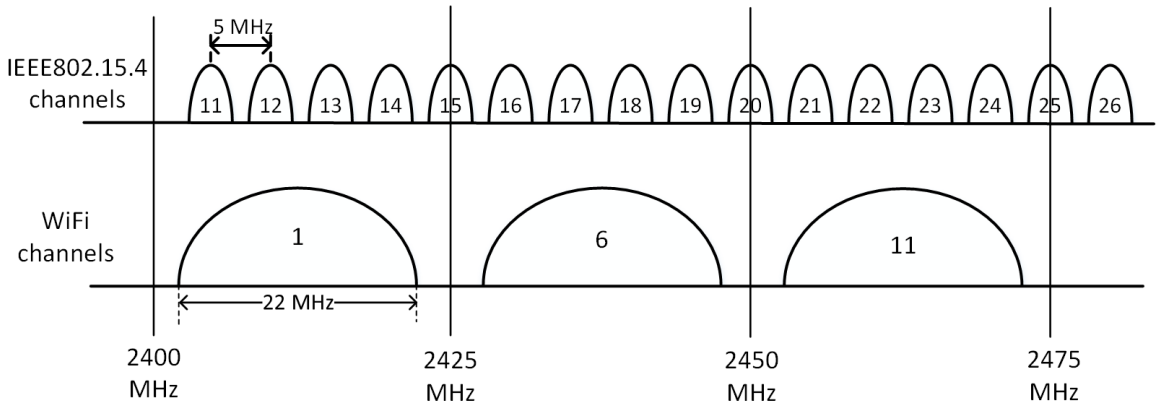

Fig. 1.4 Comparison of LR-WPAN and Wi-Fi channels in 2.4 GHz band

A channel is a smaller continuous section of the RF spectrum in a radio band. Typically, multiple channels are included in a band. Wireless technology can select a channel as a medium for communication. Channels help wireless network manage spectrum resource and deploy a network to cover a large area without interference. For example, LR-WPAN specifies 16 channels in the 2.4Ghz band, as shown in Fig. 1.4. In the same time, Fig. 1.4 also shows that Wi-Fi defines channels differently. There are only three non-overlapping channels (1, 6 and 11) specified for Wi-Fi. It easy to tell that some of Wi-Fi and ZigBee channels are overlapped in term of RF spectrum, which indicates they could interfere with each other if LR-WPAN and Wi-Fi nodes are using radio at the same time.

1.2.2 Out-of-band Emission

As mentioned previously, wireless technology defines radio channels to avoid interference among multiple networks. Ideally, the transmission power is limited within its channel. However, a real radio transceiver has out-of-band emission that is unwanted and results in adjacent channel interference. IEEE802.11a/g/n modulate signal by using Orthogonal frequency-division multiplexing (OFDM), which is also very promising for the future radio system. Nevertheless, OFDM has significant out-of-band emission [46]. They point out that

reducing out-of-band emission is a major technical challenge for the OFDM signal. Angelakis et al. [6, 7] work on a theoretical model for adjacent channel interference in IEE802.11a and the results indicate that equipping a single node with multiple radio transmitters can lead to a severely degraded wireless performance in term of throughput, even if each transmitter is on a different channel because out-of-band emission cannot be ignored when transmitter distances are close enough. Their studies deduce channel power leakage theoretically as in Table 1.1:

Table 1.1 IEEE802.11a out-of-band emission power

Interfere Power (dB)	Receiver Bandwidth (MHz)	Adjacent Channel Power Leakage (dB)	Next Adjacent Channel Power Leakage (dB)
0	20	-22.04	-39.67
0	∞	-19.05	-36.67

Practically, testbed based experiments are performed in both laboratory and outdoor to evaluate the impact of adjacent channel interference (ACI) on dual-radio 802.11a nodes [21, 63]. Their work includes both directional and omnidirectional antennas. Their experiments empirically show the methods to reduce ACI effects, including increasing channel separation and antenna distance as well as using directional antennas.

An experiment is carried out to acquire IEEE802.11g signal spectrum as shown in Fig. 1.5a, which matches the spectral mask suggested by NXP [83] as shown in Fig. 1.5b. The experiment adopts Atheros 9331 [9] Wi-Fi modules as AP. One USRP-X310 is introduced to monitor the signal spectrum when a smartphone connects to the AP and downloads a big file. The graph depicts the Wi-Fi signal spectrum for Wi-Fi channel one that is 22Mhz channel with frequency from 2.401Ghz to 2.423Ghz (the green area in the graph), and the central frequency is 2.412Ghz. It indicates the signal spectrum doesn't stop at the channel frequency boundary, though the signal spectrum strength decreases slowly. Unwanted emission is about 20dB lower than in-band. Although the power leaked into the neighbouring channels is quite low compared to the transmitted signal power, it is sufficient to interfere or even block some

low-power wireless technologies, e.g. ZigBee and Thread, especially when those transceivers are integrated into one node.

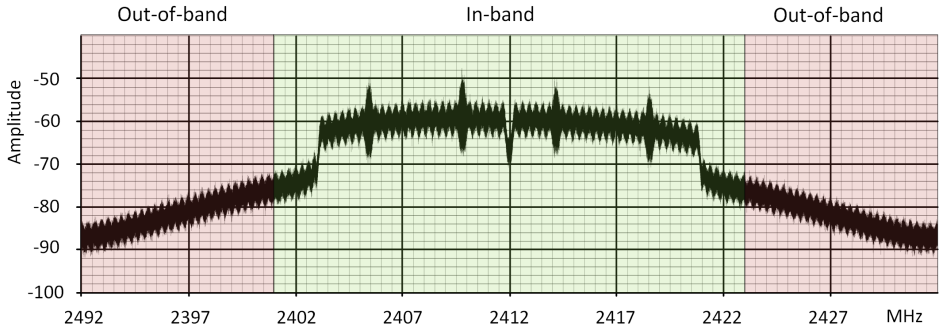

(a) Measured spectrum for Channel 1

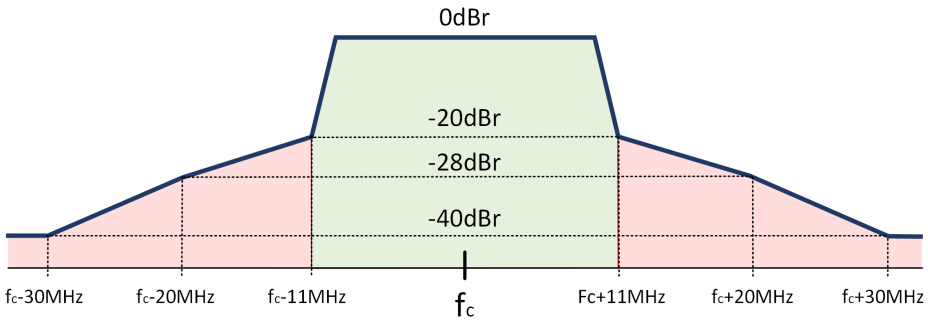

(b) Spectral Mask

Fig. 1.5 IEEE802.11g signal spectrum

Besides Wi-Fi radio, LR-WPAN also gets unwanted emission when transmitting signals. LR-WPAN adopts offset quadrature phase-shift keying (OQPSK) with a half-sine pulse-shaping filter to reduce the channel side effect. Many researchers [33, 88, 100, 38] have revealed that OQPSK transmits only 90 percent of total power in a given bandwidth of $W = \frac{1}{T_b}$, where T_b is the symbol interval. Remaining 10 percent energy is the out-of-band emission, as depicted in Fig. 1.6b. LR-WPAN define channels with 2MHz bandwidth, while the channel frequency space is 5MHz. Thus, the adjacent channel interference is quit small, as shown in Fig. 1.6c. SiliconLabs [108] indicates spectrum strength is 42 dB below the wanted signal level at 5 MHz offset.

Fig. 1.6a shows the experimental LR-WPAN signal spectrum. One CC2530 [49] RF module is programmed to transmit packets in channel 16 and a USRP-X310 is set up to acquire the spectrum graph. Compared with Fig. 1.6b, Fig. 1.6a confirms the signal spectrum shape matches the theoretical calculation.

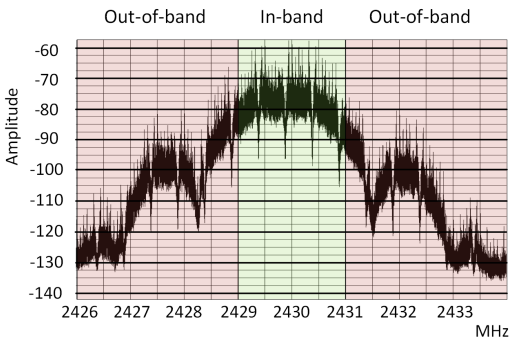

(a) Measured spectrum for Channel 16

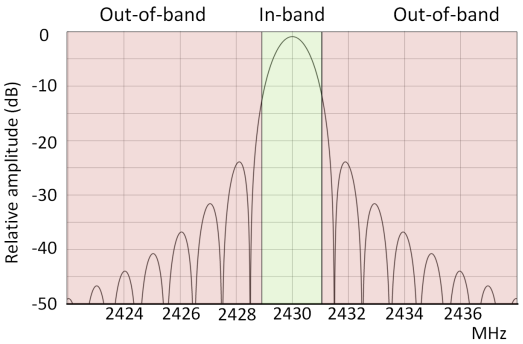

(b) Calculated spectrum for Channel 16

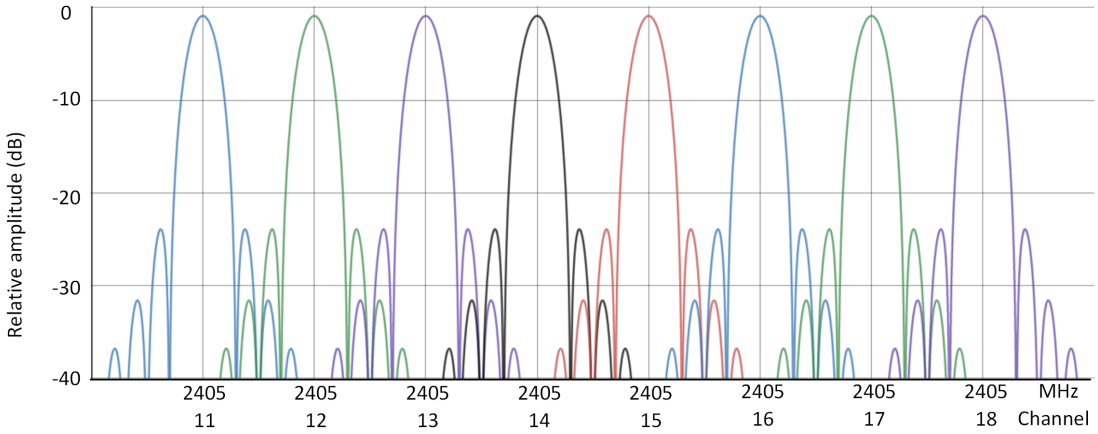

(c) Calculated spectrum for Channel 11 to 18

Fig. 1.6 LR-WPAN signal sepctrum

1.2.3 Cross Technology Interference between Wi-Fi and LR-WPAN

Many technologies, e.g., Microwave oven, Bluetooth, and Cordless telephones, work in the 2.4-GHz band due to its unlicensed feature. These technologies share the same spectrum resource and make the 2.4GHz band crowded. The high interference among them extensively degrades the experience. Particularly, Wi-Fi traffics deeply affect LR-WPAN communications

due to higher transmission power and shorter frame time duration. Wi-Fi and LR-WPAN channels are overlapped, which makes the coexistence problem more severe.

This thesis concentrates on the interference in the 2.4GHz band. Fig. 1.4 shows the detail channel distribution of ZigBee and Wi-Fi at 2.4 GHz band. IEEE 802.11 (Wi-Fi) defines only three non-overlapping channels in 2.4GHz, while IEEE 802.15.4 defines 16 channels with a frequency step of 5 MHz. It can be seen that ZigBee and Wi-Fi channels are overlapped. The overlapping channels, such as IEEE 802.15.4 channel 11 and Wi-Fi channel 1, share the same spectrum resource and is expected to interfere with each other. Non-overlapping interference (e.g., interference between Wi-Fi channel one and IEEE 802.15.4 channel 17, as shown in Fig. 1.8) must be considered as well, because of close distance and out-of-band emission. In a real-life environment where a heterogeneous gateway integrates Wi-Fi AP and LR-WPAN radio module, the non-overlapping interfere is significant and fully capable of drowning out LR-WPAN transmissions. Following, we will analyses CTI problems in two aspects: (1) CTI between overlapping channels, (2) CTI between non-overlapping channels.

Cross-Technology Interference between overlapping channels

This kind of interference is similar to the CCI. In a specific wireless technology, this interference is effectively mitigated by CSMA mechanism in MAC. Both Wi-Fi and IEEE 802.15.4 introduce their CSMA mechanisms. Nevertheless, their CSMA mechanisms is not adequate to address the inter-technology interference [45, 44, 146]. Therefore, a new mechanism is required to schedule these wireless technology and achieve high spectrum resource efficiency and fair medium access.

Many researchers confirm this type of interference. Liang et al. [66] report that frequency overlap across wireless networks with various technologies can cause severe interference and reduce communication reliability. In the case of ZigBee under interference from Wi-Fi, the network performance can be significantly reduced, because of the asymmetric radio

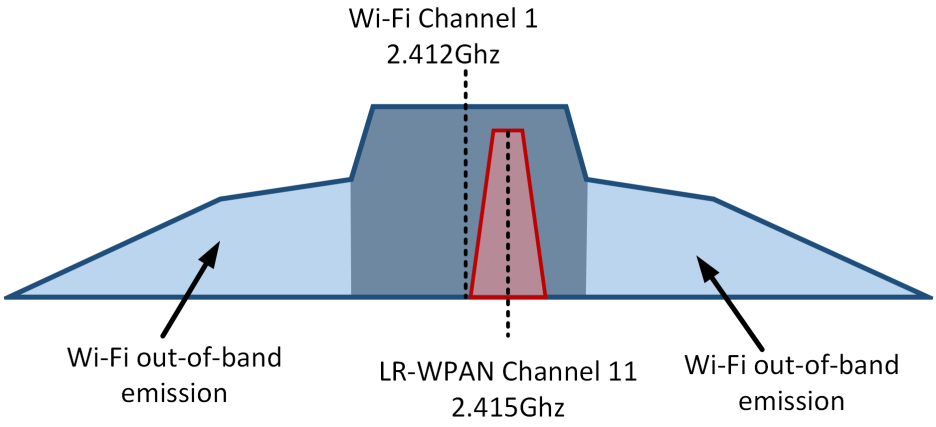

Fig. 1.7 CTI between overlapping channels

features where Wi-Fi senders are capable of 10 to 100 times higher transmission power. Under certain condition, the ZigBee signal is too weak to be detected by Wi-Fi senders, while Wi-Fi activity can arbitrarily corrupt any ZigBee packet. This problem is also confirmed by Mohammad et al. [74] and they state that the interference can be even more server in an urban environment where the CTI behaviour and unplanned Wi-Fi deployments change fast and frequently. It is often not possible for a WSN to pick a good and clear channel to stay on.

Cross-Technology Interference between non-overlapping channels

This kind of interference has similar features of ACI, which mainly caused by out-of-band emission. Thonet et al. [117] confirm this kind of interference and claim that the Wi-Fi channels with a centre frequency 20MHz away from our IEEE 802.15.4 channel can still cause severe disruption. In most cases, this problem can be resolved by separate IEEE802.15.4 and Wi-Fi nodes at a proper distance. However, in the case of CIM-HetNet gateway where Wi-Fi and IEEE 802.15.4 modules are integrated into one small box, it is not realistic to keep them at a relatively far distance. Thus the non-overlapping channel interference must be considered. Most previous researches do not consider the Cross interference between non-overlapping channels. The thesis will fill this gap.

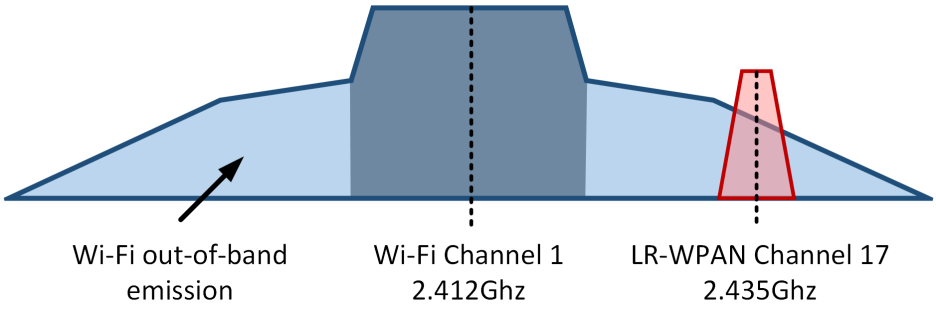

Fig. 1.8 CTI between non-overlapping channels

1.3 Major Contribution

There are many studies on CTI and its solutions. Most of them consider Wi-Fi and LR-WPAN as non-relevant networks without data intersection, without considering that both technologies may be embedded into one small box. Nowadays, some heterogeneous gateways are becoming popular. The gateway acts as a versatile network hub, allowing at lease both Wi-Fi AP and LR-WPAN coordinator functionalities available in on compact node. Wi-Fi AP serves as a high-throughput Internet provider, while the LR-WPAN coordinator works as a low-power sensor data collector. Our research fills this gap and proposes time-slot based methods to address interference problems in this scenario. The solution is confirmed to be effective by using both real-life indoor experimental testbed and NS-3 simulation. Our major contribution includes:

- To create a testbed that mimics a real-life indoor environment where both Wi-Fi and IEEE802.15.4 coexist. For this purpose, the CIM-HetNet gateway integrating both Wi-Fi and IEEE 802.15.4 modules has been designed and implemented.

- To design and to carry out indoor experiments and most importantly to provide observations of real-life experiment results. These results, in some cases, have proved Wi-Fi out-of-band emission has a significant effect on LR-WPAN transmissions. Thus non-overlapping CTI must be considered.

- To design an innovative Time-slot based scheduling mechanisms over Wi-Fi and IEEE802.15.4 for CTI mitigation. Different from most of CTI mitigation research, our work focus on separating these two types of traffic in the time domain and scheduling their access to the medium in a different time to avoid interference. It is achieved by introducing a new control frame called Access Notification (AN) into IEEE 802.15.4. Moreover, an HWN (Heterogeneous) layer on top of Wi-Fi and LR-WPAN MAC is contributed as an NS-3 simulator module.

- To propose and define the concept of slot-based congestion indicator to assess the network congestion level and crowdedness. Because it is complicated and impractical to get a precise CI value, we design CI estimation models to reduce the network statistic requirement and simplify the calculation to offer an estimated CI.

- To propose, implement and evaluate both static and adaptive time-slot based scheduling algorithms, which mitigates harmful CTI and extensively increase the network efficiency.

1.4 Thesis Organization

The thesis is organized as follows: Chapter 2 provides an overview of the related literature about CTI and the way to mitigate it. Chapter 3 carries out basic experimental study of Cross interference and design time-slot scheduling mechanism. Chapter 4 propose a static time-slot based scheduling algorithm and its evaluation by using the hardware-based system and NS-3 simulator. Adaptive time-slot based scheduling algorithm is proposed and evaluated in chapter 5. The last chapter (chapter 6) gives a conclusion and future work.

Chapter 2

Literature Review

2.1 Heterogeneous Networks

Heterogeneous network [62, 143, 70], also referred to as HetNet, is a wireless network which consists of devices using various underlying radio access technologies. They can be seen everywhere. For example, today's smartphones equip multiple wireless modules to meet diverse requirements of network [93, 70], e.g., the Wi-Fi is for high throughput video streaming and local area network resource access; LTE is for long-range network access, which enables the Internet almost available in any place on the earth; Bluetooth offers a convenient way to share small file between devices or to connect a wireless earphone. Due to every wireless network has its unique features e.g. low-power consumption, long communication range, high anti-interference and high throughput. In order to fully utilize these favour features, many works have been done. Zhang et al. [143] note that HetNet is able to increase the frequency spectrum efficiency in cellar network effectively. Moreover, because of the high pressure of cellular network from dramatically increasing cellular traffic, some researcher has proposed various HetNet technologies to enable mobile data offloading from cellular to Wi-Fi [18, 132]. The HetNet of Wi-Fi and Wireless Sensor Network (WSN) is also widely deployed in a smart building and smart home scenarios [67], where Wi-Fi

provides high-throughput Internet service. At the same time, WSN allows low-power sensors to collect ambient statistics, e.g., temperature, humidity, lightness, movements and so on.

Typically, HetNet gathers the favour features of the diverse wireless network. Meantime, many challenges are also introduced. When taking multiple networks into consideration, resource scheduling and allocation become much more complicated than in the situation of only one network. In wireless communication systems, radio spectrum resource is very precious and scarce [89]; radio resource management aims to have better utilization of the resource. In order to utilize wireless bandwidth resource, Masud et al. [70] propose a scheduling algorithm for selection of Radio Access Technology. Rapidly rising energy cost, Peng et al. [89], Xie et al. [131] study the energy efficiency aspect of spectrum sharing and power allocation in HetNet. Moreover, Miao et al. [71] investigate the HetNet effective capacity by considering both the bandwidth and power. With emerging of new wireless technology, resource scheduling will be a long term challenge. Cross interference is another big challenge. If two or more wireless technologies works in an overlapping frequency band, they inevitably interfere with each other, especially in the case of no effective scheduling management in between. Wi-Fi, Bluetooth and WSNs typically work in an overlapping frequency band [133]. This thesis will focus on cross-interference mitigation in the way of time-slot based scheduling.

2.2 Coexistence Challenges

Because the need for bandwidth keeps increasing while the available wireless spectrum resource is limited, the coexistence problem is one of the major challenges for wireless communication towards IoT and IIoT(Industrial Internet of Things), which is confirmed by relevant studies [52, 109, 16]. According to Yang et al. [135], the essence of the coexistence problem is the collision of spectrum resource, and the basic principle of mitigating coexistence interference is to avoiding collision in term of frequency, time and space. As a

license-free radio band, 2.4Ghz ISM has been widely used by many wireless technologies. Because of the high transmit power, wide deployment and large coverage range, IEEE802.11 devices contribute major impact on IEEE802.15.4 [136, 135]. Sikora and Groza [107] also confirm that IEEE802.11 is the major factor to interfere IEEE802.15.4 communication in comparison with other wireless systems including Bluetooth, microwave oven and cordless phone. For this reason, It is critical and valuable to study and analyse the CTI between these two techniques. This section reviews the research on seriousness and cause of CTI from coexistence.

2.2.1 Medium Access control

In a 7-layer OSI (Open Systems Interconnection) model for wireless networks, MAC (Medium Access control) and PHY (Physical) layer are the main layers to achieve channel sharing in the multi-nodes communication system. In order to reduce interference among nodes in a wireless network and share medium in term of time, frequency as well as space, diverse mechanisms and algorithms are proposed and built into each node by default, e.g. CSMA/CA (Carrier Sense Multiple Access with Collision Avoidance) [124], CSMA/CD (Carrier Sense Multiple Access with Collision Detection) [125], TDMA (Time-division multiple access) [127] and FDMA (Frequency-division multiple access) [126]. Both Wi-Fi and LR-WPAN employ CSMA/CA, also known as LBT (Listen Before Talk), as an interference avoidance method in the MAC layer. LR-WPAN also specifies TDMA as an option, but it is less commonly adopted because of beacon conflict problem [58] that may result in unexpected network panic when considering a number of LR-WPAN networks coexistence.

CSMA/CA process in the real case can be complicated. However, the simplified key process can be concluded as in Fig. 2.1. Before sending a data frame, a transceiver needs to perform CCA (Channel Clear assessment) that evaluates if a channel is clear to send a packet. In other words, it tries to ensure only one node sending a packet at the same

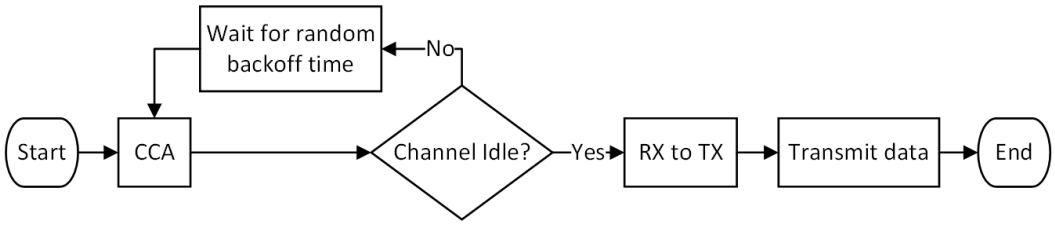

Fig. 2.1 CSMA/CA brief flowchart

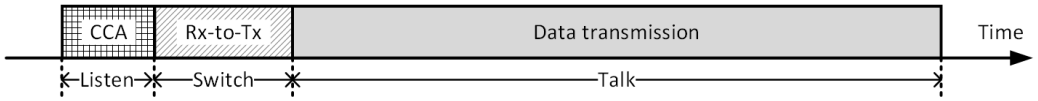

Fig. 2.2 An example of packet send based on CSMA/CA

time to avoid packet conflict. If the channel is clear, the transceiver will switch from RX (receiving mode) to TX (transmitting mode) and then send the data frame out. Otherwise, the transceiver will wait for random backoff time and repeat the process above by performing CCA again until the data is transmitted. Fig. 2.2 gives an example how a packet is successfully sent. The Time windows of CCA and TX-to-RX, as well as frame-in-air time, vary from one wireless technology to another. For example, regular CCA window time for Wi-Fi is $4\mu s$ while for ZigBee is $128\mu s$ [119]. What is more, different technologies may adopt disparate CCA modes (e.g. Energy Detection mode and carrier sense mode) and diverse parameters such as ED (Energy Detection) threshold values. Thus, it isn't easy to anticipate the performance of the coexistence of two wireless technologies, even if both of them adopt the CSMA/CA mechanism in the MAC layer. In consequence, one or both networks suffer degraded performance.

2.2.2 Coexistence Interference Review

The coexistence of heterogeneous wireless networks is a critical issue in unlicensed ISM bands. CSMA/CA algorithm is built-in mechanisms for Wi-Fi networks and LR-WPANs. Plenty of research shows that CSMA/CA is an effective algorithm to resolve the collision between the same type of networks. However, these built-in algorithms become less effective

for the coexistence of various MAC/PHY protocols/standards, because of disparate transmission/interference ranges and incompatible communication mechanisms [146]. In order to address this problem, some related works have been investigated by analysing Packet Error Rate (PER) when Wi-Fi and ZigBee coexist [137, 32, 105, 43].

As shown in Fig 2.3, both Wi-Fi and LR-WPAN node may act as an interferer. The experiment carried out by Bertocco et al. [14] shows the PER (Packet Error Rate) of ZigBee network can be up to 75% with a Wi-Fi access point 1 meter away, and they conclude that CSMA/CA is not optimal for monitoring system and even not adequate in an industrial system. Zhen et al. [149] study this interference by the probability of CCA and conclude that the IEEE 802.15.4 may lose the chance for successful transmission, because of the asymmetric CCA leave IEEE 802.15.4 very low possibility to access the medium even if Wi-Fi enables energy-based CCA instead of feature-based. They also point that IEEE 802.15.4 oversensitive to Wi-Fi, while Wi-Fi is insensitive to IEEE 802.15.4. Similarly Petrova and Gutierrez [90], Howitt and Gutierrez [43] confirm that IEEE 802.15.4 has a little impact on the IEEE 802.11 performance.

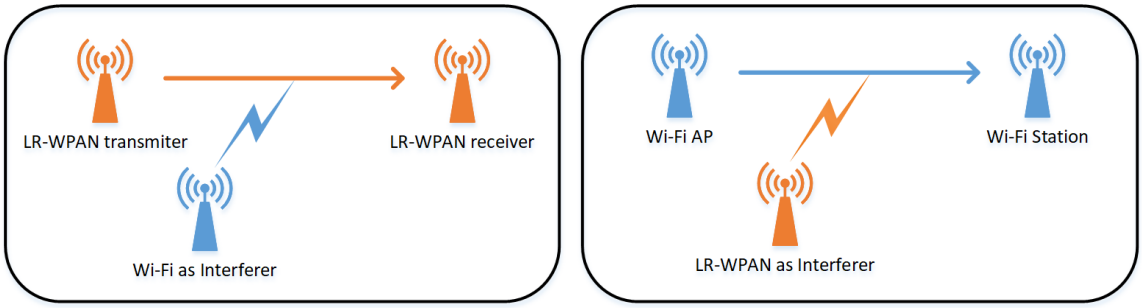

(a) Wi-Fi interferes LR-WPAN (b) LR-WPAN interferes Wi-Fi

Fig. 2.3 Wi-Fi and LR-WPAN Interference

- Wi-Fi interfere LR-WPAN as in Fig 2.3a: Yuan et al. [139] present a coexistence model of IEEE 802.15.4 and Wi-Fi based on both power and timing in a simulation way. They claim that IEEE 802.15.4 throughput can drop to only 5.75% of its original value under the interference of Wi-Fi. With the real experiment, Thonet et al. [117]

found 85% IEEE 802.15.4 Packet Loss Rate (PLR) due to Wi-Fi traffic. Golmie et al. [32] also analyse the PLR under Wi-Fi interference but in a medical scenario and note that the PLR is 100% when the Wi-Fi is Wi-Fi always has higher priority to access the wireless medium and cause unfairness to the LR-WPAN nodes.

- LR-WPAN interferes Wi-Fi as in Fig 2.3b: There also are many studies about how IEEE 802.15.4 interfere Wi-Fi. By analysing packet error rate (PER) of Wi-Fi, Myoung et al. [78] indicates that IEEE 802.15.4 has negligible impact on Wi-Fi network performance. Yoon et al. [137], by using a method of simulation, present an interference model of Wi-Fi affected by IEEE 802.15.4 at various distances and the safe distance ratio that is obtained from the PER. They conclude that either the distance longer than 4m or the safe distance ratio is 0.8, the interference effect of the IEEE 802.15.4 can be negligible with low PER less than 3.5×10^4. Wang and Yang [123] claim that the interference from IEEE 802.15.4 to Wi-Fi is still negligible in the situation that the wireless nodes are tightly designed into one box.

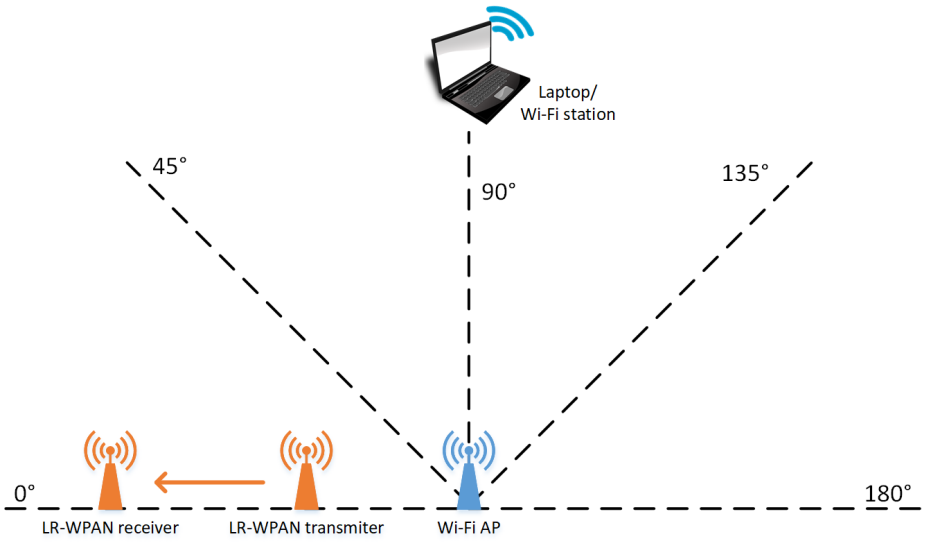

Fig. 2.4 Wi-Fi transmission orientations: the laptop is placed at different direction in different measurements

The coexistence interference can be complex and complicated in various scenarios. For example, Shuaib et al. [106] suggest data flow direction should be considered in the case of CTI. They define two directions:

- **uplink** where packets transmit from a Wi-Fi station/client to a Wi-Fi AP
- **downlink** where packets transmit from a Wi-Fi AP to a Wi-Fi station/client

The experiment in [106] reveals Wi-Fi uplink data encounter stronger interference than the downlink data when coexisting with LR-WPAN. As explained by Yang et al. [136], the reason could be the asymmetry transmission power of APs and stations. Specifically, the transmission power of APs is higher than stations. For this reason, they also advise the researcher to distinguish uplink and downlink for LR-WPAN based network on the study of CTI. Another study [91] evaluates LR-WPAN performance by considering orientations of Wi-Fi transmission, because the beam-forming feature in IEEE 802.11n focuses a wireless signal towards a specific receiving device. The experiment collects data by placing the laptop in different location and direction as indicated in Fig 2.4 and Wi-Fi UDP traffic is from the AP to the laptop. The laptop is the only node changing the position during the experiment. LR-WPAN has the highest packet delivery ratio when the Wi-Fi transmission direction is 90°. When the laptop is placed at 0°, LR-WPAN channels were heavily affected by the Wi-Fi traffic.

Basically, the seriousness of CTI follows some rules. Both Sikora and Groza [107] and Pollin et al. [95] summary four factors for severe interference:

- interferer and victim channels are fully or partially share the same spectrum frequency, namely overlapping channels
- the channel utilization rate is high for Wi-Fi or LR-WPAN or both
- interferer and victim are close to each other

- the transmission power of interferer is high

Sikora and Groza [107] also suggests that interference over non-overlapping channels cannot be ignored in some cases, because the out-of-band emission of Wi-Fi is still rather high comparing with LR-WPAN signal strength. Petrova et al. [91] study non-overlapping interference by experiments and conclude that the impact of Wi-Fi transmission on the non-overlapping channels is not directly caused by the channel error, but mainly the consequence of high sensitive CCA threshold setting.

2.2.3 Coexistence Interference Analysis

Wireless nodes work by sharing the same channel and frequency band because the Wireless spectrum resource becomes increasingly scarce. It won't be a serious issue when only one type of wireless is deployed in an area, because the default built-in MAC layer guarantees that the nodes access medium in a fair and efficient way, e.g. the CSMA/CA algorithm in Wi-Fi and LR-WPAN. Nevertheless, it is not the case when multiple types of wireless technologies coexist. Plenty of studies reveal that the default build-in CSMA algorithm is not adequate for coexistence of Wi-Fi and LR-WPAN [146, 105, 116, 69, 54]. This section analyses coexistence interference in various perspectives including hidden nodes, asymmetric transmission power, CCA working mode and parameters, CSMA timing and so on.

Hidden node problems

The hidden node problem, also known as hidden terminal problems, are studied by many researchers [98, 57, 76, 3, 80, 15]. Tseng et al. [118] deduce in theory that probability of any two nodes having a hidden node relationship is up to 41%, under the assumption of all nodes having the same transmission radius. The work of Koubâa et al. [60] and Hung and Marsic [47] shows that more than 40% packets are being lost because of the hidden node problem and this percentage can be larger with more nodes in the network.

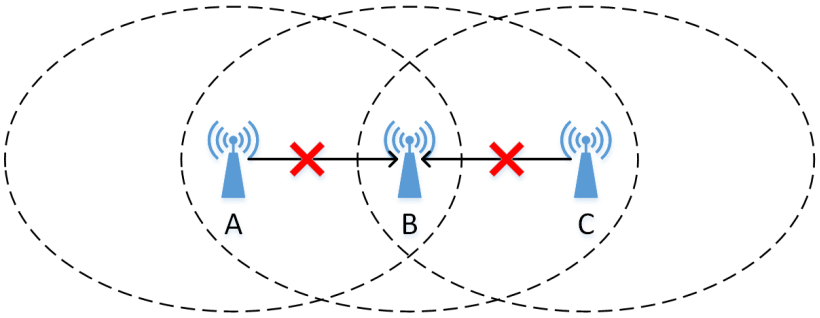

Fig. 2.5 Hidden node problems: both nodes A and C can communicate with B, but signals of A and C cannot reach each other. In another word, A and C are hidden from each other. The problem is node A and C may send data to C at the same because they cannot receive each other's signal. CSMA doesn't work in this case and collisions occur, which then corrupt the packets received by B.

Fig 2.5 shows an example of a hidden node problem, where each node gets the same transmission power and receiving sensitivity. According to Kapadia et al. [57] and Hwang et al. [48], hidden node problem can be observed easily in both Wi-Fi and LR-WPAN network, especially for uplink data. IEEE802.11 partially addresses this problem by introducing RTS(Request To Send)/CTS(Clear To Send) acknowledgement, which uses NAV (Network Allocation Vector) functionality to protect packets sending from station to AP.

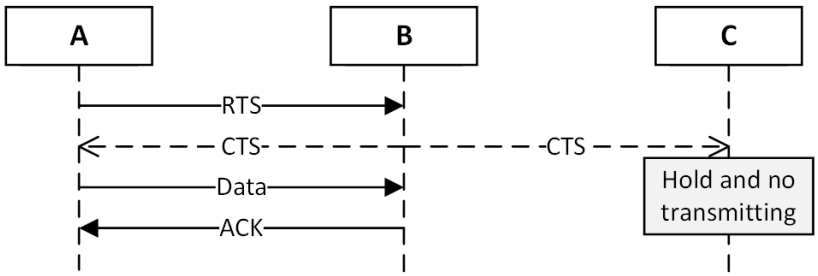

Fig. 2.6 RTS/CTS mechanism

Fig. 2.6 shows how the data is protected from interference of C when A sends data to B. Prior to A transmits long data to B, it estimates the time required for the data packet and includes this information into an RTS frame, which then is sent to B. Because the RTS frame is a short frame with only a few bytes, it is unlikely conflicted and corrupted. After

receiving the RTS, B sends out CTS frame, which is like a broadcast frame that all the nodes nearby can receive. The CTS frame includes a time duration that is assigned to A for data transmission, and all the other nodes in this area (except A) keep silence without sending any frame for this period to allow the A's data is transmitted without interruption. Finally, B replies an ACK frame to A, indicating the packet is successfully received.

The hidden node problem becomes even more complex and server in heterogeneous networks [142], where Wi-Fi and LR-WPAN coexist in an area. CSMA/CA is only effective under the assumption that the transmission power of all the nodes is at the same level. However, due to the limited power resource in WSN, the radio transmission power tends to be lower than other wireless technology. In particular, the maximum transmit power of Wi-Fi is 19dBm for AR9331 chips [9] while LR-WPAN radio is only 4.5dBm for CC2530 chips [49]. As a result, even though they perform the same CSMA/CA mechanism to access the channel, Wi-Fi is still possibly failed to sense the ongoing LR-WPAN packet because of asymmetric transmission power. In other words, IEEE802.15.4 can sense Wi-Fi traffic but not vice versa. Therefore, Wi-Fi can easily terminate and preempt IEEE802.15.4 transmission. Fig. 2.7 illustrates an asymmetrical scenario where Wi-Fi nodes have higher

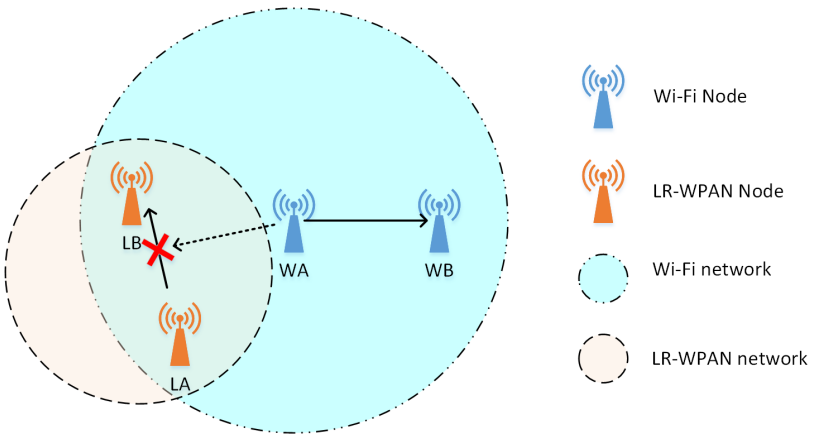

Fig. 2.7 Hidden node problem in asymmetrical scenario

transmission power than LR-WPAN nodes. Node WA in Wi-Fi network cannot be aware of the transmissions of node LA in LR-WPAN network but not vice versa. Thus, when

node WA is transmitting, node LA is waiting, but when node LA is transmitting, node LB cannot detect it and simply proceed to transmit, resulting node WA can arbitrarily interrupt LR-WPAN communication. In the case of this kind of hidden terminal problem, LR-WPAN nodes normally act as the victims and are severely affected by Wi-Fi.

Considering significantly different transmission power and receiver sensitivity for LR-WPAN and Wi-Fi, the hidden node problem can be further complicated. For example, Yuan et al. [139] and Yang et al. [136] advise three distinct ranges (R1, R2 and R3) to analyse coexistence interference, shown in Fig 2.8.

- **R1** A range where LR-WPAN nodes and Wi-Fi nodes can sense each other. The distance of Wi-Fi and LR-WPAN senders is within d1.
- **R2** A range where LR-WPAN nodes can sense Wi-Fi nodes, but not vice versa. The distance of Wi-Fi and LR-WPAN senders is from d1 to d2.
- **R3** A range where neither can sense the other, but they still suffer interference. The distance of Wi-Fi and LR-WPAN senders is from d2 to d3.

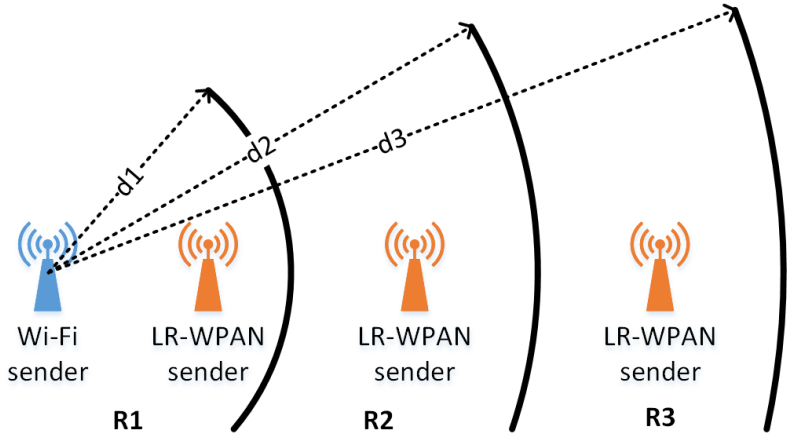

Fig. 2.8 Three interference ranges

Incompatible CCA mode

As described in section 2.2.1, radio transceiver with the CSMA/CA algorithm is required to perform CCA before data transmission. According to IEEE 802.1.5.4 and IEEE 802.11, the PHY layer should perform CCA by adopting at least one of the following three CCA modes:

- **CCA mode 1 (Energy detection)** *CCA shall report a busy medium upon detecting any energy above the ED (energy detection) threshold.* It is important to note that the ED(Energy detection) threshold may vary from different specification, possibly result in asymmetric hidden node problem.

- **CCA mode 2 (carrier sense only)** *CCA shall report a busy medium only upon the detection of a signal compliant with this standard with the same modulation and spreading characteristics of the PHY that is currently in use by the device. This signal may be above or below the ED threshold.* Different wireless technologies may not detect transmission of each other.

- **CCA mode 3 (carrier sense with energy detection)** *CCA shall report a busy medium using a logical combination of Model 1 and Model 2.*

Considering the CCA modes, we could extend the interference range by introducing the fourth range (R4), where Wi-Fi nodes can sense LR-WPAN nodes but not vice versa. Table 2.1 list the ranges and possible CCA modes.

The CTI can be worse when considering incompatible CCA mode of CSMA. For example, most commodity Wi-Fi chips perform CCA carrier sensing 802.11-modulated preamble [36] to get better anti-interference performance. In other words, Wi-Fi will not sense IEEE 802.15.4 traffic at all, even if the signal is strong enough. Thus, Wi-Fi will transmit Wi-Fi data, regardless of ongoing LR-WPAN traffic. This will definitely corrupt ongoing LR-WPAN transmission. Pollin et al. [95] confirm that the Wi-Fi may block LR-WAPN communication. Furthermore, Yang et al. [136] declare that these nodes may work in a range in which neither

Table 2.1 Interference ranges

R	case 1[a] Detectable?	case 2[b] Detectable?	Possible CCA modes
R1	Yes	Yes	CCA mode 1 for LR-WPAN and Wi-Fi
R2	Yes	No	Mode 1 for LR-WPAN while any mode for Wi-Fi
R3	No	No	Mode 2 for both LR-WPAN and Wi-Fi
R4	No	Yes	Mode 2 for LR-WPAN while mode 1 for Wi-Fi

[a] LR-WPAN nodes are able to detect ongoing Wi-Fi packet
[b] Wi-Fi nodes are able to detect ongoing LR-WPAN packet

LR-WPAN nodes nor Wi-Fi nodes can sense each other, but LR-WPAN may still suffer from the Wi-Fi interference because both networks can adopt a non-ED based CCA mode, namely carrier sense only, which is described as blind transmission [104]. This means both of LR-WPAN and Wi-Fi nodes can freely transmit packets without deferring the other. In this case, the network performance can be significantly reduced.

Different CSMA/CA timing parameters

Both of Wi-Fi and LR-WPAN implement CSMA/CA mechanism in their MAC layer as mentioned in section 2.2.1 and simplified flow diagram is given in Fig. 2.1. The operating principle of a CCA-based CSMA/CA algorithm includes three steps:

1. **Perform CCA in RX (receiving mode).** This process take time T_{CCA}
2. **Switch from RX mode to TX (Transmitting mode)** this process take time T_{Rx2Tx}
3. **transmit the packet.** The time reuiqred for data transmission depends on the packet size.

However, the operating parameters, especially timing parameters, are different. Because Wi-Fi consists of specifications of IEEE 802.11a/b/g/n at 2.4Ghz and the parameters have minor differences, we select the specific IEEE802.11g for comparison. As shown in Table 2.2,

LR-WPAN is "slow" with significant lower transmit power than Wi-Fi. The "slow" is not only for the data rate but also for all the CSMA/CA steps.

Table 2.2 Wi-Fi and LR-WPAN parameters [8, 34, 84]

	LR-WPAN	IEEE 802.11g
Transmit power	0 dBm	20 dBm
Power spectrum density	-3 dBm/Mhz	6.6 dBm/Mhz
Data rate	250 kpbs	6-54 Mbps
T_{CCA}	$128\mu s$	$\leq 4\mu s$
T_{Rx2Tx}	$192\mu s$	$\leq 5\mu s$
Backoff unit T_{bs}	$320\mu s$	$9\mu s$
Min. data packet time	$512\mu s$	$28\mu s$

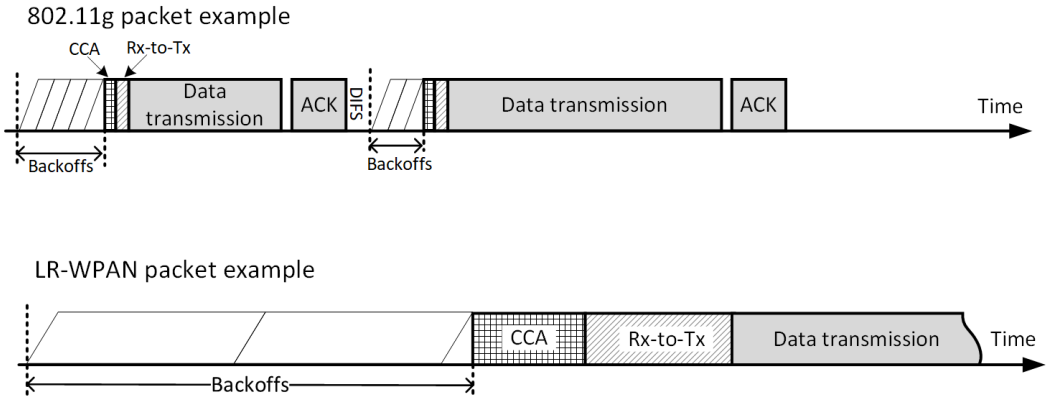

Fig. 2.9 Comparison of Wi-Fi and LR-WPAN timing parameters

Fig 2.9 compares timing parameters in Wi-Fi and LR-WPAN by using packet transmission examples. To simplify the analysis, we could assume that LR-WPAN and Wi-Fi are close enough and can perfectly sense the other. It is not difficult to observe that LR-WPAN node is unlike to get chance to transmit a packet when Wi-Fi is on heavy load because the gaps between data Wi-Fi frames are too small to allow LR-WPAN perform CCA. For this reason, although both of them have a listen-before-send prior to every transmission, LR-WPAN is not able to compete with Wi-Fi, and the network performance is severely impacted. Yuan et al. [139] claim that the shorter timing gives Wi-Fi nodes priority over LR-WPAN nodes to access the medium. Similarly, Hu et al. [44] and Zhen et al. [149] conclude that Wi-Fi

has shorter CCA time and CCA-to-transmit switching time than IEEE802.15.4's, and this gives a higher chance to access channel. Thus, Wi-Fi always has higher priority to access the wireless medium and cause unfairness to the LR-WPAN nodes. Their coexistence model and simulation show that LR-WPAN throughput reduces to only 5.75% even if Wi-Fi and LR-WPAN CCA can avoid all cross-technology collisions. Moreover, Pollin et al. [95] indicate that network's own listen-before-send algorithm is inadequate to avoid an inter-technology collision, because a Wi-Fi packet starting during LR-WPAN's CCA/Tx-to-Rx windows may not be detected by LR-WPAN node, as demonstrated in Fig. 2.10. This causes that LR-WPAN is vulnerable when competing with Wi-Fi. If Wi-Fi keeps heavy traffic, it is hard for WPAN nodes to transmit frames.

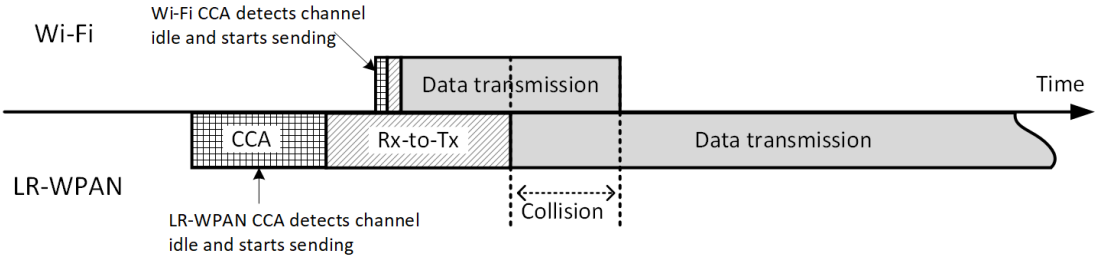

Fig. 2.10 Inter-technology collision of Wi-Fi and LR-WPAN caused by timing differences

Different frame-in-air time is another problem in relation to CSMA/CA timing parameters. Table 2.2 shows that the shortest LR-WPAN data frame lasts $512\mu s$ while this number decreases to only $28\mu s$ in a Wi-Fi network. The data frame transfer time is $4256\mu s$ for an LR-WPAN payload at 114 bytes [84], while it takes only $212\mu s$ for a 1278-byte Wi-Fi frame at a data rate of 54Mbps [119]. Hidden node problem is a well-known problem in CSMA/CA network. According to Zhang and Yoo [144], frames with longer transmission time are more likely to be interrupted by other hidden wireless nodes. Experiment from Tao et al. [116] confirms that the interference from Wi-Fi to Zigbee network is mainly constituted by short and frequent interference and this type of data corruption can not be mitigated effectively by typical approach, e.g. duplicating data and retransmitting in multiple times.

Therefore, LR-WPAN tends to be largely harmed by Wi-Fi because it has significantly longer frame-in-air time.

2.3 Cross Technology Interference Mitigation

As coexistence of various wireless technologies can result in severe interference, the mitigation of CTI has been studied by a great number of researchers. Yang et al. [136] advise categorizing the coexistence solution by three domains, including frequency, space and time because the principle of interference mitigation is to avoid conflict by sharing these resources. The work of Wu et al. [128] indicates a possible fourth domain, code domain, by utilizing specific codes that a side-channel could be constructed for transmitting control messages on top of data packets. Zhang et al. [142] mention some alternative classifications; for example, the coexistence solutions can be categorized into centralized and distributed approaches, depending on if there is a central mediator for scheduling or not. What is more, according to whether a control channel is required, they also divide solutions into two parts: control channel free and coexistence approaches requiring a control channel. This section reviews methods of CTI mitigation with these classifications in mind.

2.3.1 General Coexistence Solutions

In view of the fact that LR-WPAN tends to be the victim when coexisting with Wi-Fi, IEEE 802.15.4 based networks have introduced some built-in solutions to address the CTI. In the frequency domain, IEEE802.15.4 employs DSSS (direct sequence spread spectrum) to transmit the signal over additional bandwidth. The DSSS maps 4-bit symbol to a 32-chip symbol that is RF modulated. It acts like redundant coding in the PHY layer to improve perform. In addition, IEEE802.15.4 defines 16 communication channels in 2.4Ghz ISM band and each channel are 5 MHz apart, allowing non-interfering channel plan over LR-

WPAN and Wi-Fi. For some IEEE802.15.4 based network, such as ZigBee [111], the network coordinator is required to scan all the available channels. The channel with the least interference is selected to create the network. In the time domain, IEEE802.15.4 specifies listen-before-talk strategy and limits the PHY data payload at maximum 127 bytes, because a shorter packet can generally reduce the collision possibility. However, as explained in section 2.2, these built-in mechanisms are still inadequate for CTI mitigation.

A great amount of literature suggests solutions in frequency domain that is achieved by changing to a clean channel when interference is detected. Xu et al. [134] claim that a wireless node can detect the interference and retreat from the interference by dynamic channel switching. Moreover, Chen et al. [19] and Cheng and Ho [20] propose and implement multi-channel MAC protocol that dynamically assigns a channel to sensor nodes and improves PDR in a Wi-Fi interference environment. Phunchongharn et al. [92], Vikram and Narayana [120] developed a cross-layer multi-channel MAC protocol, which can predict future interference based on HMM (Hidden Markov Model) and mitigate interference by choosing the channels with minimum interference. They also introduce Hidden Markov Model to predict a channel that has minimum interference. Sahoo et al. [101] propose load-aware channel estimation to assess the possibility of traffic weight assignment before moving to a new channel. To ensure all the node switch to the same channel to communicate, Yun et al. [140] and Musaloiu-E and Terzis [75] adopt a centralized approach and dedicated interference-free channel to delivery channel switch information. The centralized coordinator in [140] checking other channels periodically and notice all the others in the network to switch the channel when sensing interference. However, the new channel may not suit for all the nodes. In order to minimize interference in IEEE 802.15.4 multi-hop WSN, Musaloiu-E and Terzis [75] advise that the scope of channel change can be based on a path. This solution requires all the nodes on the path find the channel with the least interference and later the best channel across the whole path is agreed with the coordinated by the centre gateway. The dedicated interference-free

channel for IEEE 802.15.4 may not be practical and realistic in most case. Thus Nishikori et al. [81] propose a cooperative channel control method for Zigbee and Wi-Fi, in which the Wi-Fi is requested to stop using the channel for a certain period that ZigBee can exchange message to switch to a more appropriate channel together. Different centralized approaches, Pollin et al. [94] design a distributed channel selection algorithms, in which the channel interference is assessed by hearing beacons in a given period. All the nodes run the same algorithm, and they always move to the channel that is next to current channel. The algorithm is simple, but it cannot guarantee that adjacent devices move to the same channel. Zhou et al. [151] address this issue by introducing methods, such as toggle snooping, modified CCA, and receiver ID. Zhou et al. [150] improve the work in [94] by design a middleware for WSN called SAS (Self-Adaptive Spectrum) management. It enables single-frequency MAC protocols with multi-frequency capability and allows existing MAC protocol to automatically adapt to the least congested physical channel at runtime. However, the distributed approaches consumption extra energy to perform environment scanning, and the packet may suffer a long delay because of the channel switching. Moreover, IEEE 802.15.4 has limited channel number in 2.4 GHz band; there may not be enough channels for a retreat from interference. Due to the out-of-band emission, especially when two nodes are close to each other, the Wi-Fi channels with a centre frequency 20MHz away from the IEEE 802.15.4 channel can still cause severe disruption [117].

Spectrum sharing in space domain allows spatial reuse of the frequency spectrum. According to Yang et al. [136], it is impractical to move a wireless sensor frequently, but there is a close relationship between signal power fading and distance. For this reason, space sharing is usually achieved by transmitting power control and receiving power sensitivity (CCA ED threshold). Simulation results in Haron et al. [39] reveal effectiveness for Coexistence. Hauer et al. [40] and Myers et al. [77] conduct experiment and suggest that adaptive TPC (Transmission Power Control) can be helpful for LR-WPAN and Wi-Fi coexistence. Empiri-

cal studies or analytical models in [28, 68] indicate that adaptive TPC generally improves overall performance in terms of communication quality and energy consumption. Vikram and Sahoo [121] improve network efficiency under diverse network conditions by designing interference aware adaptive TPC algorithm. The algorithm performs data communication with consideration of communication features, e.g. interference level, signal strength, node distance and power level. In addition to TPC in the sender side, CCA sensitivity control is another wide studied method. Petrova et al. [91] observe that LR-WPAN can suffer serious interference from Wi-Fi even in non-overlapping channels because the highly sensitive CCA threshold settings in IEEE 802.15.4 nodes. They also suggest that LR-WPAN performance can be improved in the overlapping and non-overlapping channels through adaptive CCA ED threshold according to the interference level.Bertocco et al. [13] provide useful information and hits to optimize CCA settings, in presence of white Gaussian noise interference. Zhen et al. [149] investigate CCA on the coexistence of Wi-Fi and LR-WPAN in 2.4 GHz. Because asymmetric CCA ED thresholds in different wireless technologies can result in unfairness of medium access and reduction of network performance, they define HECR (heterogeneous exclusive CCA range) in which different systems in the heterogeneous environment can reliably sense the transmissions of the other. Different from the work in [149], Yuan et al. [138] propose a decentralized approach by adaptively and distributively adjusting CCA thresholds of LR-WPAN nodes in the presence of heavy interference and the result shows the approach can significantly increase LR-WPAN performance because of the substantial reduction of the amount of discarded packets caused by channel access failure. Furthermore, Sha et al. [103] design AEDP(Adaptive Energy Detection Detection) protocol, which can dynamically adjusts a node's CCA threshold to improve network reliability. In addition to the work of [138, 103], Sparber et al. [110] propose and implement DynCCA approach on a real testbed to minimize the impact of both unintentional and malicious interference. Their experiment shows the algorithm can increase the packet reception rate by up to 50%. However, these

work in space domain require both Wi-Fi and LP-WPAN adopt ED-based CCA approach and under light Wi-Fi traffic. In the cause of carrier-sense based CCA, LR-WPAN still cannot survive under the heavy interference of Wi-Fi [36, 95]. Moreover, the space sharing approaches cannot address the problem of unfairness caused by different CSMA/CA timing parameters [139, 44, 149].

Besides the coexistence in frequency and space domain, there are plenty of studies about spectrum sharing in the time domain. Most time sharing method involves scheudling between victims and interferes [55, 56], or introduce extra hardware or algorithm in MAC to reduce collision probability, e.g. CACCA (coexistence aware CCA) by using extra hardware [119], RTS/CTS protected LR-WPAN transmission[42, 42]. Jung et al. [55] propose UWC-Aided (Ubiquitous Wearable Computer) coexistence algorithm in the overlaid network environment. The algorithm using the Wi-Fi module on UWC nodes to transmit an RTS request to the desired AP that reserve the channel for a specified duration for ZigBee data transmission. In considering of algorithm in [55] require the device has Wi-Fi module available, and it is impractical in most cost, Jung et al. [56] make improvement and introduces a mediation scheme in an overlaid network environment of Wi-Fi and ZigBee by using a centralized interference mediator, which allows two network access medium different time windows to avoid harmful interference. However, the work in [56] is not evaluated by implementation on network simulation platform nor real hardware, it may be changeable to synchronize ZigBee superframe and WLAN PCF(Point Coordination Function) duration because of the feature of the randomness of underlying CSMA/CA packet transmission. For the IEEE 802.15.4 operating in the beacon-enabled mode, ElSawy et al. [30] propose a distributed coexistence method, which checks the surrounding environment and schedules LR-WPAN superframe properly to minimize the mutual interference. Different from the work in [30], [23] try to detect interference by performing CCA at the beginning of the GTS(Guaranteed Time Slots), which enables LR-WPAN nodes to avoid collisions with minimum overhead. However, their

methods may not work when Wi-Fi in on heavy load because server interferes from Wi-Fi may block all the GTS. Hou et al. [42] and Hou et al. [42] suggest using RTS/CTS to reserve Wi-Fi interference-free slot, allowing the LR-WPAN packet to be protected, but it requires each LR-WPAN node to equip a Wi-Fi transceiver. In order to address the timing problem that the CCA process of LR-WPAN is substantially slower than that of the Wi-Fi, similarly, Tytgat et al. [119] equip an LR-WPAN node with a Wi-Fi transceiver and conclude that deploying proposed CACCA on Wi-Fi and ZigBee nodes reduces packet loss by 99.6%. However, it may not be an option to equip a Wi-Fi transceiver on an LR-WPAN node in most cases, because it can ruin the low-power feature of LR-WPAN.

Some researchers study the coexistence from other points of view. For instance, [61, 53, 99] investigate how to use optimized dynamic packet size to improve the network performance and reduce interference, because smaller packets have less chance to conflict with other ongoing packets, while it requires more overhead to send the same amount of data [102]. Zhang and Shin [147] propose CCS (cooperative carrier signalling) mechanism that employs a separate ZigBee node to emit busy tone during the desired ZigBee data transmission. Because Wi-Fi channel has much wide bandwidth, there is always some ZigBee channels that are different from the desired ZigBee data channel, but they can be sensed by Wi-Fi. The busy tone is a ZigBee signal that is scheduled in those channels to enhance the ZigBee's visibility to Wi-Fi without affecting ZigBee data. Their experiment shows that CCS reduces collision between ZigBee and Wi-Fi by 50% in most cases. However, it requires to equip an extra ZigBee transceiver to send busy tone, which can double the energy consumption. In the worst case, if the Wi-Fi CCA works in carrier sense only mode or Wi-Fi get heavy load, LR-WPAN can still get less chance to access the medium and even be blocked by Wi-Fi [36, 139, 44, 149].

2.3.2 Scheduling Algorithms for Cross-Interference Mitigation

In order to harmonize Wi-Fi and LR-WPAN interference, different mechanisms have been proposed to schedule between victims and interferes and allow them access channel in interference-free time window or slot. Zhang and Shin [147] adopt a CCS (cooperative carrier signalling) mechanism to schedule Wi-Fi and ZigBee; this mechanism can also be seen in the work of Zhang and Shin [145]. Fig. 2.11 shows the principle behind CCS. A

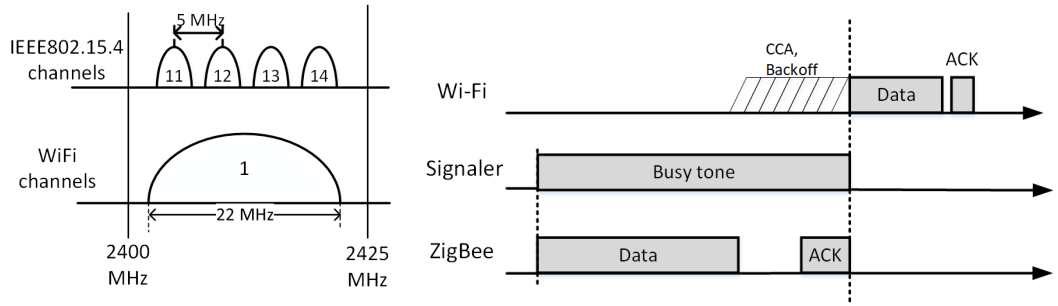

(a) Channels of Wi-Fi and ZigBee

(b) CCS working example

Fig. 2.11 The principle behind CCS

great number of studies have shown ZigBee's performance to be severely interrupted by Wi-Fi because Wi-Fi gets much higher transmission power and fast CCA. CCS employs a additional ZigBee node, called signaler, to emit a high-power busy-tone during the packet transmission, which increases the visibility of ZigBee transmission to Wi-Fi and protect the ZigBee channel from being prompted by Wi-Fi during RX/TX switching. For example, If there is no ZigBee signaler in Fig. 2.11b, the Wi-Fi nodes would transmit data while ZigBee sender is waiting for ACK. Therefore, Collision occurs, and ZigBee would not receive ACK and result in transmission failure. The ZigBee signaler works in a different channel from ZigBee sender; thus, there is no interference between them, while the signaler can be sense be Wi-Fi because each Wi-Fi channel is overlapped with four ZigBee channels as depicted in Fig. 2.11a. They also work on CCS scheduler that employs an algorithm to schedule the signaller in the correct channel and decide the length of busy-tone duration.

Ock et al. [85] improve the work in Zhang and Shin [147] by proposing a simple scheduling algorithm about periodical busy-tone generation and simulation in MATLAB confirms that periodic busy tones enhance the performance of ZigBee transmissions. The signaler is schedule busy tones periodically, irrespective of the ZigBee transmission and ZigBee nodes have no knowledge about when the busy tone is generated. Because ZigBee data and busy tones are not synchronised, ZigBee transmission can occur when in either busy-tone period and off-period. The ZigBee traffic is protected in the busy-tone period, while not in off-period. In considering long busy-tone can significantly reduce Wi-Fi performance, it would be a waste to use a long busy tone all the time. Thus, With the Markov chain model, they analysed the performance of ZigBee systems mathematically and suggested to schedule busy tone dynamically to reduce the impact on Wi-Fi.

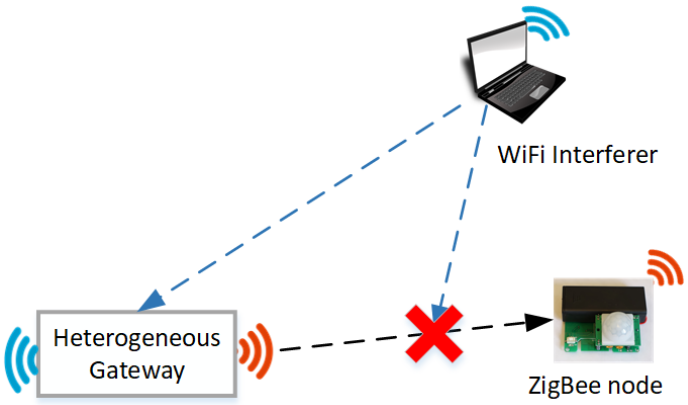

Fig. 2.12 Wi-Fi corrupts ZigBee transmission in the scenario of heterogeneous gateway

An alternative way to schedule LR-WPAN and Wi-Fi is to use RTS/CTS control command in Wi-Fi that is defined in the IEEE 802.11 standard. The basic idea is to RTS/CTS clear Wi-Fi traffic for a period time allowing IEEE 802.15.4 traffic. For example, forcing AP to send out CTS fame will block all 802.11 devices from transmitting for a specified period of time. In a heterogeneous network, CTS can be used for protecting ZigBee transmission [42, 51]. As shown in Fig. 2.12, a laptop may break the ongoing ZigBee transmission from Gateway to ZigBee node in the scenario of a heterogeneous gateway that integrates both

technologies. The conflict can be avoided if the gateway sends out a CTS frame to block surround Wi-Fi devices for a period before transmitting ZigBee messages.

Hou et al. [42] schedule ZigBee and Wi-Fi traffic by using a similar idea in [85], which Periodically block Wi-Fi traffic to allow ZigBee to transmit packets. However, differently, the work in [42] uses a CTS jammer to block Wi-Fi traffic for a 32ms period instead of busy tones. As shown in Fig. 2.13a, ZigBee and Wi-Fi coexist in an area, and Fig. 2.13b depicts the timeline of how CTS block Wi-Fi and allow ZigBee to access the channel without Wi-Fi interference in the CT block period. However, the CTS jammer just schedules CTS messages periodically without aware of Wi-Fi or ZigBee traffic. The algorithm gets the same problem in the work of [85] in which the ZigBee may try to access channel in non-block period and result in a collision. Although the algorithm improves ZigBee performance in their experiments, it can cause a significant drop to the Wi-Fi throughput. In order to not block Wi-Fi when ZigBee does not use the channel, they conduct an experiment in which each ZigBee node is equipped with an Wi-Fi jammer. ZigBee nodes are required to send an CTS message out prior to any ZigBee transmission. They observed that interference drops significantly, as low as 3%. However, this approach has a drawback that it requires an 802.11 transmitter on each ZigBee node.

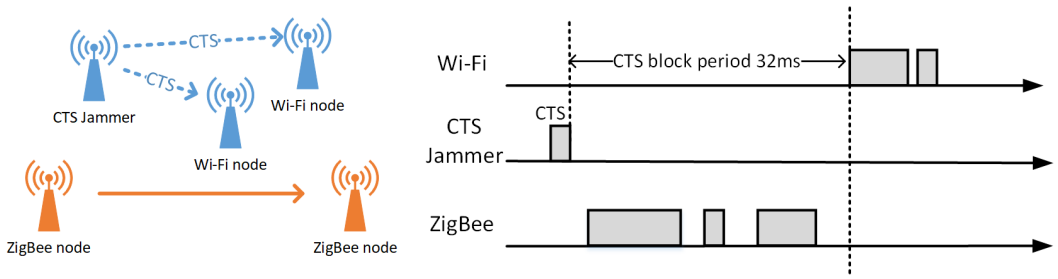

(a) Setup

(b) CTS block Wi-Fi example

Fig. 2.13 Wi-Fi ZigBee scheduling by CTS

Ishida et al. [51] propose a coexistence scheme named AA CTS-blocking (AP-assisted CTS-blocking). Differently, the scheme introduces a helper AP as shown in Fig. 2.14a. The ZigBee network is a single-hop data collection network, where the ZigBee end devices send

data to the coordinator. The coordinator is connected to a laptop that supports Wi-Fi. The laptop does send CTS to block the Wi-Fi traffic. Instead, it sends RTS to a helper AP that has the strongest RSSI. According to IEEE802.11 specification, on receiving RTS frame, the AP sends a CTS frame that blocks all the other Wi-Fi nodes nearby except the laptop. However, the laptop does not send any Wi-Fi packet to allow ZigBee network communication freely. Moreover, they also propose a TDMA-based MAC protocol that enables the end device transmission without the CSMA/CA mechanism as depicted in Fig. 2.14b. Specifically, the coordinator broadcasts a synchronization frame immediately after receiving CTS from helper AP. Each end device sends data to the coordinator in a slot specified by the device ID. However, most of the slot may not be used by end devices if the slot is not well scheduled, which leads to waste of spectrum resource. Furthermore, it may be challengeable for the coordinator to send data to the end device, and the TDMA-based required well-synchronized that may not work for low-power ZigBee nodes.

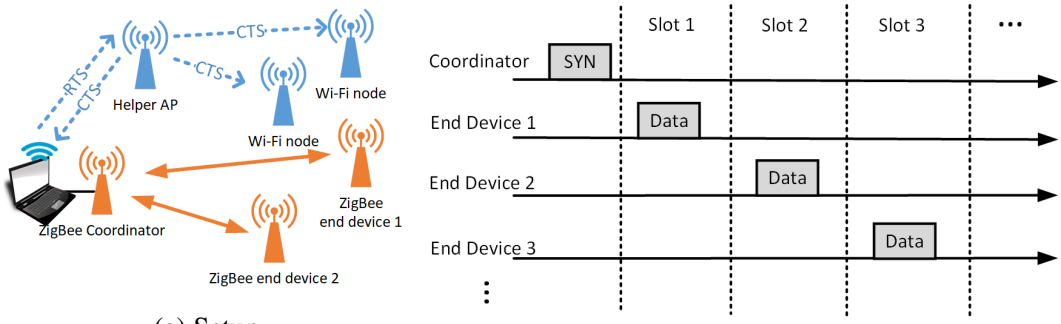

(a) Setup

(b) TDM-based scheduling of ZigBee communication

Fig. 2.14 AP-assisted CTS-blocking for WiFi-ZigBee Coexistence

Jung et al. [56] combine superframes of Wi-Fi and ZigBee, and propose a centralized interference mediation scheme by using an IM (interference mediator). The IM plays an important role as a coordinator that schedules Wi-Fi and ZigBee superframes to allow both networks to access the channel in different time periods, as shown in Fig. 2.15. The main idea is to use Wi-Fi PCF (Point Coordination Function) duration to transmit ZigBee data and

to use the inactive duration of ZigBee to transmit Wi-Fi data. The scheduling works under the assumption that other Wi-Fi nodes do not reserve the PCF duration to transmit. They also indicate that the main concern of the TDMA method is the ratio of time occupancy between Wi-Fi and ZigBee networks. They present two simple, fair schemes, including a time-based fair scheme and a throughput-based fair scheme. The time-based fair scheme is schemed by set the same channel occupancy time for Wi-Fi and ZigBee, while the throughput-based fair scheme tries to achieve the same throughput for both networks. The throughput-based fair scheme requires ZigBee to be allocated much more time to access the channel. Thus the Wi-Fi throughput is reduced to an unusable level. As for the time-based fair scheme, it may be a waste of the spectrum resource if the ratio keeps fixed. For example, The ZigBee network may be idle in some time, while the Wi-Fi network may be on heavy load. It may be better to "borrow" ZigBee duration to Wi-Fi in this case. In order to overcome this shortcoming, Jung et al. [56] further propose per-data transmission time-based fair scheme, which considers the difference between two networks and eliminates the waste of resources in the existing unbalanced channel activities. Their analysis shows the aggregated throughput of the proposed scheme is bigger than the original time-based fair scheme. However, the algorithm requires the number of successful and collided transmission and the time they occupied of both networks in a duration. It is not realistic because gather this kind of information requires to collect statistics from all the nodes in the network, and the central mediator has no knowledge about this information. Moreover, the work in [56] does not consider the network delay. In the real case, ZigBee superframe is designed for the low-power device. Thus the beacon interval can be more than 250s to allow the nodes works in a low duty cycle. If the number of nodes increases in a network, the ZigBee active period can be very long. In other words, the algorithm in [56] may result in long latency of the Wi-Fi network, which leads Wi-Fi unusable.

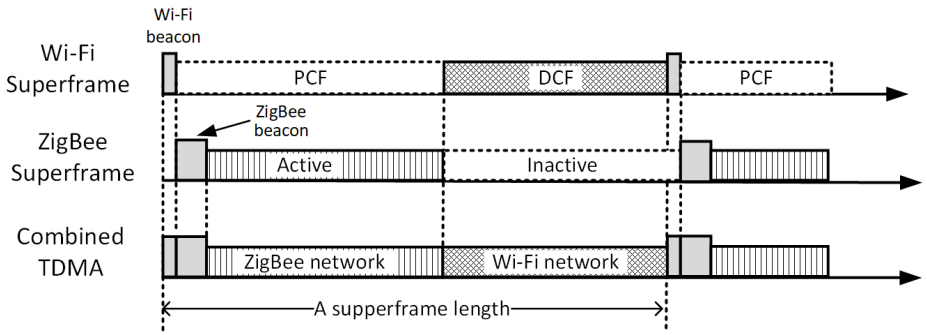

Fig. 2.15 TDMA-based superframe structure for interference mediation

2.4 Summary

Various wireless networks share the same frequency band, which lead to unavoidable interference. Many wireless technologies operate in the crowded 2.4GHz band, e.g., Wi-Fi, ZigBee, Bluetooth, ZWAVE, Thread, Rime. Most of them enable a MAC, which effectively avoids interference when only one wireless technology presents in a particular area. Wi-Fi and IEEE 802.15.4 both employ CSMA/CA mechanism in their MAC layer. However, the CSMA/CA mechanism is powerless when facing CTI between Wi-Fi and IEEE 802.15.4, because of asymmetric transmission power, incompatible CCA and different timing parameters. Plenty of studies have shown that Wi-Fi always has higher priority to access the wireless medium and even block LR-WPAN transmission in the worst case.

Most literature investigates the Cross interference between overlapping channels. However, the non-overlapping channel interference should be taken into consideration, especially when Wi-Fi and IEEE 802.15.4 nodes are close to each other. The CTI from LR-WPAN to Wi-Fi can be ignored in most cases, but LR-WPAN network performance is excessively interrupted by Wi-Fi network.

When it comes to Interference mitigation, the most popular ways are channel switching and power adjusting. However, the total channel number is limited, and there may be no extra channels to perform channel switching. Especially when two kinds of wireless nodes are near each other, the channel switching is possible to become useless due to non-overlapping

interference. Power adjusting does not suit for the heterogeneous network of Wi-Fi and LR-WPAN, where the power adjusting to avoid interference is not efficient due to their large transmission difference. WISE provides a model to improve LR-WPAN performance under Wi-Fi interference, but it is under the assumption of low Wi-Fi traffic and lack of resource scheduling between Wi-Fi and LR-WPAN. Thus it does not suit for heavy Wi-Fi traffic.

Some researchers work on the scheduling algorithms to address cross-interference mitigation. The work in [147] adopts a high-power busy tone during the ZigBee transmission, which can effectively resolve part of coexistence issues, but it can still be blocked by heavy Wi-Fi traffic because of slow CCA of ZigBee. Ock et al. [85] present a simple scheduling algorithm by periodically emitting busy-tone. Because ZigBee data and busy tones are not synchronized, it is not efficient enough. Moreover, fixed duration of long busy-tone significantly reduces Wi-Fi performance. By employing the RTS/CTS control frame in Wi-Fi, there are some scheduling algorithms designed to guarantee LR-WPAN traffic. The CTS blocking mechanism is effectively, but it is not realistic because an extra Wi-Fi module is required to be equipped on each low-power LR-WPAN node. Ishida et al. [51] propose a coexistence scheme named AA CTS-blocking. The TDMA-based MAC protocol that enables the end device transmission without the CSMA/CA mechanism and improves Zigbee performance significantly. However, most allocated ZigBee slots may not be used, result in waste of spectrum resource and reduce Wi-Fi performance. Their TDMA-based required well-synchronized that does not work for low-power ZigBee nodes. Jung et al. [56] combine superframes of Wi-Fi and ZigBee, and design a centralized interference mediation scheme. Their per-data transmission time-based fair scheme eliminates the waste of resources in the existing unbalanced channel activities and effective avoid harmful CTI by analysis. However, the algorithm is not realistic because it requires some statistics that the mediator does not know in the real case. Moreover, they do not consider the network delay, and the algorithm may result in long latency for a Wi-Fi network, which leads Wi-Fi unusable.

The thesis presents a novel centralized scheduling mechanism in the time domain to harmonize coexistence of Wi-Fi and LR-WPAN, also refer to as time-slot based scheduling mechanism. The thesis considers a scenario where a centralized heterogeneous gateway is required, in which Wi-Fi and LR-WPAN nodes are closely embedded into a gateway. In this case, the non-overlapping CTI cannot be ignored; thus, most literatures cannot directly apply. Different from other studies, the scheduling mechanism is achieved by introducing a new command frame, named Access Notification (AN), into the IEEE802.15.4 Medium Access Control (MAC) layer. Compared with idea of high-power busy tone [147] and superframes [56], the proposed mechanism does not require occupying extra channels and enable more flexible and advanced control on the LR-WPAN communication. Together with Wi-Fi CTS command frame, Wi-Fi and LR-WPAN traffic can be scheduled in a synchronized manner. Based on this mechanism, a static time-slot based scheduling algorithm is designed and evaluated on both real hardware-based system and NS-3 simulator. The result shows the algorithm improves LR-WPAN Packet Loss Rate (PLR) significantly, but at the cost of reducing Wi-Fi throughput. The proposed algorithm is able to achieve shorter message latency than medication scheme suggested by Jung et al. [56]. The static algorithm allocates Wi-Fi and LR-WPAN at fixed interval, resulting in low channel efficiency. To address this issue, the thesis proposes and defines a concept of slot-based congestion indicator (CI) to tell whether an allocated time slot is adequate for data transmission or not in an allocated time slot. The CI is able to indicates crowdedness of a network that enables adaptive allocation of the time slot. Based on the CI, an adaptive time-slot based scheduling algorithm is proposed. The evaluation shows that the adaptive algorithm covers the shortage of the static algorithm and offers a distinct improvement on LR-WPAN Packet Transmission Rate (PTR).

Chapter 3

Experimental Study and Overall System Architecture Design

This chapter includes three sections. The experiment in the first section reveals the seriousness of the cross-technology interference based on a heterogeneous gateway, in which ZigBee coordinator and Wi-Fi AP are integrated very close to each other. Following, overall system design is described by explaining application scenario, design features and challenges. The last section discusses and explains the time-slot based scheduling mechanism in detail, in terms of the new introduced AN frame, time-slot design and scheduling overhead.

3.1 Experimental Study of CTI between Wi-Fi and ZigBee

Due to ZigBee is widely adopted as a network layer on top of IEEE 802.15.4 (LR-WPAN) MAC, the ZigBee is chosen to do research about cross-technology interference between Wi-Fi and LR-WPAN in this section. Some basic experiments were conducted to get first-hand statistics about cross-interference between ZigBee and Wi-Fi, including (a) ZigBee PLR (Packet Lost Rate) versus AP Transmission Power and Wi-Fi Traffic Speed, (b) ZigBee PLR versus ZigBee Channel Shifting and (c) ZigBee PLR versus Antenna Distance and Direction.

3.1.1 Experiment Setup

In our experiment, we investigate Wi-Fi and ZigBee coexistence interference in a scenario where Wi-Fi and LR-WPAN radio modules are integrated into the small box to form a heterogeneous gateway. A gateway is designed as shown in Fig. 3.1. Based on this real hardware, we setup testbed to get first-hand statistics about cross-technology interference between ZigBee and Wi-Fi. The gateway consists of three parts, including (A) an AP module, (B) a ZigBee module and (C) an Ethernet port. The AP module is based on an Atheros AR9331 chip, which is a Wi-Fi System-On-Chip (WiSoC) with a MIPS 24Kc @400MHz CPU [9] and support 802.11b/g/n at 2.4 GHz band. The ZigBee module (also is IEEE 802.15.4 radio module), as a ZigBee coordinator, is designed based on CC2530 MCU [49]. Both ZigBee and Wi-Fi adopts a monopole PCB antenna. The ZigBee coordinator is 10 cm away from the AP module.

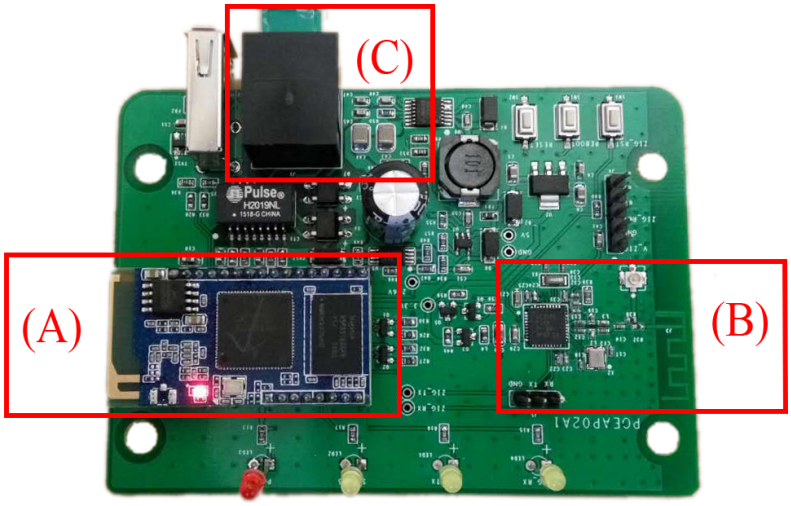

Fig. 3.1 the gateway PCB layout

As shown in Fig. 3.2, a laptop and a ZigBee node are connected to the gateway. Both the laptop and the ZigBee node are two meters away from the gateway. A desktop is connected to the gateway through Ethernet port. The desktop runs an iperf3 server, and the laptop runs iperf3 client. The client generates Wi-Fi traffic at maximum rate and exchanges data with the

server. A ZigBee program is designed in such a way that it allows the ZigBee node generates ZigBee packets and sends to the gateway. The gateway counts the number of the correct messages received. Then ZigBee Packet Loss Rate (PLR) can be calculated.

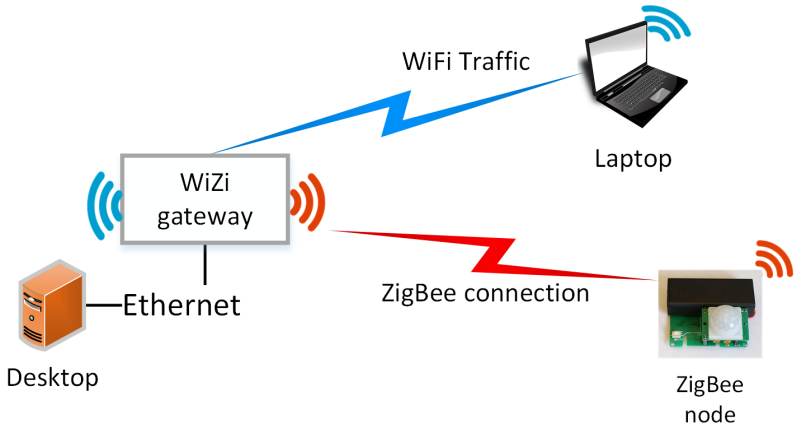

Fig. 3.2 Experiment topology

Due to most studies has shown that the impact from ZigBee to Wi-Fi is negligible, so we mainly concerned about ZigBee performance in this experiment. Instead, we will mainly focus on the interference from Wi-Fi to ZigBee by analysing ZigBee PLR. During experiments, the ZigBee node sends out packets with sequence number every 32ms. The number of the packets is set to be 1000 packets for each run. To get reliable results, each data point is measured for three runs. In order to evaluate ZigBee network performance under Wi-Fi interference in the gateway scenario, ZigBee PLR is measured by adjusting AP power, changing Wi-Fi traffic, shifting ZigBee channels, adjusting ZigBee antenna direction and antenna distance of Wi-Fi and ZigBee.

3.1.2 ZigBee PLR versus AP Transmission Power and Wi-Fi Traffic Speed

This experiment is conducted to evaluate ZigBee performance with overlapping channel interference. Specifically, ZigBee nodes operate in ZigBee channel 11 and AP is in Wi-Fi channel 1. By changing AP transmission power and Wi-Fi traffic speed, Fig. 3.3 is acquired.

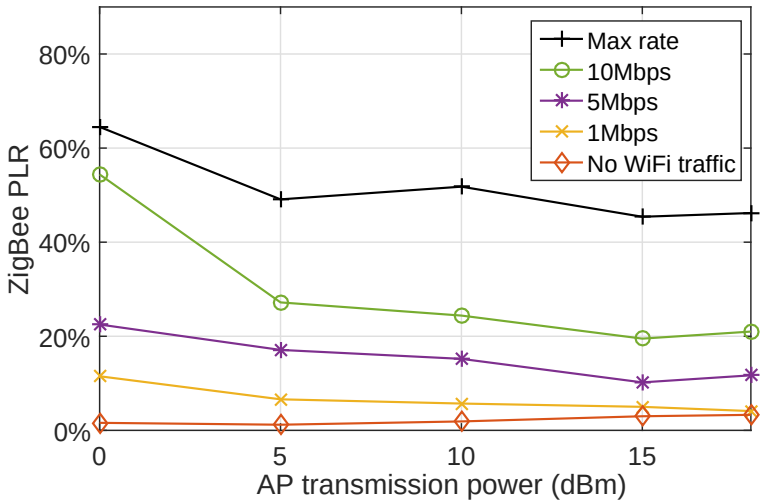

Fig. 3.3 ZigBee PLR versus AP transmission power and Wi-Fi traffic speed

Four curves are acquired when transmitting Wi-Fi data at a different rate. Without Wi-Fi traffic, the ZigBee network keeps at very low PLR, indicating high network performance. When the AP transmission power keeps fixed, the ZigBee PLR goes up when Wi-Fi traffic increases. For example, if the AP transmission power is 0dBm, the worst ZigBee network performance is observed at high PLR 64.5%. Thus, as expected, the ZigBee network performance is reduced as the increase in Wi-Fi traffic, because more Wi-Fi traffic introduces more cross-technology interference. In consideration of short CCA time and frame-in-air time, the Wi-Fi traffic is able to preempt ongoing ZigBee transmission. In addition, the short Wi-Fi-ZigBee distance makes the problem more serious.

The graph shows a common trend that PLR slightly drops as the increase of AP transmission power. In other words, ZigBee network performs better as the increase of AP trans-

mission power, which is in contrast to the intuitive understanding of wireless interference. Actually, there are some studies [40, 77] that minimize the interference by reducing transmission power. Nevertheless, the experiment in this thesis reveals a different phenomenon in which reducing AP transmission power cannot reduce interference in the presented application scenario. This can be explained by the difference between the application scenarios. In consideration of the short distance between Wi-Fi AP and ZigBee, even though AP reduces its transmission power to 0 dBm, its power is still high enough to interrupt ZigBee communication. Reducing AP power can increase Wi-Fi frame error and trigger the retransmission mechanism that results in more spectrum resource usage and more interference when over a poorer channel; then more interference is introduced.

In summary, this experiment shows that interference can be reduced by transmitting less Wi-Fi data, but a low AP transmission power is not helpful for ZigBee performance improvement in the gateway scenario.

3.1.3 ZigBee PLR versus ZigBee Channel Shifting

This experiment aims to evaluate ZigBee performance by shifting ZigBee channels. Specifically, AP is fixed at channel one, and ZigBee channel is shifted from 11 to 19. During the experiment, we cover both overlapping and non-overlapping cross interference analysis: (1) ZigBee channel 11 to 14 are overlapped with AP channel 1; (2) ZigBee channel 15 to 19 are not overlapped with AP channel 1. By considering two situations, with maximum Wi-Fi traffic and without Wi-Fi traffic, Fig. 3.4 is acquired. As shown in the diagram, the curve without Wi-Fi traffic shows that the ZigBee network has low PLR and high network performance over all the tested channels, which plays a role of a reference curve when analyzing the ZigBee network performance. With Wi-Fi traffic, however, ZigBee PLR increases up to 50% over a wide ZigBee channel distribution. In particular, this cover can be interpreted into two segments: (1) in overlapping channels where ZigBee PLR just keeps high and (2) in

non-overlapping channels where the PLR goes down from 47.3% to 16.7% as the channel shifts from 15 to 19. This result shows that the non-overlapping cross interference cannot be negligible, especially when the channel distance is not so far. For example, Wi-Fi channel 1 occupy spectrum over 2401MHz to 2423MHz, while ZigBee channel 16 occupy spectrum over 2427.5MHz to 2432.5MHz. It is clear that no frequent overlaps between these two channels. Compared with the experiment result, however, the Wi-Fi traffic in channel 1 affects ZigBee channel 16 seriously.

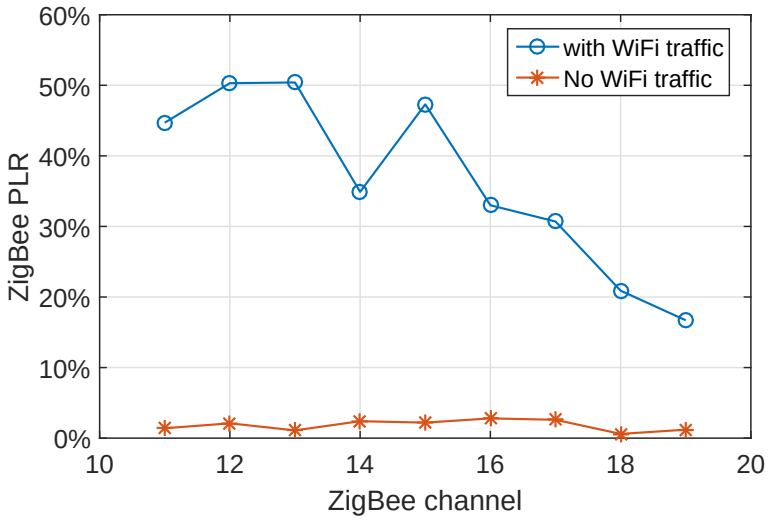

Fig. 3.4 ZigBee PLR versus ZigBee channel shifting

In some research, non-overlapping channels are allocated to Wi-Fi and ZigBee networks aims to eliminate the cross interference without considering non-overlapping channel interference, but we argue that channel allocation algorithm may not be efficient in heterogeneous gateway scenario where the ZigBee and Wi-Fi module are designed to be close to each other.

3.1.4 ZigBee PLR versus Antenna Distance and Direction

This experiment evaluates the ZigBee performance by considering the antenna distance of ZigBee and Wi-Fi modules as well as the antenna direction of the Wi-Fi module. In this experiment, Wi-Fi nodes are equipped with inverted-F PCB antenna, while Zigbee adopts

meander line PCB antenna. Both types of antennas are omnidirectional monopole antennas. As shown in Fig. 3.5, during the experiment, the Wi-Fi AP is separated from the gateway and slowly moved away from the ZigBee coordinator (ZigBee receiver). Because the research is under heterogeneous gateway scenario, the antenna should not be too far, e.g., within 80 cm. The ZigBee transmitter and ZigBee receiver stay fixed and keep two meters away from each other. In order to get general results, we test five antenna directions of the AP: four antenna directions (labelled by 0 to 90 degree) that stay on the same plane of ZigBee antenna and one direction that is orthogonal to the ZigBee antenna.

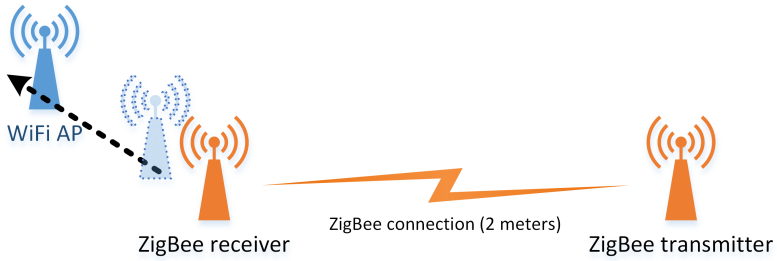

Fig. 3.5 Experiment method

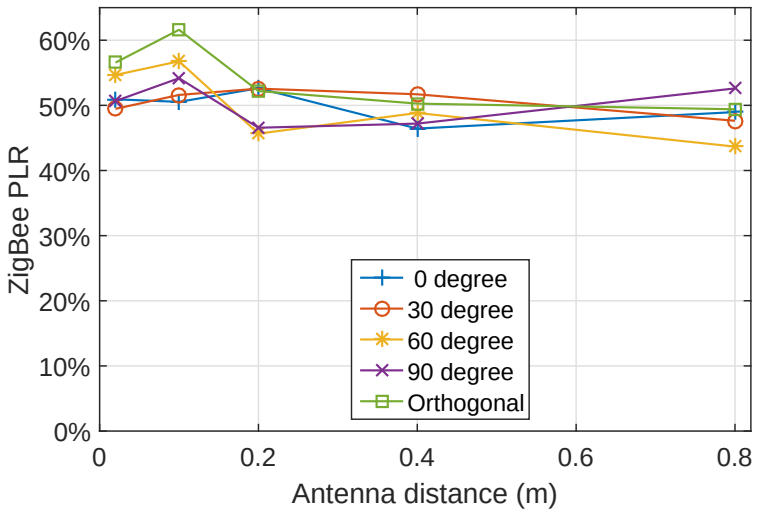

Fig. 3.6 ZigBee PLR in overlapping channels

By measuring ZigBee PLR on both overlapping channels (ZigBee channel 11 and AP channel 1) and non-overlapping channels (ZigBee channel 16 and AP channel 1), Fig. 3.6

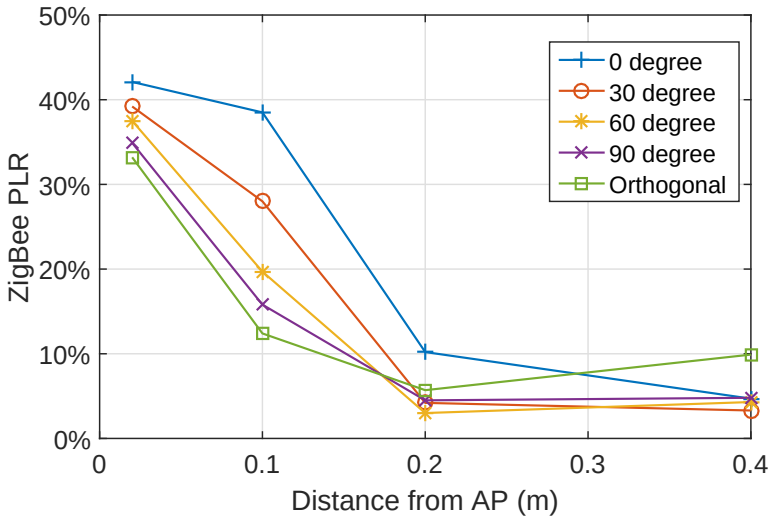

Fig. 3.7 ZigBee PLR in non-overlapping channels

and Fig. 3.7 are acquired. These two figures show different patterns. In Fig. 3.6, the ZigBee channel overlaps with the AP channel, and the ZigBee PLR keeps around 50%. There is not obviously performance improvement when changing antenna distance or adjusting the AP antenna direction. When it comes to Fig. 3.7, which is measured with non-overlapping ZigBee and Wi-Fi channels, the curves show obvious trends over antenna distance and AP antenna directions. Firstly, each curve has a common trend that ZigBee PLR reduces along with the increase of the antenna distance between Wi-Fi and ZigBee modules. When the antenna distance is not more than 20 cm, changing AP antenna directions also help to improve ZigBee network performance. For example, if the antenna distance is 10 cm when AP's antenna is orthogonal to ZigBee's, we get the best ZigBee performance at PLR 12.4%, which is hugely better than the case where AP antenna direction is 0 degree to ZigBee's, give a poorer performance at PLR 38.5%. An explanation is that the antennas are not perfectly omnidirectional. Further research on the antenna is beyond the scope of this thesis. The experiment also shows that the antenna distance is the most significant factor that gives rise to the interference over the non-overlap adjacent channel. When the distance greater than 20

cm, the experiment indicates an acceptable ZigBee PLR at around 10%. Due to the small size of the gateway, however, it is not practical to have the antenna distance more than 20 cm.

3.1.5 Conclusion

The experiment in this section reveals the seriousness of the cross-technology interference based on one heterogeneous gateway, in which ZigBee coordinator and Wi-Fi AP are integrated very close to each other. Due to the short antenna distance between ZigBee and Wi-Fi modules, we observe some interference phenomenon that is not intuitive. For example, the ZigBee PLR unexpectedly goes up as AP transmission power reduces, indicating that lowering AP power is not good for ZigBee packet transmission. A reasonable explanation for this is that the lower AP transmission power actually causes more retransmission at the same throughput. Consequently, the channel became even crowded and leas worse ZigBee performance. What is more, the non-overlapping channel interference becomes so significant that researchers must take it into consideration. Many existing studies aim to mitigate cross-technology interference by adaptive transmission power control or dynamic channel switching, but these approaches will not be effective in such kind of real-life environment. The last experiment confirms that the non-overlapping channel interference mainly comes from the short antenna distance. Moreover, adjusting the AP antenna direction also helps to improve ZigBee network performance. Thus, we suggest increasing the antenna distance and adjusting antenna direction when designing a heterogeneous gateway to achieve better network performance. However, it still has a limitation, because a practical gateway tends to be small, and there is not enough room to separate the transmitters far away from each other. The experiments on CTI indicates that ZigBee channel switching and AP radio power adjusting are not an effective way to mitigate the interference from Wi-Fi in the scenario of short ZigBee-Wi-Fi distance. Thus, we need to develop new mechanisms to address the coexistence problem between ZigBee and Wi-Fi. Because the gateway provides a platform

integrating Wi-Fi and ZigBee, it is possible to do time-slot based resource scheduling to eliminate interference and guarantee network performance. In the following sections, a novel centralized scheduling mechanism in the time domain are proposed.

3.2 Overall System Design

3.2.1 Application Scenario

This thesis focuses on an application scenario as shown in Fig.3.8. The network includes a heterogeneous gateway, some Wi-Fi nodes and LR-WPAN nodes. The gateway, as a central point of the network, integrates a Wi-Fi AP and LR-WPAN coordinator. It does not only provides data service for LR-WPAN and Wi-Fi but also schedules both network communication and mitigate harmful CTI. Therefore, we call the network as CIM-HetNet (Cross-Interference Mitigation Heterogeneous Network), and the gateway is named CIM-HetNet gateway.

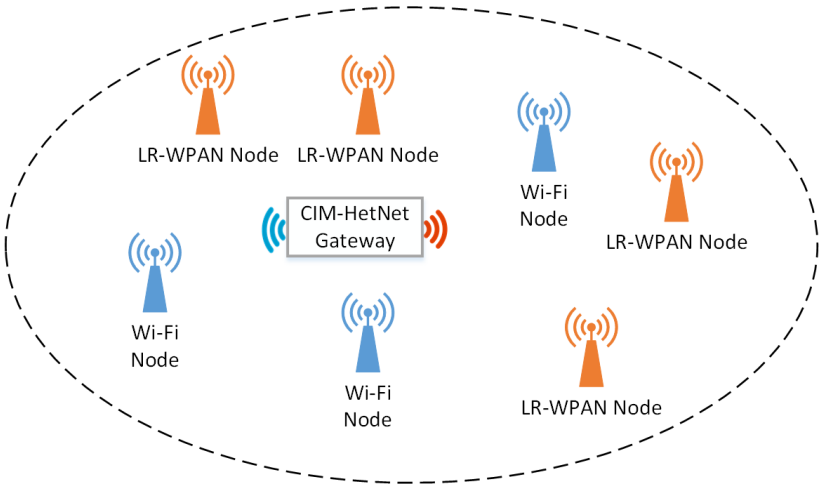

Fig. 3.8 Application scenario: single gateway

Sometimes, large area coverage is required. For example, there is an increasing demand for both Wi-Fi and LR-WPAN available in the public area, such as airports, shopping malls, universities and so on. The LR-WPAN is mainly used for low-power sensors while Wi-Fi

can be used for some high throughput application. In this case, CIM-HetNet can be planed in a dedicated way that each different CIM-HetNet work in non-interference channels. For example, Fig. 3.9 shows a simple example of channel planning for two CIM-HetNet gateway. IEEE 802.11 specifies three non-overlapping channels and plenty of studies have investigated how to make a dedicated channel plan to cover a large area, which is out the scope of this thesis.

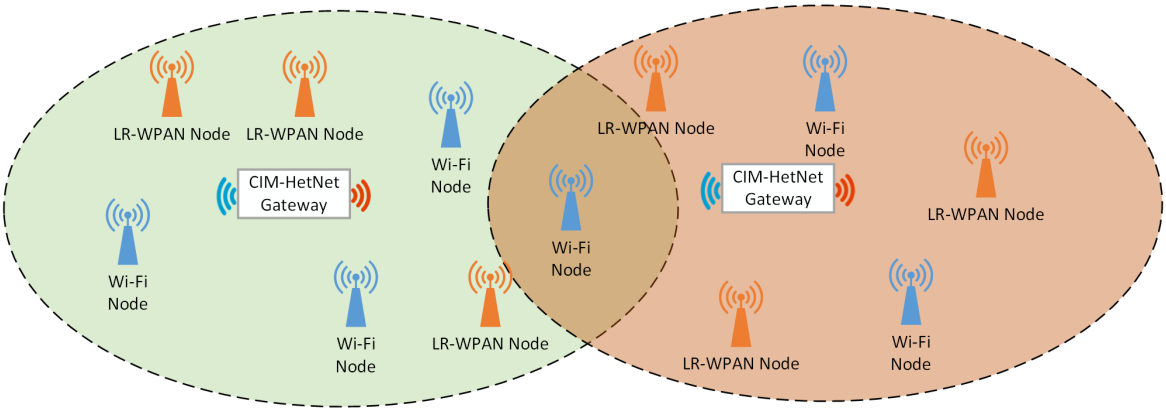

Fig. 3.9 Application scenario: large area coverage

3.2.2 Design Features

The thesis aims to propose a coexistence mechanism to harmonize Wi-Fi and LR-WPAN networks. As depicted in Fig. 3.10, the proposed CIM-HetNet MAC includes three key components, including CIM-HetNet scheduler, Wi-Fi MAC and LR-WPAN MAC. The CIM-HetNet scheduler sits on top of the both MAC layer to take charge of scheduling tasks. In the design, the channel is accessed in a time-slot manner that Wi-Fi and LR-WPAN are scheduled to access channel at different time duration without CTI as shown in Fig. 3.11. This is achieved by periodically blocking and activating of Wi-Fi and LR-WPAN. In a time slot, multiple nodes may access medium by using the CSMA/CA algorithm. Ideally, both networks are well synchronized that the Wi-Fi is activated while the LR-WPAN is blacked, and vies versa. Because there is not a standard way available to schedule these two networks,

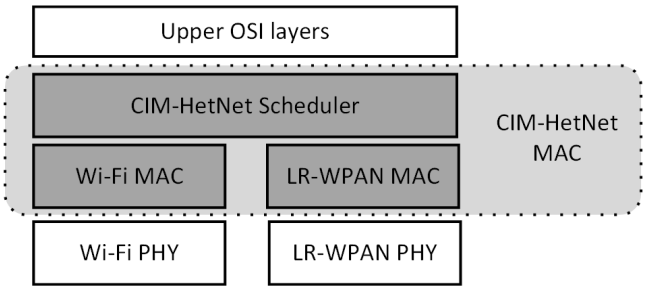

Fig. 3.10 CIM-HetNet MAC

modification and extension in the MAC layer of a gateway are required to enable scheduling mechanisms. For example, a new MAC command frame in LR-MAC is designed in our research to notify LR-WPAN nodes the status of the coexistence.

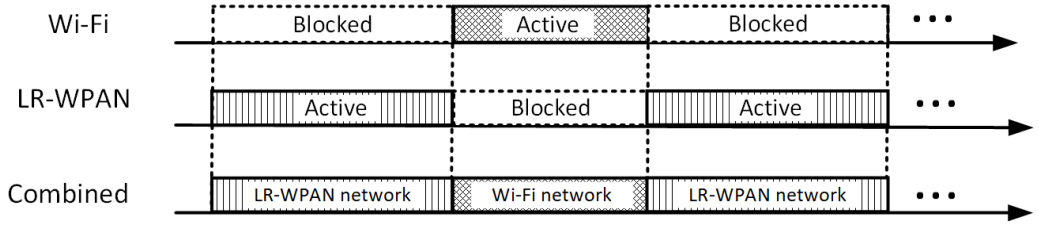

Fig. 3.11 time-slot based scheduling for coexistence of Wi-Fi and LR-WPAN

The system gets features:

- The mechanism is designed as a MAC layer functionality (IEEE 802.15.4 and IEEE 802.11) rather than for specific network technology, e.g., ZigBee, Rime or Contiki-6LoWPAN. Thus, the coexistence mechanism can be generally applied in most of the LR-WPAN networks. The mechanism is achieved by introducing a new MAC command frame into both LR-WPAN coordinators and end nodes.

- The mechanism scheduling Wi-Fi and LR-WPAN traffic in the time domain, in a centralized slot-based manner. It acts as a high-level TDMA on top of the CSMA/CA instead of replacing standard CSMA/CA. Therefore, the end nodes that use standard MAC may not have optimal network performance, but can still work with the gateway.

- It does not require any hardware or software modification on Wi-Fi stations. Because Wi-Fi stations, e.g., smartphones, laptops and tablet PCs, are owned by different individuals. It is impractical to apply modification on all of these devices.
- Wi-Fi AP and LR-WPAN coordinator are integrated into one box for easy deployment.

3.2.3 Challenges

Designing an effective time-slot based scheduling mechanism over Wi-Fi and LR-WPAN network can be challenging because these networks are designed for completely different applications and have distinctive features. For example, Wi-Fi is high-throughput and low-latency that is critical for applications like VoIP and video stream, but is power-hungry. LR-WPAN tends to be slow and not sensitive to latency, but the low power features enable it to be extensively popular for sensors. Therefore, application differences needs to be considered when designing a scheduling scheme.

The first challenge is how to schedule the nodes. In a Wi-Fi network, sending a CTS frame can block Wi-Fi communication for a short period. By repeating this process periodically, we can manage Wi-Fi to access medium in a specific time slot. In other words, it schedules Wi-Fi nodes to access medium, and it can be a promising method to synchronize Wi-Fi communication. In an LR-WPAN network, there is IEEE 802.15.4 superframe available. However, as explained in the literature review, the long interval time of superframe lead to Wi-Fi not usable. Moreover, the superframes often have a big frame size, which results in high scheduling overhead. Therefore, there is not a proper scheme available to schedule the LR-WPAN node.

Another challenge is the synchronization of scheduling. A perfectly synchronized scheduling should work as demonstrated in Fig. 3.11, in which the end of one network's time period is exactly the start of the others. In proposed design, the CIM-HetNet scheduler mediates the network by broadcast controlling frame in the MAC layer to block or activate a network.

Nevertheless, CSMA/CA has a random backoff feature. therefore, the controlling frame is unlikely to be transmitted immediately, and random delay for scheduling is applied. Fig. 3.12 shows a case where the scheduling is not well synchronized. Specifically, the LR-WPAN is scheduled falls behind Wi-Fi. It is easy to observe that some time is wasted because both Wi-Fi and LR-WPAN are blocked. In some duration, Wi-Fi and LR-WPAN coexist, incinerating that harmful CTI may occur. The situation in the real case can be even more complex because the transmitting delay of a controlling frame is completely random and cannot be anticipated.

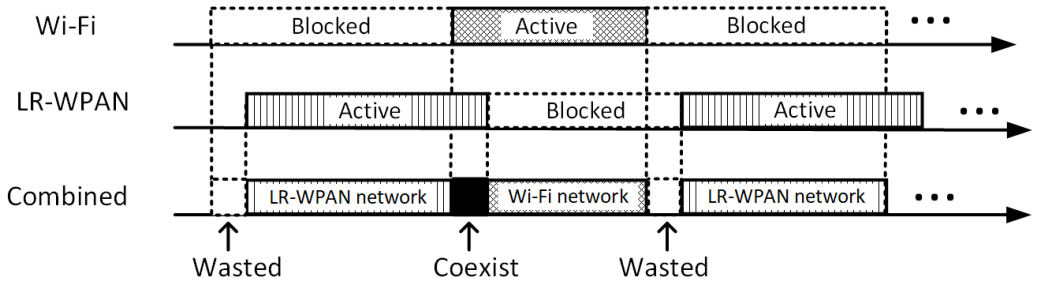

Fig. 3.12 time-slot based scheduling: a case of not well synchronized scheduling

The third challenge is that the scheduling overhead needs to be low. In order to schedule both networks, CIM-HetNet gateway has to broadcast some beacon-like packets to allocate slot-length in real-time. Transmitting these packets requires additional wireless channel time that is the scheduling overhead. The work in [56] employs Wi-Fi and LR-WPAN superframes as a scheduling scheme. However, the length of a superframe tends to be very long because it includes lots of information that is not used for scheduling. Long packet requires more time to transmit, and the real-time scheduling repeats at high frequency can result in high scheduling overhead.

Finally, it is challengeable to deal with different features of Wi-Fi and LR-WPAN. For instance, Wi-Fi is latency-sensitive while LR-WPAN is not. Thus, LR-WPAN slot can not be too long, or it can result in severe Wi-Fi packet latency, and the Wi-Fi-related application

Table 3.1 Wi-Fi and IEEE 802.15.4 frame comparison

	Wi-Fi (54Mbps) frame length		IEEE802.15.4 (256kbps) frame length	
	MSDU(Bytes)	Frame-in-air time(μs)	MSCU(Bytes)	Frame-in-air time(μs)
Maximum Frame	2358	349	114	4256
medium Frame	1000	148	30	1568
Minimum Frame	0	28	0	512

like VoIP recommends a maximum of a 150 ms one-way latency. What is more, Wi-Fi tends to be high-throughput, while LR-WPAN usually light traffic. It is important to consider that slots in Wi-Fi should be longer than LR-WPAN in most case. Therefore, the maximum slot duration for Wi-Fi and LR-WPAN should be different. As shown in Table 3.1, it may need to be aware of the different frame-in-air time when deciding the minimum slot duration, because an LR-WPAN packet generally take more time to transmit compared to Wi-Fi.

3.3 Time-slot based Scheduling Mechanism

This section proposes a time-slot based scheduling mechanism over Wi-Fi and LR-WPAN with the consideration of different network features. In Wi-Fi network, there is RTS/CTS command frame that can be used for scheduling active and blocked periods. However, the LR-WPAN network does not provide a proper way for this purpose. Thus, we introduce a new command frame, name Access Notification (AN), into IEEE 802.15.4 MAC. Base on proposed AN command frame, a time-slot based scheduling mechanism is presented with the features of low scheduling overhead, optimized synchronization of scheduling and low Wi-Fi latency.

3.3.1 Access Notification For LR-WPAN

This section first explains why the superframe in LR-WPAN is not a proper command frame for time-slot based scheduling. Then AN frame format is presented.

IEEE 802.15.4 superframe

IEEE 802.15.4 can operate MAC in two modes: non-beacon mode and beacon-enabled mode. Non-beacon mode follows CSMA/CA MAC. Beacon-enabled mode divides channel time into an active period and an optional inactive period, as shown in Fig. 3.13. An active period includes Content-Access Period (CAP) and Content-Free period (CFP). In CAP, nodes follow CSMA/CA and access medium. In CFP, the Guaranteed Time Slot (GTS) are allocated to specific devices, and the devices access medium directly without CSMA/CA. The active period and inactive period can be managed by setting Superframe Duration (SD) and Beacon Interval (BI).

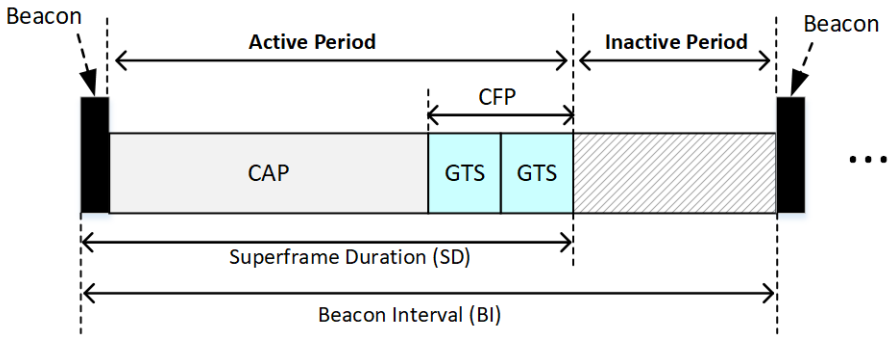

Fig. 3.13 IEEE 802.15.4 Superframe

It appears that the superframe can be used for scheduling masochism over Wi-Fi and LR-WPAN. Nevertheless, it has three main problems:

- Long active period. The minimum SD is 15.36ms [34, 64], and this number can increase dramatically if LR-WPAN needs to transmit more data. Because the Wi-Fi needs to be blocked in the LR-WPAN active period, it can cause long latency for the Wi-Fi network.

- Long packet size. The packet size of a superframe is often large, which can result in high scheduling overhead.

- Low granularity for period settings. The active period and inactive period can be managed by setting Superframe Duration (SD) and Beacon Interval (BI). The SD and BI is get from *macBeaconOrder* (BO) and *macSuperframeOrder* (SO), where $0 leq SO leq BO leq 14$. They have relations of $SD = aBaseSuperframeDuration \times 2^{BO}$ and $BI = aBaseSuperframeDuration \times 2^{SO}$, where *aBaseSuperframeDuration* corresponds to 960 symbols, corresponding to a duration of 15.36 ms, considering a bit rate of 250 kbps, frequency band of 2.4 GHz. Therefore, the possible period settings increase exponentially, such as 15.36ms, 30.72ms, 61.44ms, 122.88ms, 245.76ms and so on. If employing a CTS frame to block Wi-Fi traffic, the longest duration is 32.767ms, which does not allow a long LR-WPAN period. Therefore, we have only two period options: 15.36ms and 30.72ms. This granularity of the period is too low for an adaptive slot-based scheduling logarithm.

In summary, the superframe in LR-WPAN is not a proper command frame for time-slot based scheduling.

Introducing a New Command Frame

According to [34], four frame types are specified, including Beacon frame, Data frame, ACK frame and MAC command frame. Fig. 3.14 depicts a general MAC command frame format. The command frame is defined in MAC layer with a MAC Header (MHR) where frame type subfield in Frame Control Field (FCF) is set to "3", indicating frame type is a MAC command.

IEEE 802.15.4 has nine command frame types, as shown in Table 3.2 with command frame identifier from 0x01 to 0x09. The command frame with identifier 0x0a is not defined in IEEE 802.15.4. Thus, we use this identifier for our newly introduced command frame, AN frame, to achieve flexible time-slot management. An FFD shall be capable of transmitting and receiving all command frame types, with the exception of the GTS request command.

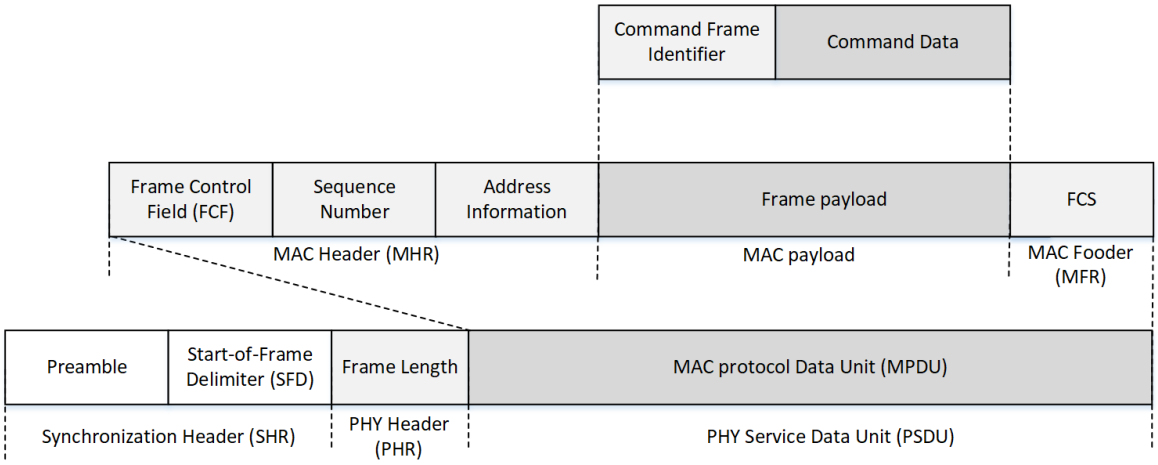

Fig. 3.14 IEEE 802.15.4 MAC command frame format

As for an RFD device, some MAC command is not supported. The table gives the what command an RFD device should include, which is indicated by an "X" in the table. For example, an RFD can not send but is able to receive an AN frame.

Table 3.2 IEEE 802.15.4 MAC Command Frames

Command frame identifier	Command name	RFD	
		Tx [a]	Rx [b]
0x01	Association response	X	
0x02	Association request		X
0x03	Disassociation notification	X	
0x04	Data request	X	
0x05	PAN ID conflict notification	X	
0x06	Orphan notification	X	
0x07	Beacon request		
0x08	Coordinator realignment		
0x09	GTS request		
0x0a [c]	**Access notification**		**X**

[a] If a RFD can transmit a specific command frame
[b] If a RFD can receive a specific command frame
[c] New introduced command frame in our thesis

Access Notification Format

The detail AN frame format as in Table 3.3. It is important to know that Guaranteed period (GP) and Suppressed Period (SP) have different maximum values. For example, the LR-WPAN CTI-free (Cross-Technology-Interference-free) period can only be guarantee within maximum Wi-Fi block period. Thus we design the maximum time duration for GP is 32.64, which is almost the same as the maximum CTS block period (32.767ms) in Wi-Fi. Because LR-WPAN can accept long latency and the network traffic tends to be lighter than Wi-Fi, LR-WPAN can be in an inactive period for a long time to allow longer scheduling duration and lower scheduling overhead. In other words, the Maximum SP should be larger than GP, as designed in this thesis.

- MHR field: the MHR field includes many subfields and the detail setting for this field will be described in detail later.
- Command Frame Identifier: this field is always 0x0a to differentiate from other MAC command frame.
- Guaranteed Period Field (GPF): this field has a value of 0 to 255. GP is given by $GP = 8 \times GPF$ in a unit of symbol. According to IEEE 802.1.54, one symbol is 16 μs for 2.4Ghz MAC in this thesis unless stated otherwise. Thus, the maximum GP is 32.64 ms.
- Suppressed Period Field (SPF): this field has a value of 0 to 255. SP is given by $SP = 64 \times SPF$ in unit of symbol. Thus, the maximum SP is 261.12 ms.

Table 3.3 AN Command frame format

Bytes: 7/9	1	1	1
MHR field	Command Frame Identifier (0x0a)	GPF	SPF

The settings for the subfields in the MHR field shall be as below:

- The Security Enable field, Frame Pending field and Acknowledgement request of the Frame Control field shall be set to zero.
- The PAN ID Compression subfield of the Frame Control field shall be set to one. In accordance with this value of the PAN ID compression subfield, the Source PAN Identifier field shall be omitted. If the Destination PAN Identifier is not a broadcast PAN identifier (i.e., 0xffff), the ASN is just limited in one PAN. Otherwise, all the nearby PANs are affected.
- The Source Address field should contain the coordinator's short address.
- Typically, Destination Addressing Mode subfield of the Frame Control field should be set to zero, and the Destination Address field shall be omitted. If the Destination Addressing Mode subfield of the Frame Control field should be set to one, except for the node with the short address contained in the Destination Address field, all the child nodes may behave in the way notified by the AN command.

Access Notification Functionality

AN frame is designed to be sent by an LR-WPAN coordinator and received by other nodes in an LR-WPAN network. Specifically, this frame is sent by CIM-HetNet gateway in our implementation. As shown by the frame format, it contains two important fields: GPF and SPF, which indicates the channel states that child nodes or the nodes nearby may access channel based on the received notification. The GPF and SPF divide channels into three types of states that is immediately after the AN framed transmitted, indicating that following specific duration is recommended or suppressed to access medium. The AN frame from the coordinator allows child nodes to pick advised, safe and guaranteed time slots when sending data. As shown in Fig. 3.15, the three channel states include GP, SP and Normal Period (NP) and each period has features as below:

- GP: this period is guaranteed Wi-Fi interference-free. LR-WPAN nodes access channel in a GP-aware CSMA/CA algorithm, which is discussed later in the following section.
- SP: this period is not recommended being accessed by LR-WPAN node. This period is reserved for Wi-Fi in this thesis. In order to be compatible with the nodes that do not support AN MAC command, LR-WPAN communication is not thoroughly blocked in this period, but accessing medium in SP may experience reduced channel quality and high packet loss ratio, because of the possible Wi-Fi interface. LR-WPAN nodes that support proposed time-slot based scheduling mechanism should hold back transmission and try to send in GP or NP.
- NP: this period is beyond scheduling periods. LR-WPAN nodes access channel in a normal CSMA/CA algorithm that is specified in the IEEE 802.15.4 standard. Both Wi-Fi and LR-WPAN may coexist in this period.

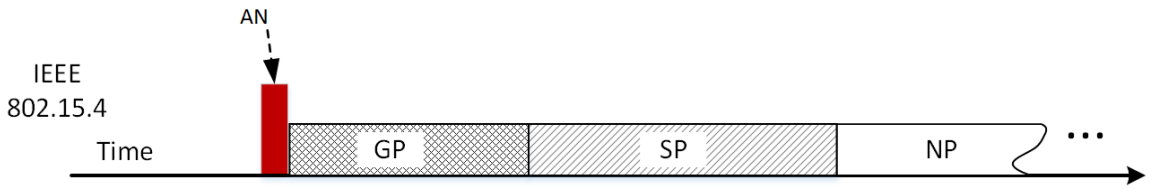

Fig. 3.15 AN frame: GP SP NP

If the GPF and SPF are non-zero values, A GP is right after the AN framed transmitted with a period of $GPF \times 128\mu s$ and A SP is right after GP with a period of $GPF \times 1024\mu s$. The channel state returns to NP and accesses the channel in a normal way. If any field is zero, the corresponding period is removed, but GPF and SPF cannot be zero at the same time. Fig. 3.16 demonstrates three possible cases when GPF and SPF are set to different values.

As illustrated above, the channel states transit happens when the previous period expires. For example, GP transits to SP when GP is timeout. It is important to note that the NP never expires. However, it may not always be this case, and coordinator does not need to wait

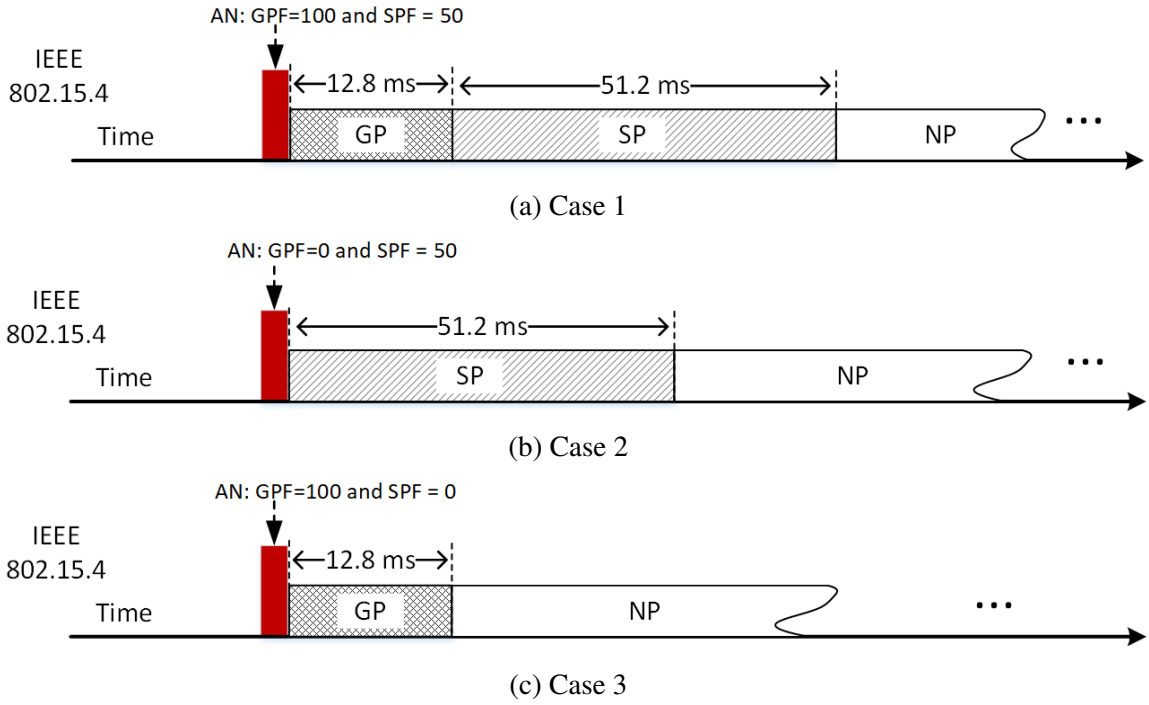

(a) Case 1

(b) Case 2

(c) Case 3

Fig. 3.16 Examples of GP SP and NP

for GP or SP period completed before sending another AN command frame. For instance, an AN command frame may be sent while the channel is still in SP period, and this can cause forced transition of the channel states. Fig.3.17 gives a finite-state machine for all the possible transitions among three channel states.

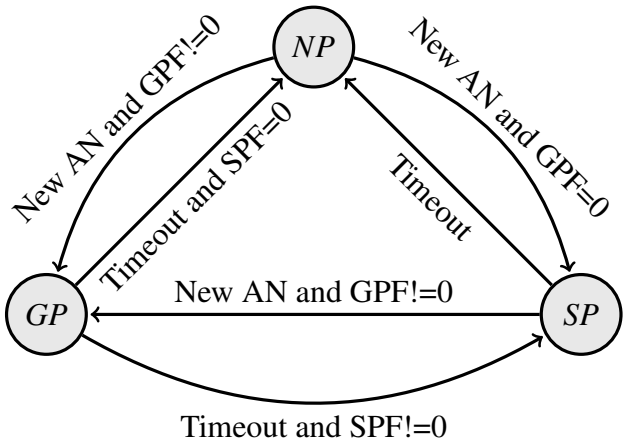

Fig. 3.17 Finite-state machine for three period transition

GP-aware CSMA/CA algorithm

The thesis proposes an enhanced channel access algorithm in GP to improve channel efficiency and help mitigate CTI. In addition to CSMA/CA algorithm, GP-aware CSMA/CA algorithm needs to hold back packet transmission if it cannot fit into the remaining GP time. As shown in Fig. 3.18, standard CSMA/CA has no knowledge of GP expiring time thus it may send a packet just before the end of GP, as long as CCA reports a clear channel. When the time left is not enough to for data transmission and ACK receiving, the packet would occupies some time in SP. In the scenario of Wi-Fi and LR-WPAN coexistence, this transmission tends to be failed because of interference from Wi-Fi, particularly when there is heavy Wi-Fi traffic. In addition, the Wi-Fi network can also be interfered by this LR-WPAN packet.

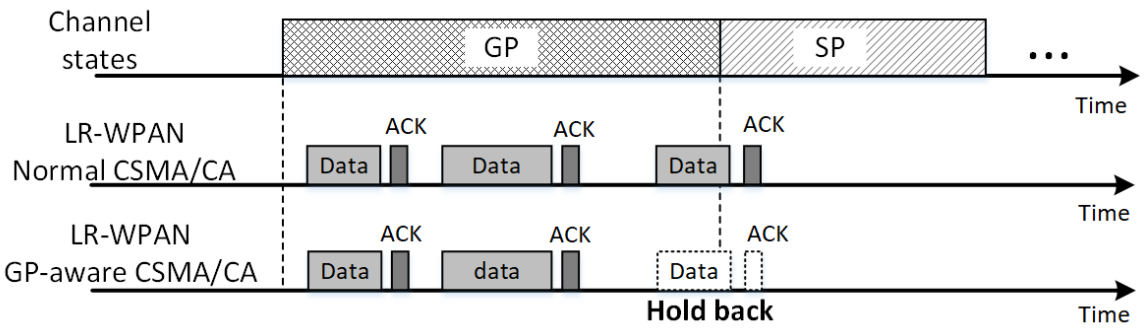

Fig. 3.18 Normal CSMA vs GP-aware CSMA/CA

With a GP-aware CSMA/CA algorithm, the node defers that there is not enough time left for the transmission and then it can hold back the transmission. In the meantime, other nodes in the network may have a shorter packet that can be fitted in, which improves channel efficiency. It is especially true when many nodes are in an LR-WPAN network.

Fig. 3.19 gives an example of a successful transmitted packet with ACK. Therefore, in order to successfully transmitting an LR-WPAN data packet, the time required (exclude CCA

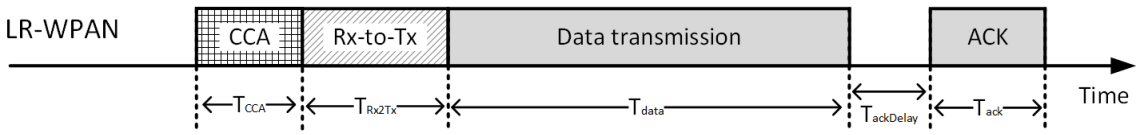

Fig. 3.19 An example of a successful transmitted packet with ACK

time) is given as below:

$$T_{packet} = T_{Rx2Tx} + T_{data} + T_{ackDelay} + T_{ack} \tag{3.1}$$

Where $T_{ackDelay}$ may change for each transmission, but there is a maximum delay limitation for the ACK. It is a reasonable estimation for T_{packet} by use maximum ACK to replace $T_{ackDelay}$.

Fig. 3.20b gives a GP-aware CSMA/CA flow chart. Compared with the standard CSMA/CA in Fig. 3.20a, the GP-aware CSMA/CA needs to check if the T_{packet} is less than or equal to the remained GP time. If there is adequate time left, it reports success. Otherwise, it needs to wait for the next GP or NP to retry the transmission and the parameter NB is left untouched.

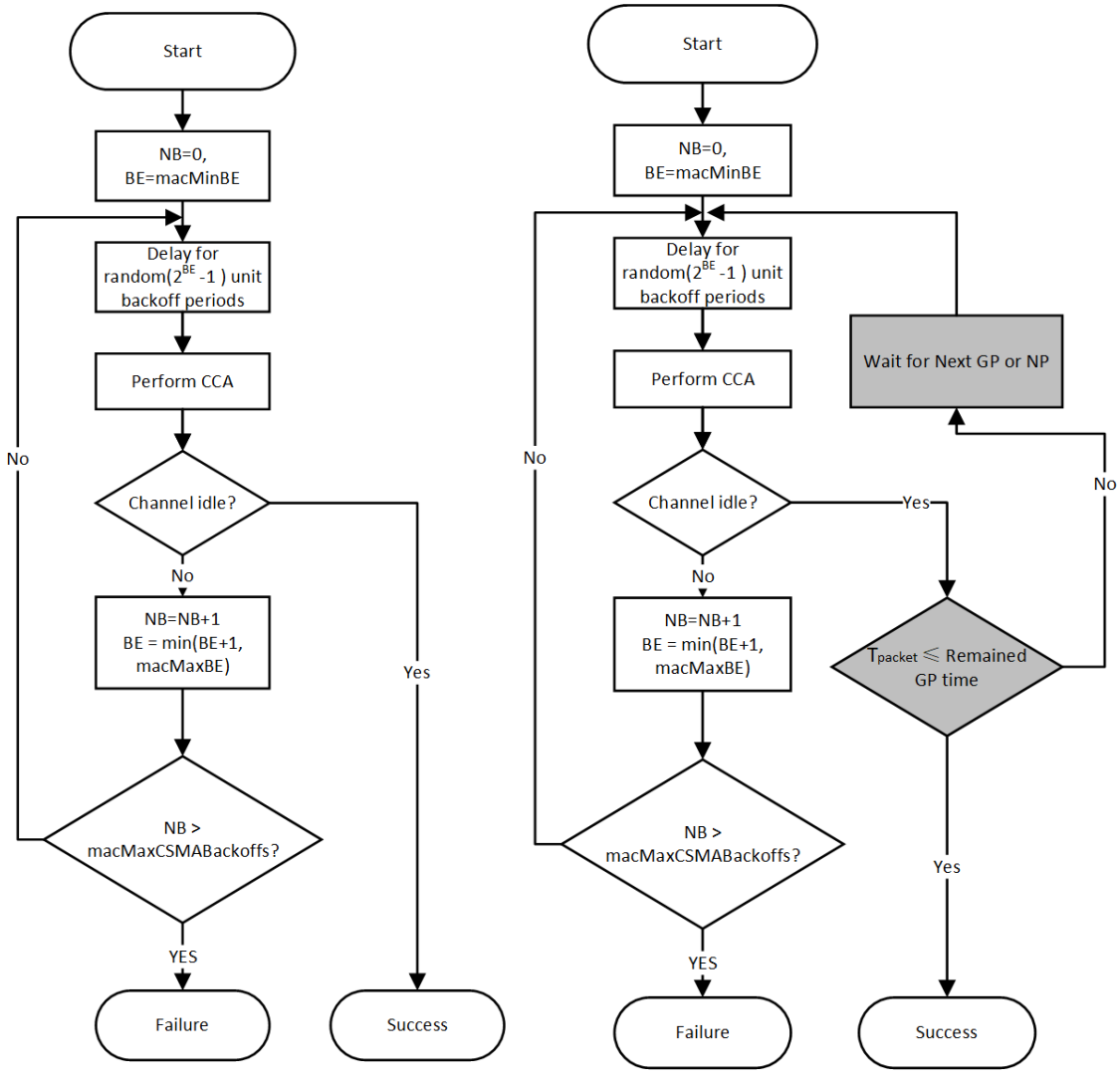

(a) Standard CSMA/CA (b) GP-aware CSMA/CA

Fig. 3.20 standard CSMA/CA algorithm vs GP-aware CSMA/CA algorithm in LR-WPAN

3.3.2 Time-slot Design

The idea for time-slot design in the thesis is depicted in Fig. 3.21. There are three periods to achieve a time-slot design, including scheduling management period, LR-WPAN slot and WI-Fi slot. Each scheduling allocates two slots; one is for LR-WPAN and the other one for Wi-Fi. During the period of scheduling management, neither Wi-Fi nor LR-WPAN can send the data packet. In this period, CIM-HetNet gateway periodically broadcast shingling frames in both networks to achieve an allocation of the slot in real-time. In our design, we employ

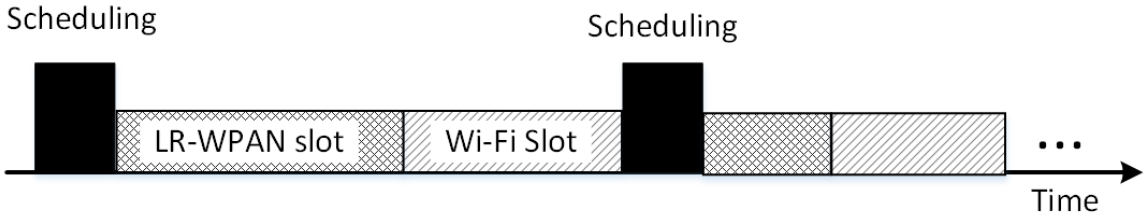

Fig. 3.21 Time slot idea

CTS in Wi-Fi and proposed AN in LR-WPAN to design time slot. This section explains the mechanism in detail.

Combination of CTS and AN

The Fig. 3.22 shows how to combine CTS and AN. Considering that LR-WPAN tends to be severely interfered by Wi-Fi, it is important to send the CTS first and then sending AN while the Wi-Fi is blocked. In order to synchronize the GP and CTS-blocking period, the fields in AN and CTS need to be set properly. The combination of these two command frames consists of three periods:

- LR-WPAN period is a Wi-Fi interference-free period. Wi-Fi traffic is blocked by CTS in this period, while LR-WPAN is in GP.
- Wi-Fi period is dominated by Wi-Fi traffic. Wi-Fi traffic is enabled because CTS duration expires, while the LR-WPAN network is suppressed in SP.

- coexistence period has both Wi-Fi and LR-WPAN network communicated. Therefore, this period is out of scheduling and tends to have severe CTI.

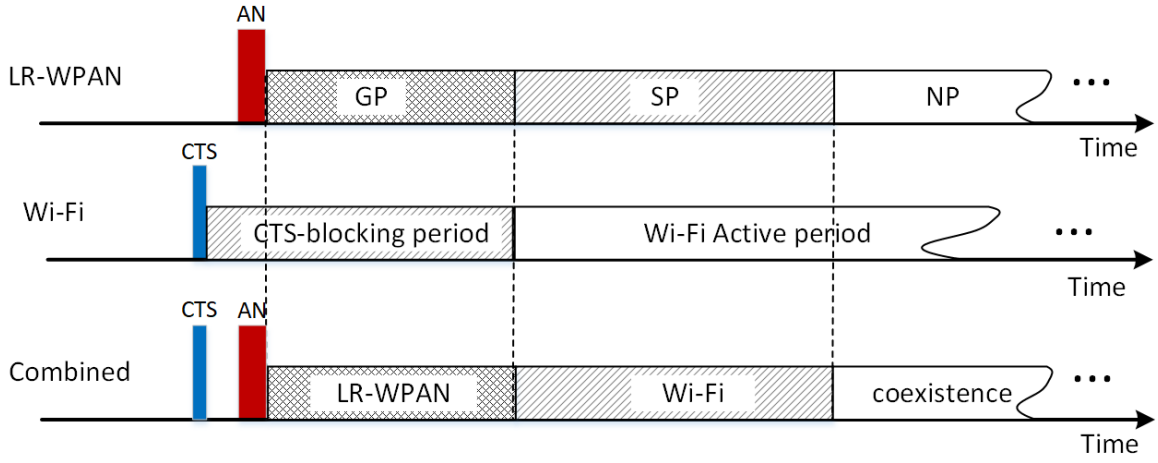

Fig. 3.22 How to combine CTS and AN

The scheduling frames can not be sent immediately, and there is always a random delay because of the randomness of the underlying CSMA/CA nature. Fig. 3.23 reveals the detail of these problems. The first problem is at the beginning of the scheduling. The CTS cannot be sent immediately, and the gateway needs to perform CCA and send the CTS frame out only when a clear channel is sensed. Therefore a random delay occurs from the start of the scheduling to the CTS transmitted. Another problem is the random delay of AN frame transmitting. If the GPF field of AN frame is set like other types of frames, the random delay makes it hard to align the end of GP with the end of the CTS-block duration. Therefore, we need to design a special CSMA/CA algorithm that fills the GPF field after a successful CCA and right before triggering Tx in the PHY layer. In this thesis, we design a high priority CSMA algorithm to address this problem. Moreover, this algorithm also has a shorter random delay in comparison with the standard CSMA/CA algorithm.

In order to send AN at a high priority mechanism to achieve real-time scheduling, a high priority CSMA algorithm is introduced as depicted in Fig. 3.24a. The algorithm gets features as below:

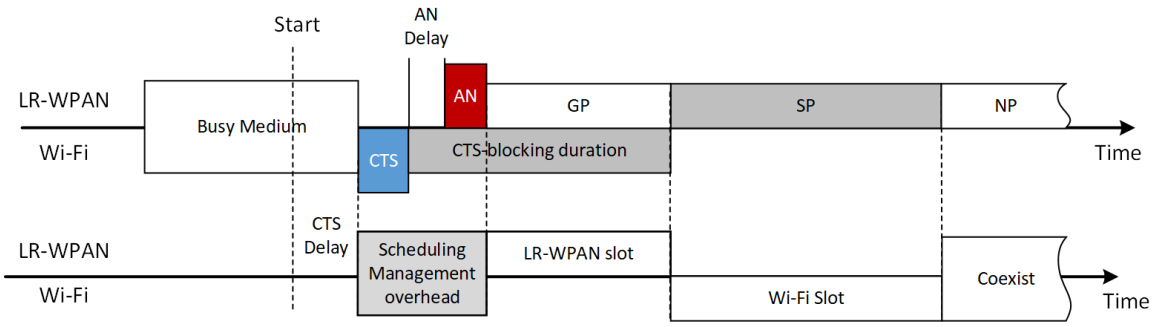

Fig. 3.23 How to combine CTS and AN

- Small BE. BE decides the maximum number of backoff windows. A small BE, such as two, can increase the possibility of winning the right to access a channel. In the other side, small BE also indicated higher chance to encounter packet collision with other nodes.

- Retry times policy is different. Unlike standard CSMA/CA that gets limited attempts for a frame transmitting, the proposed algorithm does not limit trial times but limited by disparate criteria: $GP \leq macMinGP$, where $macMinGP$ is the configured minimum GP.

- The GPF needs to be updated after gain access to the channel according to the remaining GP time.

The whole process about how to schedule CTS and SN frames is given by Fig. 3.24b. It is import to note that $CTSD$ (CTS duration)is given by upper layer and GP is calculated as below:

$$GP = CTSD - T_{CCA} - T_{Rx2Tx} - T_{ANF} \tag{3.2}$$

where T_{CCA} is the LR-WPAN CCA, T_{Rx2Tx} is the Rx-to-Tx switch time in LR-WPAN and T_{ANF} is the AN frame-in-air time.

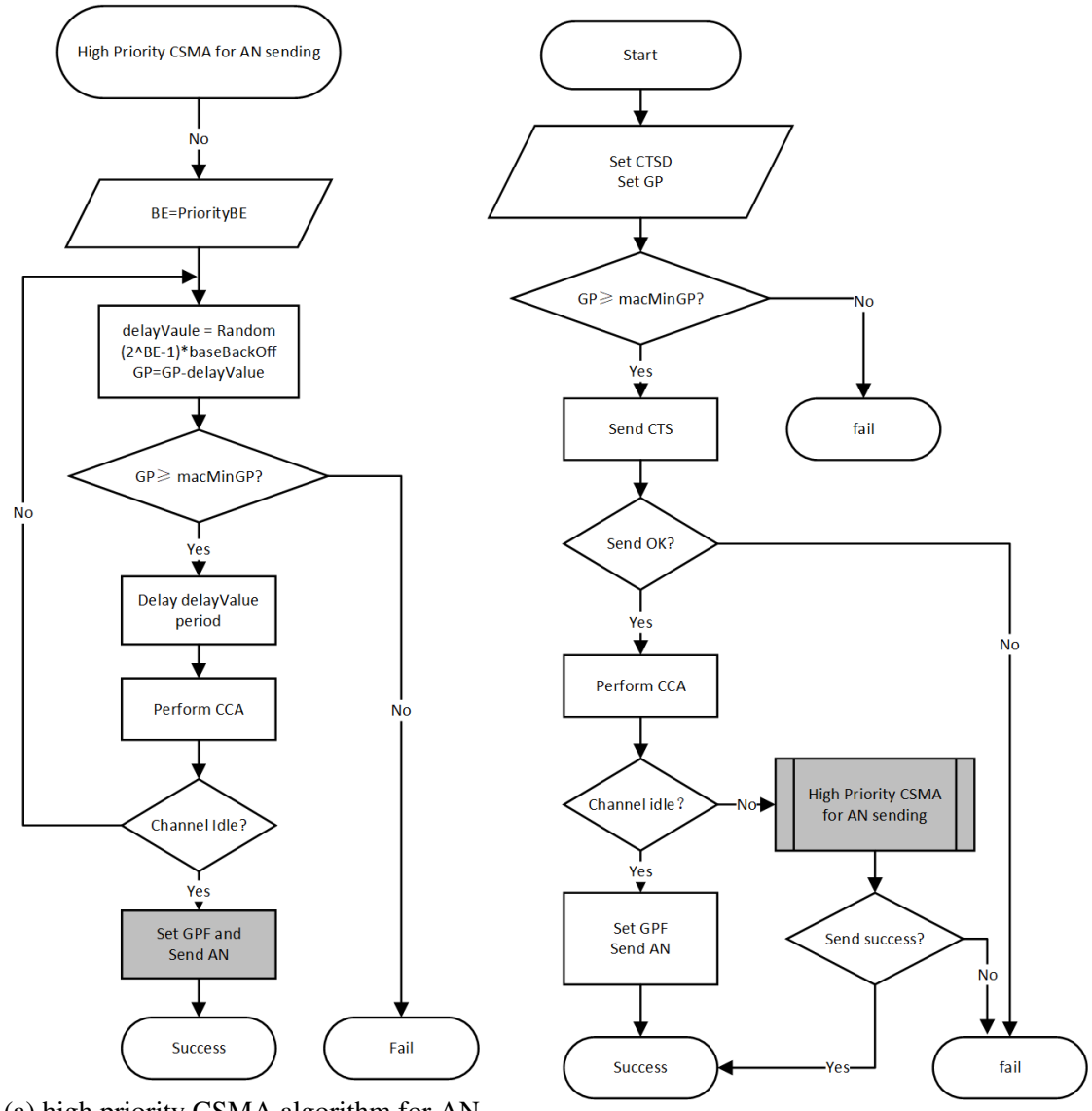

(a) high priority CSMA algorithm for AN sending

(b) The flowchart for CTS and AN frame scheduling

Fig. 3.24 The flow chart for Combination of CTS and AN

Coexistence-free time-slot design

If the CTS and AN frame are scheduled periodically, the Wi-Fi and LR-WPAN can be scheduled to access in a time-slot manner. Thus, the harmful CTI is avoided. Nevertheless, because of the random delay in transmission of the command frame, the exact period is impossible to anticipate in advance. This section studies the problems cause by this random feature and solve the problem by using excess SP and CSMA random delay compensation.

If the SP is set to exact length that we want, the unwanted coexistence period can be observed as shown in Fig. 3.25. Our design is built on top of CSMA. Thus the scheduling can experience unavoidable delay. Especially the scheduling delay can be even longer in a busy Wi-Fi network because it takes more time until a clear channel is sensed. Practically, the delay is normally a few milliseconds, but it can be more than ten milliseconds if the network is excessively busy.

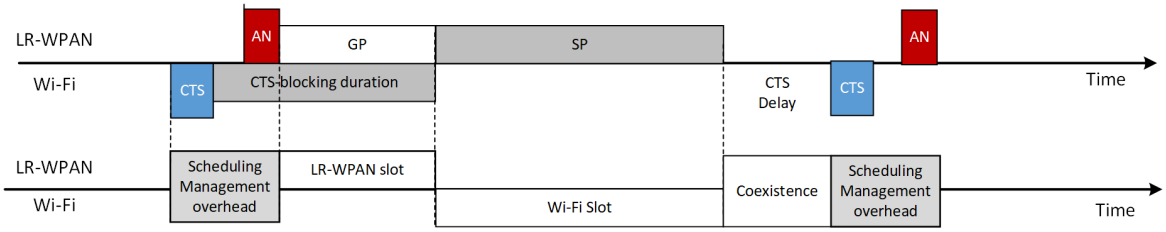

Fig. 3.25 Unwanted coexistence period

In order to overcome this problem, SP is advised to set more than the wanted length, named excess SP. For example, we may set 10 ms more SP. Fig. 3.26 shows how it works. As stated in Fig. 3.17 in section 3.3.1, the channel state can be changed from SP to GP by sending a new AN frame. Therefore, it is a good idea to set the SP more than the wanted length, and it can remove unwanted coexistence period.

However, using excess SP has a drawback that Wi-Fi slot is always more than expected length. To eliminate this limitation, CSMA random delay compensation is required as shown in Fig. 3.27. Basically, the algorithm records the CSMA random delay time t_1 and deduct this time when starting following schedule. In other words, the algorithm tries to trigger the

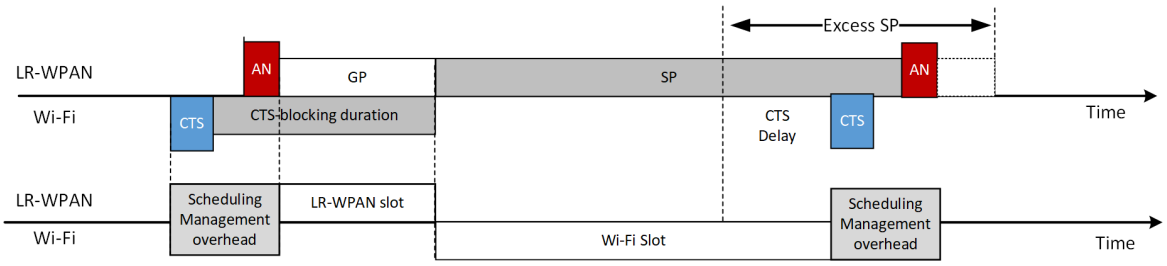

Fig. 3.26 Coexistence-free time-slot design by using excess SP

scheduling t_1 time in advance, which compensates an unexpected long Wi-Fi slot to some extent.

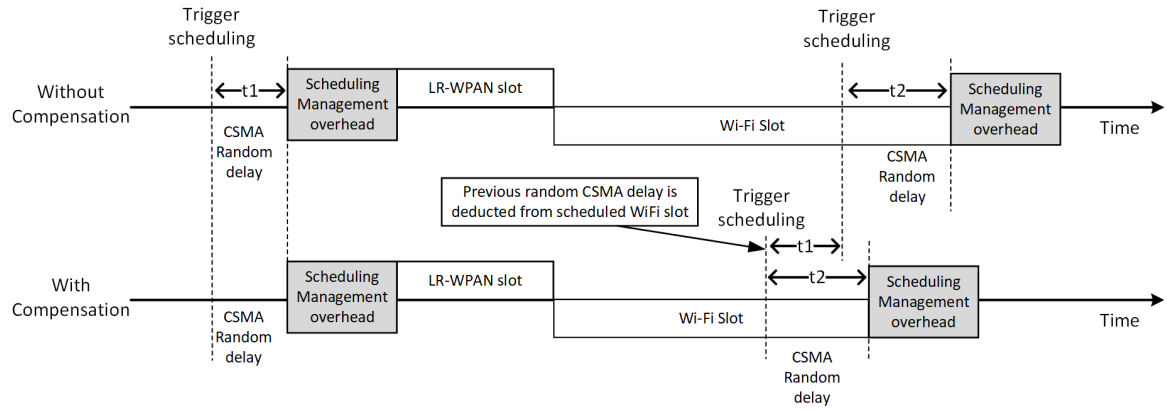

Fig. 3.27 CSMA random delay compensation

In summary, a Coexistence-free time-slot design is achieved by sending periodical Wi-Fi CTS and AN frames. The fields of the command frames must be set with the consideration of randomness of CSMA/CA transmission. Here, we adopt the idea of excess SP and CSMA random delay compensation. We also employ an enhanced CSMA/CA for AN frame, named high priority CSMA algorithm and the GPF field is updated after PHY layer CCA returns success CCA, which removes the GPF error from random backoff. To make thing simple, the Coexistence-free time-slot design can be briefly depicted in Fig. 3.28

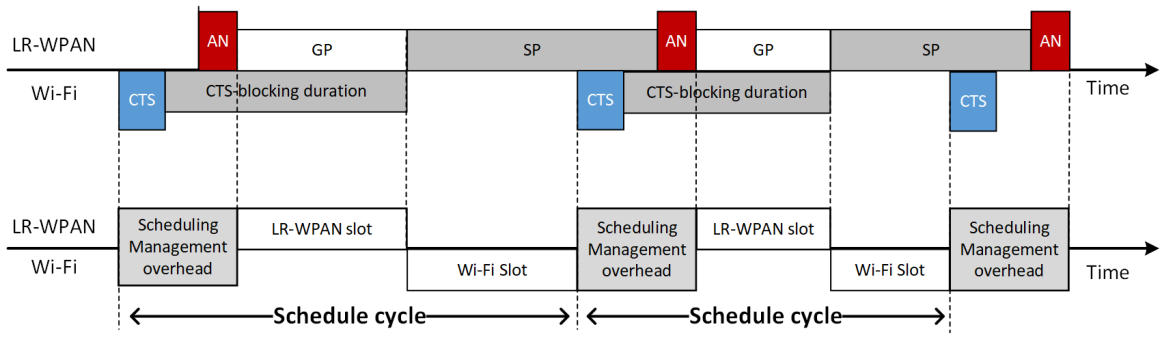

Fig. 3.28 Brief view of the Coexistence-free time-slot design

3.3.3 Overhead of Scheduling Frames

Wireless Frame Transmission Time

In a wireless technology with CSMA/CA mechanism applied, the actual transmission time (T_Z) varies under different network background, such as variable backoff time, failure re-transmission and so on. In order to simplify the calculation, we assume the transmission succeeds in first-time trial and one Back Off time ($T_{Z,BF}$) is expected. Thus, IEEE 802.15.4 frame-in-air time (T_Z) includes CCA ($T_{Z,CCA}$), Tx-to-Rx turnaround ($T_{Z,Rx2Tx}$), Synchronization Header ($T_{Z,SHR}$) containing both preamble sequence and start of frame delimiter, PHY Header (TZ,PHR), MAC Protocol Data Unit (TZ,MPDU). We have

$$T_Z \approx T_{Z,BF} + T_{Z,CCA} + T_{Z,Rx2Tx} + T_{Z,SHR} + T_{Z,PHR} + T_{Z,MPDU} \tag{3.3}$$

As for WiFi transmission time (T_W), the frame includes PHY Header ($T_{W,PHR}$) containing both PLCP preamble and PLCP Header, MAC PDU ($T_{W,MPDU}$), PHY pad ($T_{W,PPad}$). Similarly, we also expect one back off and CCA time (also refer DCF Interframe Space, T_{DIFS}) and the transmission succeeds in first trial. We have

$$T_W = T_{W,DIFS} + T_{W,PHR} + T_{W,MPDU} + T_{W,PPad)} \tag{3.4}$$

Typical AN and CTS frame transmission time

In the project, we make a reasonable assumption that AN frame has a payload size of 2 bytes and operates in 2.4 GHz bands. Hence, according to the [113], we get typical T_{ASN} transmission, about 1216 microseconds, as shown in Table 3.4:

Table 3.4 Typical AN transmission time

Variables	$T_{Z,BF}$	$T_{Z,CCA}$	$T_{Z,Rx2Tx}$	$T_{Z,SHR}$	$T_{Z,PHR}$	$T_{Z,MPDU}$	T_{ASN} (sum)
Value (us)	320	128	192	160	32	384	1216

Compared with AN, the transmission time of WiFi is typically short. As shown in Table 3.5, due to the various channel data rates, four typical channel data rates are chosen and analysed. T_{CTS} is the CTS frame transmission time.

Table 3.5 WiFi CTS typical transmission time

Channel Rate Mbps	$T_{W,DIFS}$ us	$T_{W,PHR}$ us	$T_{W,MPDU}$+$T_{W,PPad}$ us	T_{CTS}(sum) us
1	50	192	112	354
6	28	20	24	72
24	28	20	8	56
54	28	20	4	52

Scheduling Overhead Ratio (OR_S) Estimation

In a given heterogeneous network with time-slot based coordination mechanism, the overhead can be estimated by defining overhead Ratio of scheduling frames (OR_S) Estimation)

$$OR_S = \frac{T_{ASN} + T_{CTS}}{T_{cycle}} \tag{3.5}$$

Where $T_{cycle} = T_{Z,slot} + T_{W,slot} + T_{ASN} + T_{CTS}$ is the scheduling cycle.

$T_{Z,slot}$ is scheduled IEEE 802.15.4 slot duration and $T_{W,slot}$ is scheduled WiFi slot duration. We assume WiFi has a channel rate at 54 Mbps. Table 5 gives a list of scheduling overhead.

Table 3.6 Overhead Ratio of scheduling frame

$T_{Z,slot}$ (ms)	$T_{W,slot}$ (ms)	T_{cycle} (ms)	OR_S
5	5	11.27	11.3%
5	10	16.27	7.8%
10	10	21.27	5.9%
15	32	48.27	3.5%
32	32	65.27	2.0%
50	100	151.27	0.84%

It is obvious that the OR_S reduces along with the increase of T_{cycle}. If the scheduling cycle is long enough, the scheduling overhead can be limited at a quite low ratio. For instance, the scheduling overhead is estimited less than 2%, when choosing a schduling cylce longer than 63.4ms.

3.4 Summary

An experiment is conducted in this chapter to reveal the seriousness of cross-technology interference between Wi-Fi and LR-WPAN in a scenario where a heterogeneous gateway works as the central node in both networks. Different from others, the experiment focuses on the interference when LR-WPAN and Wi-Fi antennas are at an extremely short distance. The experiment also indicates that ZigBee channel switching and AP radio power adjusting are not effective to mitigate the interference from Wi-Fi in this scenario.

The overall system design explains application scenario, design features and challenges. The application scenario is a heterogeneous network, called CIM-HetNet, including a CIM-HetNet gateway, some Wi-Fi nodes and LR-WPAN nodes. The gateway works as the central node of a wireless network to cover a small area. Wi-Fi and LR-WPAN nodes are connected to the gateway. In the case of large area network coverage, CIM-HetNet can be planed in a dedicated way that each CIM-HetNet operates in non-interference channels. The gateway does not only provides data service for LR-WPAN and Wi-Fi, but also schedules both network

communication and mitigate harmful CTI. With the scheduling, the channel is accessed in a time-slot manner that Wi-Fi and LR-WPAN are scheduled to access channel at different time duration to mitigate the CTI. The mechanism is more like a high-level TDMA on top of the CSMA/CA than a replacement of standard CSMA/CA. It is designed to be a MAC layer functionality; thus, it can be generally applied in most of the LR-WPAN networks. Moreover, It does not require any hardware or software modification on Wi-Fi clients. There are many challenges to achieve such a scheduling mechanism. For example, the scheduling requires to send extra scheduling frames, which can result in high scheduling overhead; non-proper time-slot allocation can result in long network latency. Furthermore, as LR-WPAN and Wi-Fi are designed for completely different applications and have distinctive features, the design of the scheduling scheme needs to meet additional requirements, e.g. the Wi-Fi application like VoIP cannot work properly with a one-way network latency more than 150 ms.

Time-slot based scheduling mechanism is discussed in the last section of this chapter. Firstly, AN frame is designed and introduced into IEEE 802.15.4 MAC as a command frame to synchronize LR-WPAN communication, which is sent by an LR-WPAN coordinator and received by other nodes in an LR-WPAN network. Specifically, this frame is sent by CIM-HetNet gateway in our implementation. The frame consists of information of GPF and SPF, which divide channels into three types of states including GP, SP and NP. GP is guaranteed Wi-Fi interference-free period. SP is the period that LR-WPAN nodes are suppressed to access channel. NP is the period beyond scheduling periods. The channel states transit happens when the previous period expires or an AN frame with special parameters is sent. In order to restrict the LR-WPAN packet within allocated GPs and improve channel efficiency, the thesis proposes an enhanced channel access algorithm called GP-aware CSMA/CA algorithm that holds back packet transmission if it cannot fit into the remaining GP time. Secondly, a Coexistence-free time-slot design is achieved by sending periodical Wi-Fi CTS and AN frames. The scheduling mechanism is designed on top of the CSMA/CA. The

random delay prior to send a CSMA/CA frame can result in large error on the real scheduled period. In order to minimize the error, a high priority CSMA algorithm is proposed and the GPF field is updated after PHY layer CCA returns success CCA, which removes the GPF error from random backoff. Finally, the overhead of scheduling mechanism is estimated by analysing wireless frame transmission. The scheduling overhead can be limited at a quite low percentage.

Chapter 4

Static Time-slot Based Resource Scheduling Algorithm

This chapter proposes static time-slot based resource scheduling algorithm, or static scheduling algorithm in short. The resource here is the channel access time. The algorithm is achieved by using the time-slot based scheduling mechanism designed in Chapter 3. The static scheduling algorithm simply allocates a fixed length of the time slot for LR-WPAN and Wi-Fi in every scheduling cycle. Fig. 4.1 give an example of static scheduling, in which LR-WPAN and Wi-Fi get fixed 32ms slot in every scheduling cycle.

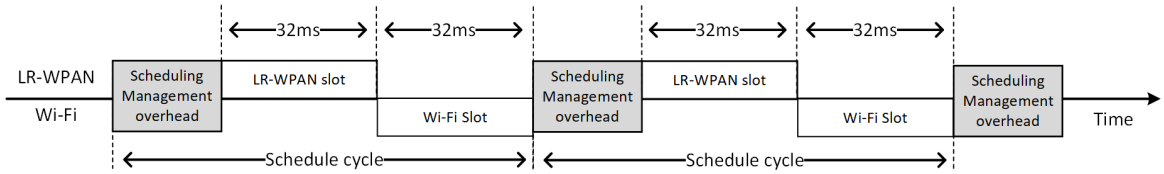

Fig. 4.1 An example of static time-slot based resource scheduling algorithm

The static scheduling algorithm is first implemented and evaluated based on real hardware. Unfortunately, due to the limitation of the hardware radio modules, only a reduced version of the scheduling mechanism mentioned in Chapter 3 is implemented. The hardware-based experiments confirm the effectiveness of the static scheduling algorithm.

We further design and implement a full revision of the algorithm in NS-3 simulator. And then it is evaluated in term of Packet Loss Ratio (PLR), Packet Transmission Rate, Network latency, spectrum usage, scheduling overhead and so on.

4.1 Hardware-based Analysis and Evaluation

4.1.1 Design and Challenge

Design overview

Fig. 4.2 describes the overall architecture of the gateway and IEEE 802.15.4 end node. The gateway, integrating Wi-Fi module radio module and IEEE 802.15.4 radio module, runs a Coordination Controller (CC). By utilizing the CTS frame and proposed AN frame, CC is able to schedule Wi-Fi and IEEE 802.15.4 traffic into separated slots.

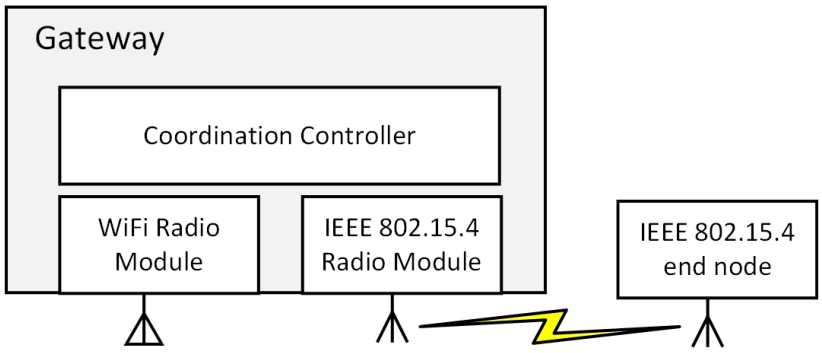

Fig. 4.2 Gateway component

The detailed design of the architecture is depicted in Fig. 4.3. Generally, CTS is directly controlled by hardware, and Operating System (OS) doesn't to allow user send CTS by default. In order to send arbitrary CTS frame, the OS kernel modifications are necessary. The implementation is based AR9331 [R58] SoC that runs an embedded Linux OS, named OpenWRT. AR9331 chip integrates an 802.11 b/g/n radio module. As shown in Fig. 4.3, MAC80211 and ath9k driver for the Wi-Fi module are modified to enable Wi-Fi CTS frame

injection. The IEEE 802.15.4 AN frame proposed in this paper is implemented in Contiki-OS, thanks to its flexible radio control, rich features, support of simulation. We design new Radio Duty-Cycle (RDC) layer to enable AN support. The RDC layer in the IEEE 802.15.4 coordinator module provides control API by serial port, allowing CC to send a signal to it. Once the RDC layer receives the signal from a serial port, it sends out proper AN fame and holds its upper MAC layer data transmission for a specific period. The transmitted AN frame will be received by IEEE 802.15.4 end node and the RDC layer in the end node will also block its upper MAC layer data transmission. Thus the AN is implemented and able to suppress IEEE 802.15.4 traffic. In this project, the AN command frame is implemented on the CC2538 [R67] chip. The CC2538 chip is connected to the AR9331 by serial port. Test applications are also designed to evaluate the coordination mechanism performance.

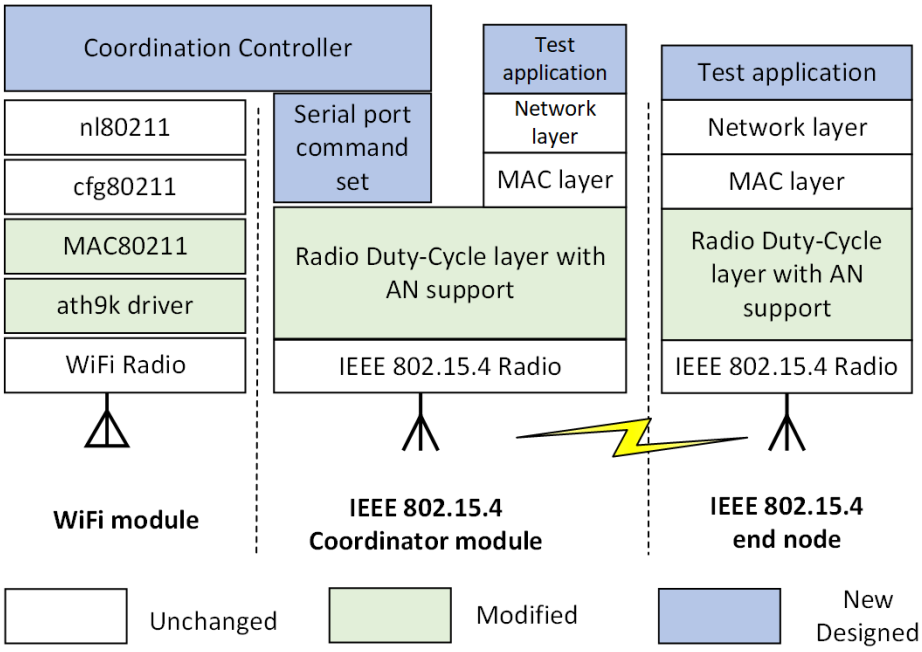

Fig. 4.3 Architecture

Challenge of Wi-Fi CTS frame injection

CTS frame is designed to block nearby Wi-Fi nodes from sending any traffic, except for the one that is chosen and allowed to send without worry about interference from other nodes. Sending numerous CTS frames can jammy Wi-Fi network and result in DoS attack. Therefore, user cannot send CTS frames without modifying the OS kernel. The gateway is built by using a AR9331 [9] SoC with linux-based OpenWRT OS. Thanks to the open-source feature of the linux kernel, the customized kernal can be compiled and used for experiment. AR9331 chip integrates an 802.11 b/g/n radio module. By modify Linux kernel and ath9k wireless driver for the radio module, Wi-Fi CTS frame injection is allowed.

Challenge of AN frame implementation

Previously, experiments about IEEE 802.15.4 are based on TI's z-stack on CC2530 chip. However, due to TI does not provide source code for their z-stack of the MAC layer, the extended MAC layer functionality proposed in this report cannot be implemented on it. After the investigation on ZBOSS [141], Open-ZB [86], and Contiki [87], we decided to use Contiki-OS, because of its flexible radio control, rich features, support of simulation. Contiki separates IEEE802.15.4 MAC layer into three sublayers.

- MAC layer: Generally for CSMA mechanism implementation
- Radio Duty-Cycle (RDC) layer: taking care of sleep period of nodes. Many power-saving algorithms are implemented in this layer, such as ContikiMAC and X-MAC.
- Framer layer: providing a collection of auxiliary functions that are called for creating a frame with data to be transmitted and parsing of data being received.

Due to AN functionality needs to be scheduled in real-time and affects sleep period of nodes, it is implemented in the RDC layer. In this project, the AN command frame is implemented

by introducing a new RDC layer and based on CC2538 [50] chip that has better support in Contiki than CC2530.

Challenge of Scheduling Synchronization

In order to schedule over Wi-Fi and LR-WPAN, As shown in Fig. 4.3, the Coordination Controller (CC) needs to access both of the wireless modules. Wi-Fi module can be accessed by nl80211 interface, but there is not a mechanism available to access LR-WPAN radio module. Thus, we connect the LR-WPAN module by serial port and design command set to allow CC to access and schedule the radio module. The command set is as below:

- **A** This command is only one letter "A", which indicates the LR-WPAN radio to transmit an AN frame with preconfigured GPF and SPF field. Even though this command is designed as short as possible with only one letter to minimum serial port delay, the delay caused by the serial port itself still affects synchronization of scheduling.
- **T:PLR:T:<packet number>,<interval>** This command notifies the *Test application module* to start PLR experiment with given number of packets and interval of each transmission.
- **T:PLR:RSTART** This command indicates an end node to prepare for reinventing PLR testing packets.
- **T:PLR:RSTOP** This command stops a PLR test and display the experiment result.
- **T:RUNICAST:<node>,<duration>** this command runs a unicast test with given node id and experiment duration
- **ping** This command tests connect status, a "pong" returned indicating that connection is in good status.

- **S:CHANNEL:<Channel number>** This command sets network channel.
- **G:CHANNEL:** This command tests command gets the network channel.

A full version of scheduling mechanism requires the AN frame is transmitted right after CTS is sent. In the hardware-based experiment, the CC can inject CTS to Wi-Fi MAC, but it cannot receive any feedback when the CTS is transmitted. It is possible to get the feedback by modifying the firmware or Integrated Circuit (IC). However, it is expensive and usually needs the IC manufacture involved. Therefore, it is unlikely to achieve in current stage and far beyond the scope of the thesis. Thus, CC can not be aware of when the CTS is sent into the air. In result, the scheduling mechanism can not guarantee AN is scheduled right after a CTS frame, which leads to a large error on scheduling, and this error mainly depends on the CSMA/CA delay.

4.1.2 Experiment One and Evaluation

Experiment Setup

Fig. 4.4a demonstrates a CIM-HetNet gateway implementation dedicated designed for static time-slot based resource scheduling algorithm. Specifically, the gateway is built with three components: A) CC2538 radio module running specially designed IEEE 802.15.4 MAC with extended AN command frame support, B) dedicated Wi-Fi module with modified kernel and able to send CTS control frame, C) normal Wi-Fi module running Wi-Fi AP and generating Wi-Fi traffic. Of these three modules, Module B and C are able to integrate into one Wi-Fi module. The reason why these two modules are separated is to get more accurate experiment results by minimizing the impact of limited CPU computing power.

Different from the previous experiment which adopts ZigBee as an upper network layer on IEEE 802.15.4, Rime is chosen in this experiment, because Contiki provides support for both 6LoWPAN and Rime, but not for ZigBee. Moreover, Rime network stack has

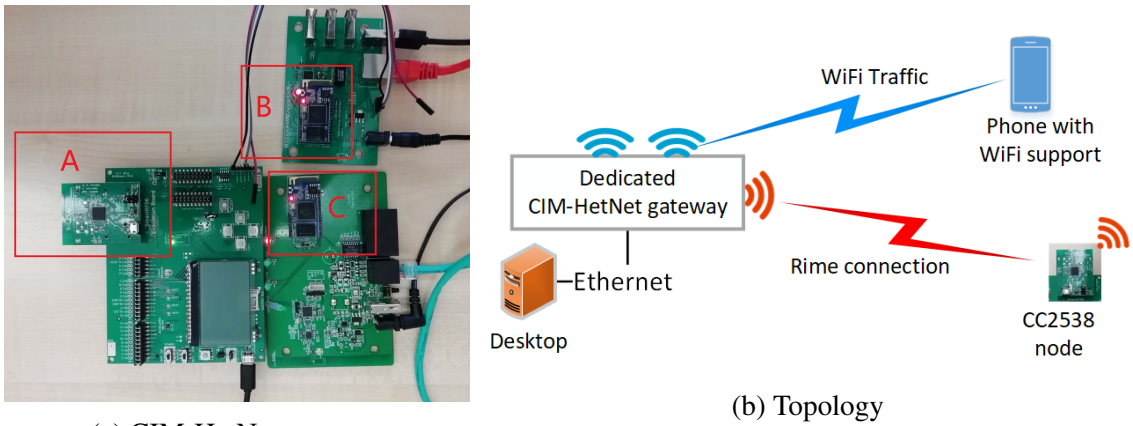

(a) CIM-HetNet gateway

(b) Topology

Fig. 4.4 Experiment setup

broadcast and reliable unicast support that is ideal for the experiment. As shown in Fig. 4.4b, the experiment platform consists of a desktop PC, a CIM-HetNet gateway, a phone and a CC2538 node. The desktop is used to access the gateway and also retrieve statics from the gateway. The Wi-Fi traffic is generated by iperf3, which is installed in both the gateway and the phone. LR-WPAN traffic is generated and recorded by a customized program running on the CC2538 module. We designed two programs to evaluate Rime PLR and PTR. They are:

- Rime broadcast PLR over various Wi-Fi transmission speed: in this experiment, the CC2538 node sends out Rime broadcast packets with sequence number every 15ms, the packet number is set to 1000 for each run. Three runs are performed at each Wi-Fi speed. Then different Rime PLR data are collected and calculated under two conditions with or without static time-slot resource.

- Rime reliable unicast PTR over various Wi-Fi transmission speed: In this experiment, the CC2538 node send out Rime reliable unicast packet to the gateway. The unicast packets are transmitted under the guarantee of an up-four-times retransmission mechanism. The transmission is successful if the packet is transmitted within four retransmissions; otherwise, the transmission is timeout. The successful transmissions are counted with a time period of 100 seconds in each run. Similarly, three runs

are performed at each Wi-Fi speed. Then Rime PTRs with static time-slot resource algorithm are compared with the PTRs without the algorithm.

Packet Loss Ratio of 802.15.4 Rime Data

As shown in Fig. 4.5, this experiment introduces desired Wi-Fi speed and real Wi-Fi speed concepts. The desired Wi-Fi speed means the Wi-Fi traffic that the iperf3 program intends to generate. However, the real generated Wi-Fi traffic may be different because the channel capacity is limited, and there are possibly multiple wireless technologies sharing the same medium. As a result, they may compete with each other. The experiment is conducted on Wi-Fi channel 6 and ZigBee channel 17. These two channels overlap in the spectrum and are expected to interfere with each other. When there is not any scheduling algorithm over Wi-Fi and Rime, desired Wi-Fi speed is set from 0 to 40 Mbits/s with a speed step of 2 Mbits/s. At each Wi-Fi speed, statistics are collected and Rime PLR is calculated. Meanwhile, the real Wi-Fi speed is also recorded. Similarly, we test and collect data when running static time-slot based resource scheduling algorithm. Thus, Fig. 4.5 is acquired. The figure depicts

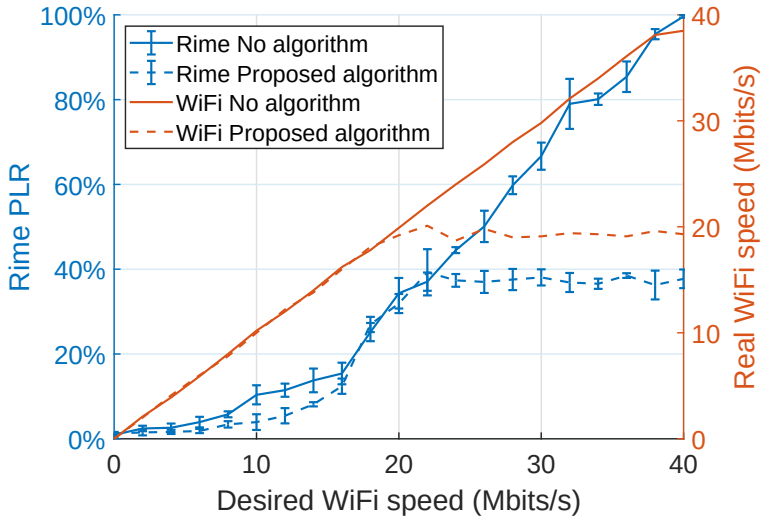

Fig. 4.5 Rime PLR versus Desired Wi-Fi Speed

that overall Rime PLR with the proposed algorithm is lower than that without any algorithm.

More detailed analysis can be done by dividing the graph into three parts according to various desired Wi-Fi speed ranges:

- Effective phase (0 to 16 Mbits/s): Wi-Fi traffic is not crowded, and the real Wi-Fi speed in both situations is basically equal with the desired Wi-Fi speed. Average of Rime PLR without scheduling is 7.41%, while Average of Rime PLR with scheduling is 4.39%. The proposed algorithm is obviously effective by reducing Rime PLR from 7.41% to 4.39% without affects Wi-Fi traffic.

- Transition phase (18 to 22 Mbits/s): Wi-Fi traffic is medium. Both PLR lines raise rapidly over this range. There is no obvious difference with or without the scheduling algorithm. At the end of this range, the scheduled Wi-Fi time slot is almost fully used.

- Stable phase (24 to 40 Mbits/s): Wi-Fi traffic become more crowded. The PLR without proposed algorithm keeps growing rapidly, while the PLR with the scheduling algorithm keeps at around 37%. The proposed algorithm shows improved performance of Rime PLR. When taking real Wi-Fi speed into consideration, the low PLR for the proposed algorithm is at the cost of Wi-Fi speed reduction. The scheduling algorithm periodically sends out CTS frames, which block Wi-Fi traffic periodically and create a time slot for Rime to send out a broadcast. With scheduling algorithm, Wi-Fi has used up all allocated time slot. Thus real Wi-Fi limited at around 19 Mbits/s. Such a mechanism works like applying protection to Rime traffic when there is too much Wi-Fi traffic.

Although the figure shows that static time-slot based resource scheduling algorithm has improved performance in term of Rime broadcast PLR, there still are some limitations and flaws on algorithm implementation. In an ideal implementation of the algorithm, a very low PLR, such as 2%, overall the Wi-Fi speed ranged is expected, because the ideal scheduling will effectively separate Rime traffic from Wi-Fi's and they will never interfere each other.

The experiment indicates that high Wi-Fi traffic affects the scheduling and results in an increase of PLR.

Unicast Packet Transmission Rate of 802.15.4 Rime Data

We measure Wi-Fi by bitrate in the unit of Mbits/s. Different from Wi-Fi, however, in WSN, application message tends to be short and only care about whether the message is successful transmitted or not, rather than the bitrate. Thus it is more reasonable to measure Rime traffic speed by successfully transmitted packets per second (packets/s). Fig. 4.6 can be study over

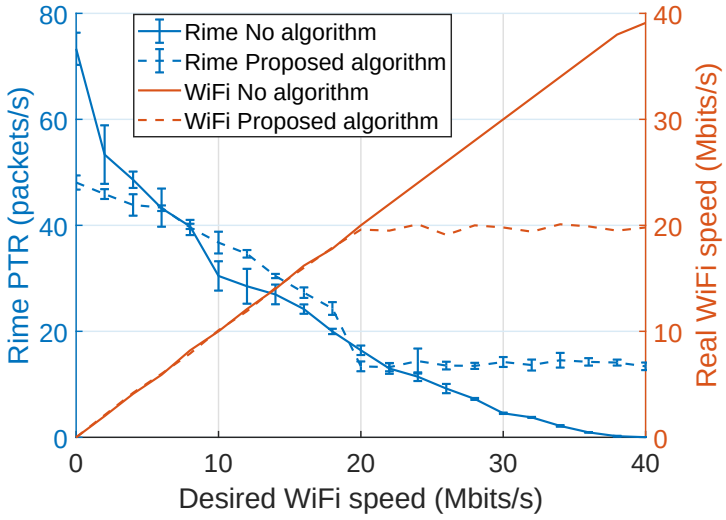

Fig. 4.6 Rime PTR versus Desired Wi-Fi Speed

four desired WiFi speed ranges:

- AN suppress phase (0 to 8 Mbits/s): Static scheduling algorithm does not help improve Rime PTR performance; instead, it reduces the performance. This is caused by periodical AN frames that static scheduling algorithm sends to suppress Rime traffic. When no scheduling algorithm is introduced, Rime PTR reach a fast speed at 73.32 packets/s while desired Wi-Fi speed is zero, but PTR drops dramatically once any Wi-Fi traffic is introduced. With the scheduling algorithm, PTR is limited at 48.08

packets/s, and this value slightly drops when there is a little Wi-Fi traffic. These two lines meet and merge quickly when Wi-Fi traffic at 6Mbits/s.

- Effective phase (10 to 16 Mbits/s): Advantages of the static scheduling algorithm starts showing up in this range. The scheduling algorithm separate Wi-Fi and Rime traffic in a different time slot. This improves PRT by avoiding potential CTI.

- Transition Phase (18 to 20 Mbits/s): with the proposed algorithm, the Wi-Fi slot usage starts reaching its limit and PTR decrease rapidly, and very soon it is stable at 13.9 packets/s.

- Stable phase (22 to 40 Mbits/s): Under the static scheduling, Wi-Fi has fully used its time slot and reached a stable state that real Wi-Fi speed is about 19 Mbits/s and PTR is about 13.9 packets/s. If without scheduling, the PTR keeps dropping until almost 0 packets/s with the increase of the Wi-Fi traffic. The proposed algorithm improves Rime PTR at the cost of reduction of real Wi-Fi speed. The scheduling protects Rime traffic and avoids that Wi-Fi takes up all the medium. If no scheduling protection, Wi-Fi traffic blocks Rime transmission and causes Rime network failure.

In summary, the scheduling algorithm implementation demonstrates an overall improvement of Rime unicast PTR. However, the implementation still needs to be improved. An ideal implementation should give a stable Rime PTR that should be half of maximum PTR. In this experiment, the maximum PTR is 73.32 packets/s, and ideal implementation should give a stable PRT at about 36.66 packets/s, but the experiment PRT drops to around 14.9 packets/s when Wi-Fi traffic use up all its scheduling time slot. In result, the algorithm works as expected in low Wi-Fi traffic situation, but it is not efficient enough when there is too many Wi-Fi traffic.

4.1.3 Analysis of the Impact of CSMA/CA Random Backoff

Experiment CSMA/CA Random Backoff

In order to figure out limitations of the implementation, we carry out extra experiment to check if the CTS and AN frames are sent out at scheduled time. In addition to previous experiments, the WiFi and IEEE 802.15.4 sniffers are deployed to acquire a CTS and AN frame when the proposed scheduling algorithm is running. WiFi and IEEE 802.15.4 both employ CSMA/CA mechanism in their MAC layer, which means that once the wireless module gets a frame, it cannot send it out until the channel is clear. If the wireless medium is crowded, it may need to wait long time before sending. This results in unpredictable delay when sending frames. This experiment estimates the frame sending-delay time, which is the time required for the radio module from receiving a frame until sending it out. The experiment has two parts:

- CTS frame sending-delay time: first make sure no WiFi traffic generated and start to capture WiFi control frames about 60 seconds. Then start to generate WiFi traffic at its maximum speed and continue capture for another 60 seconds.
- AN frame sending-delay time: first make sure no IEEE802.15.4 traffic in specified channel and start capture IEEE 802.15.4 frames about 60 seconds. Then start to send Rime uncast frame at its maximum speed and continue capture for another 60 seconds.

the Frame sending-delay time is estimated by scatter graph of the frame interval over time. Normally, if the sending-delay time is stable and predictable, the intervals between the frames will not change very much and the interval points gathers to form a line. Otherwise, if the sending-delay time is changing dramatically and unpredictable, the interval points will scatter from each other. After processing the captured frames, the CTS frame intervals over time (Fig. 4.7a) and AN frame intervals over time (Fig. 4.7b) are acquired. Fig. 4.7a shows that the intervals keep around 64 ms and nearly form a line at first, indicating a stable

sending-delay time. Nevertheless, large fluctuations appear when there is lots of WiFi traffic in air, meaning that the sending-delay time becomes unstable and unpredictable, which makes the scheduling algorithm unreliable and even failure. Fig. 4.7b show a similar pattern with Fig. 4.7a, but the fluctuations are much smaller when lots of Rime packets are transmitting when compared with CTS frame. Thus, CTS frames are very sensitive to WiFi traffic, and the main reason of the low scheduling efficiency is caused by unpredictable CTS frame sending-delay time.

This experiment explains why the scheduling algorithm is not efficient enough. Crowded WiFi traffic results in less accurate scheduling. Especially, the traffic affects CTS much more than AN. In order to improve the efficiency of the implementation, there are serval possible optimized way:

- reducing CTS frame sending-delay time, which can be achieved by reduce back-off time of CTS frame in CSMA/CA mechanism.
- Taking CTS frame sending feedback into consider and optimizing the algorithm. Instead of scheduling CTS at specific time, we may get sending feedback from wireless driver and adjust following AN sending time.
- Using a passive manner: instead of sending AN frame to perform active notification for end node, the algorithm can be designed in MAC layer to perform passive scan of CTS period.

Conclusion

The static time-slot based scheduling algorithm is implemented and evaluated. Although, proposed algorithm shows an overall improvement in terms of Rime PLR and Rime PTR, further experiment shows that there are still limitations for the implementation. the control frame may have a unpredictable sending-delay time before sending. This results in low efficiency of scheduling.

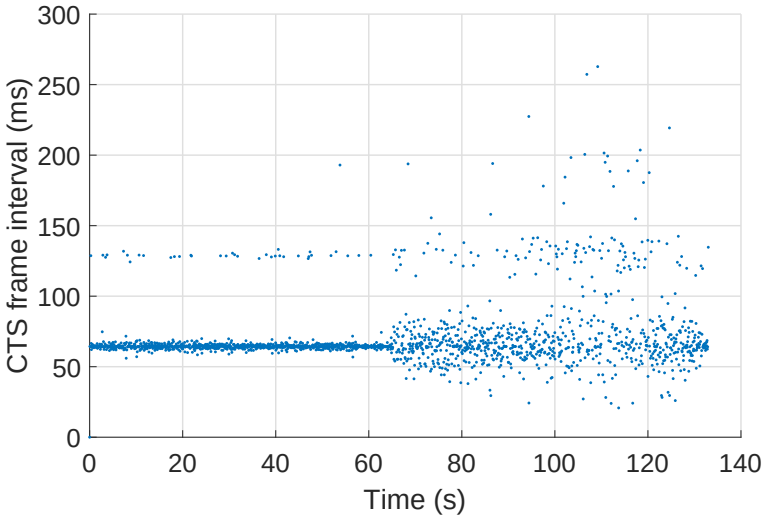

(a) CTS frame intervals

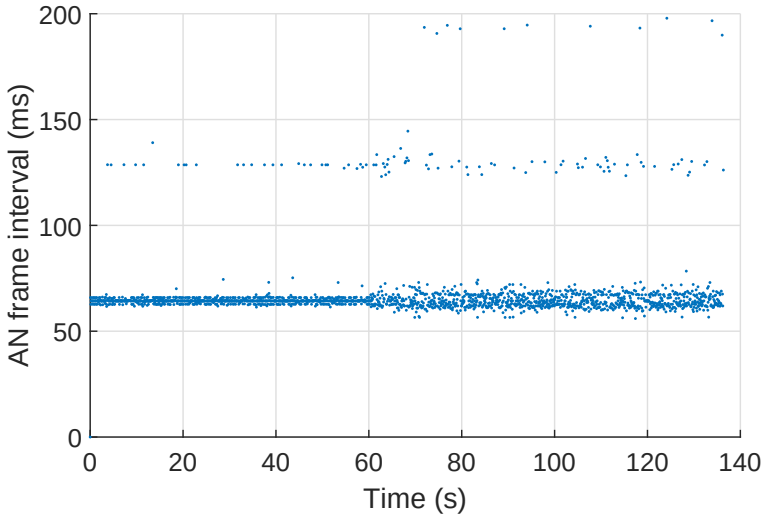

(b) AN frame intervals

Fig. 4.7 Experiment setup

4.1.4 Experiment Two and Evaluation

Reducing CSMA/CA Random Backoff time

IEEE 802.11 supports both Distributed Coordination Function (DCF) and the Enhanced DCF (EDCF) [96]. DCF can only provide best-effort services without any quality of service (QoS) guarantee, while EDCF allow some traffic to have shorter back-off time to access medium, thus reduce the frame sending delay. CIM-HetNet gateway (AR9331 [9]) has an ath9K WiFi PHY, which consist 10 hardware queue (queue0 to queue9) for EDCF. By default, only four of them are enabled in the driver. By modifying the driver, the CTS frame can be sent in a higher priority hardware queue, meaning less sending delay. As conclude in 4.1.3, less sending delay should give a better scheduling result.

In the improved implementation, we use the hardware queue7 to send CTS frames. The reason why we do not use queue9 and queue8 is that reserved for special management frame. Repeat the experiment of 4.1.3, we get Fig. 4.8.

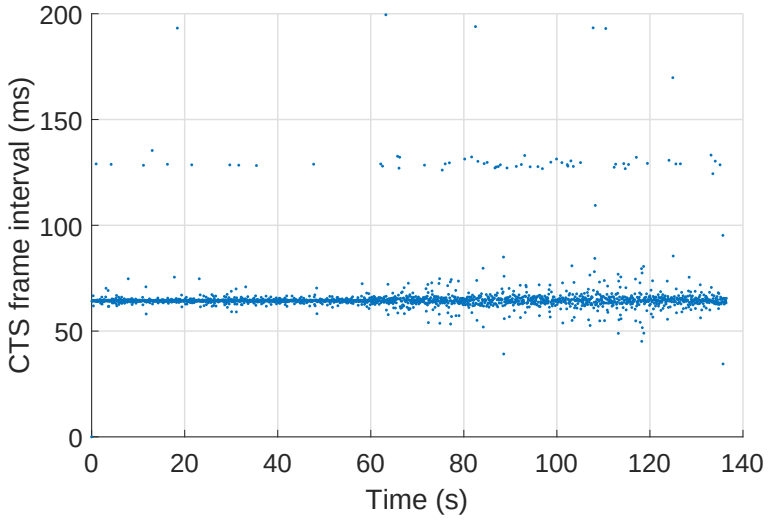

Fig. 4.8 CTS frame intervals

Compare Fig. 4.8 with Fig. 4.7a, the interval dots in Fig. 4.8 tend to gather around 64 ms line, indicating the sending-delay time of CTS frames becomes much more stable.

Packet Loss Ratio of 802.15.4 Rime Data

Repeat the experiment of 4.1.2, we get:

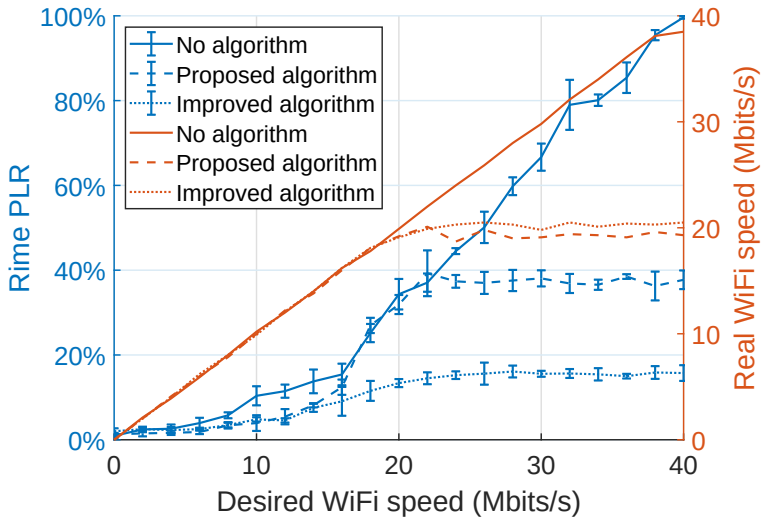

Fig. 4.9 Rime PLR versus Desired WiFi Speed

According to Fig. 4.9, The newly implemented algorithm shows lower PLR, indicating much a better performance. Roughly, the real WiFi speed keeps almost the same with the speed of the old algorithm. When desired WiFi speed increases from 0 to 20 Mbps, the real WiFi speed increases at a linear trend, while the Rime PLR gradually increases in the newly implemented algorithm. When desired WiFi speed more than 20 Mbps, both the real WiFi speed and Rime PLR tend to keep no change. Compared with the old line, the new line show improved Rime network performance.

Unicast Packet Transmission Rate of 802.15.4 Rime Data

Repeat the experiment of 4.1.2, we get:

Fig. 4.10 shows that the new implementation has higher PTR than old one. Especially in the stable phase, the PTR of the new line is about twice higher than the old one. However, when the desired Wi-Fi at the range of 0 5 Mbps, the new line is lower than no algorithm.

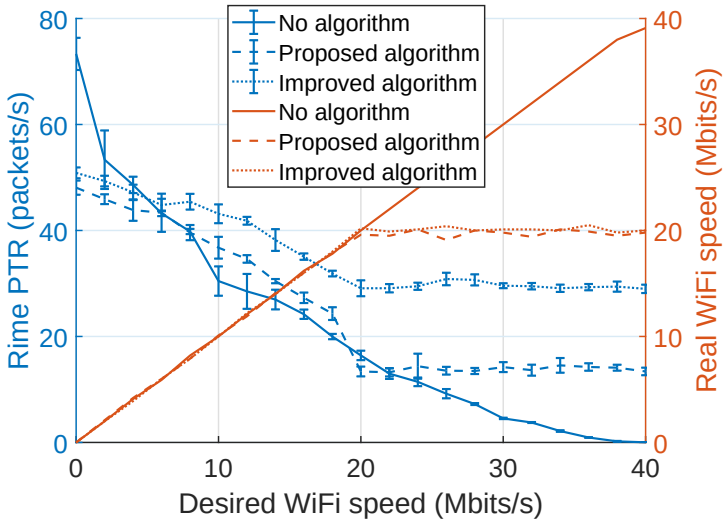

Fig. 4.10 Rime PTR versus Desired WiFi Speed

Conclusion

By changing the ath9k drive and allowing CTS frames to be sent from the high priority queue, the CTS frame CSMA/CA random backoff time is reduced. We observe that the static scheduling algorithm get improved performance, comparing with the experiment one. The LR-WPAN PLR drops by about 50% and the PTR doubles when there is heave Wi-Fi traffic.

As stated previously, the implement of time-slot scheduling mechanism on a hardware platform is a reduced version, and the CSMA/CA random delay can result in low scheduling performance. The experiment reveals this point. More importantly, the experiment also verifies and confirms the effectiveness of the idea of a time-slot based scheduling algorithm. In the following section, we design a full version of the scheduling mechanism in a simulation way and evaluate the performance.

4.2 Simulation Analysis and Evaluation

The previous hardware-based experiment has shown the effectiveness of the time-slot based scheduling mechanism. However, because of the limitation of the hardware, we are not able

to design a full version of the time-slot based mechanism on it. In result, the algorithm tends to be significantly affected by random delay caused by exponential random backoff of underlying CSMA/CA mechanism. This section studies the time-slot based algorithm by simulation. The performance is evaluated in more aspects, e.g. network latency, spectrum usage and scheduling overhead.

4.2.1 Simulation Design

Spectrum-Aware simulation

The simulation is based on NS-3 [41], a discrete-event network simulator. NS-3 manages each function block in modules. We designed a time-slot scheduling mechanism and implemented as modules. Most wireless simulation is based on an abstracted logic channel with an error mode. This type of simulation can not cope coexistence interference of multiple wireless networks, because the logic channels from different network technology are independent of each other and never interfere. Baldo and Miozzo [12] propose a spectrum-aware channel and PHY layer modelling for NS-3, which has the potential to simulate interference between two or more network technologies. The basic idea is to simulate the wireless communication by using a signal which is represented in Power Spectral Density (PSD) over a given frequency band. In order to allow Wi-Fi and LR-WPAN can "see" each other, we employ a Gaussian interference model when adding two signals. Moreover, some work has been done in the LR-WPAN MAC and PHY layer to allow the correct process of the signal interference in the spectrum level.

Fig. 4.11 shows a spectrum graph which is acquired through simulation of Wi-Fi and LR-WPAN network by using a spectrum-aware channel. The Wi-Fi works in channel 6 (2426–2448 Mhz), while LR-WPAN in channel 26 (with a central frequency of 2480Mhz). In this simulation, the Wi-Fi and LR-WPAN work on non-overlapping channel. There are two LR-WPAN nodes. one node sends packets with random payload size to the other at

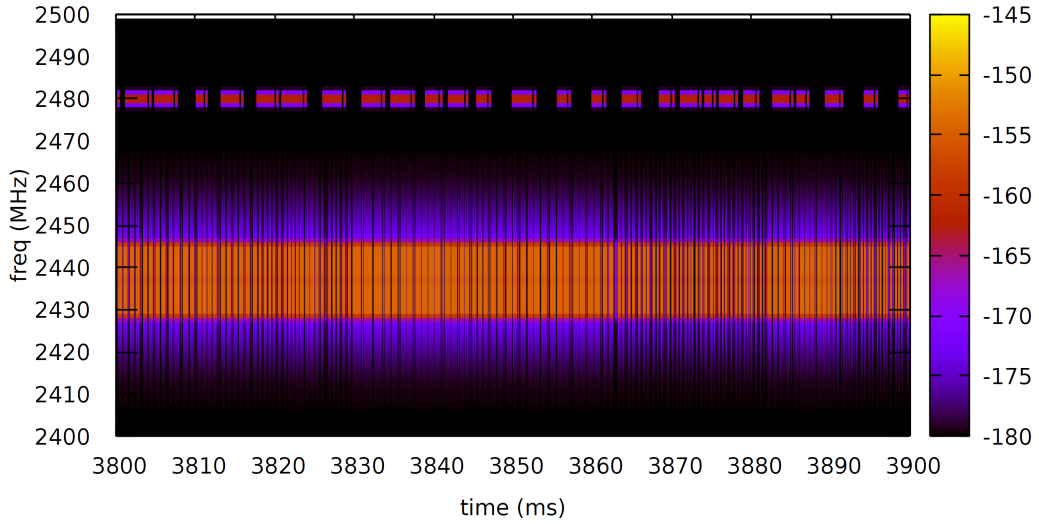

(a) 100ms time duration

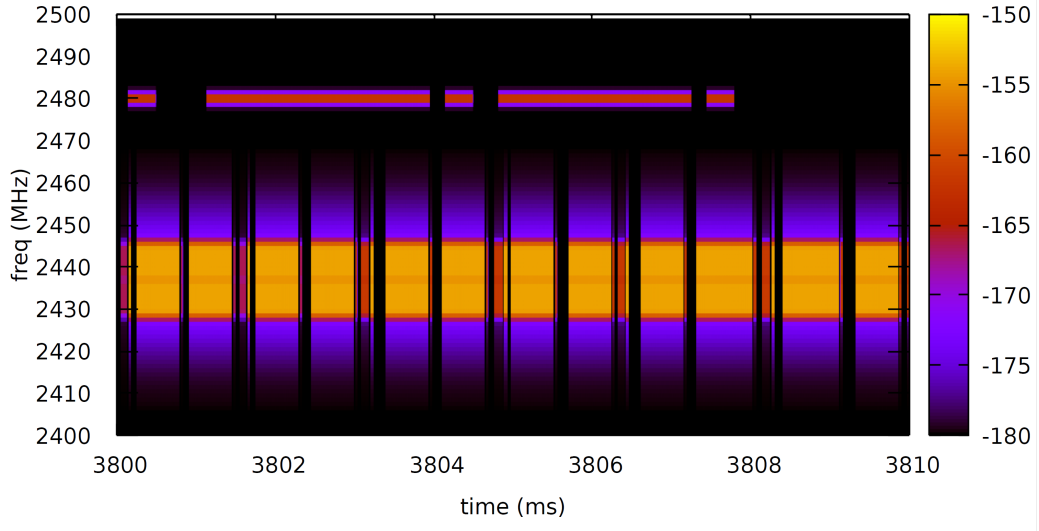

(b) 10ms time duration

Fig. 4.11 Wi-Fi and LR-WPAN spectrum comparison, the spectrum strength is in dBW/Hz

maximum speed. As for the Wi-Fi network, one AP together nine Wi-Fi station form a Wi-Fi network. Each station runs a 3GPP HTTP application [82]. The spectrum graph clearly shows the detail of Wi-Fi and LR-WPAN channel in term of bandwidth, frequency and even out-of-band emission. Fig. 4.11a shows Wi-Fi and LR-WPAN communication over 100 ms duration. It is easy to identify that each LR-WPAN frame followed by an ACK reply. Fig. 4.11b shows a 10 ms duration and can be get by zooming in on Fig. 4.11a.

Scheduling Mechanism Function Block

As shown in Fig. 4.12, in addition to standard network layers, we design the Heterogeneous Wireless Network (HWN) layer, which is an NS-3 module on top of Wi-Fi and LR-WPAN layers. In order to allow the HWN layer to perform scheduling over Wi-Fi and LR-WPAN, the underlying MAC and PHY are modified. For example, we extend the LR-WPAN MAC layer and PHY layer to support AN. High priority CSMA algorithm is also implemented in the CSMA/CA module. Moreover, the CTS frame scheduled by HWN layer is put into a high priority layer to achieve minimum scheduling delay. Unlike the hardware-based time-slot scheduling design, a callback is invoked to notify HWN layer once the CTS frame is transmitted. Therefore, we could implement the full version of the scheduling algorithm, and the CSMA/CA would not be an issue any more.

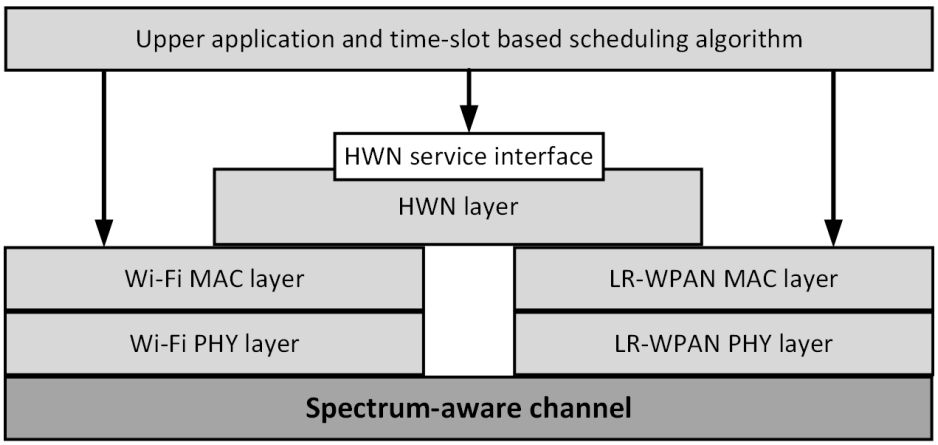

Fig. 4.12 HWN service diagram

An HWN service interface is designed to allow upper layer access the functionalities in HWN layer. It adopts in the form of request, confirm and report. The detail is as below:

- HWN.request: to request an HWN scheduling. the parameters include Wi-Fi slot and LR-WPAN slot length in milliseconds.
- HWN.confirm: to confirm an HWN scheduling. It returns if the request failed or succeeded and scheduling information like CTS sending time, real slot duration, delay compensation time and so on.
- HWN.report: to report statistic during a scheduling cycle, including Wi-Fi slot, LR-WPAN slot, Wi-Fi channel busy time, LR-WPAN channel busy time, Wi-Fi packet counter, LR-WPAN packet counter, and congestion indicators.

4.2.2 Simulation Setup

The experiment aims at providing an evaluation of the static time-slot scheduling algorithm in a simple scenario that consists of three wireless nodes. In addition, one spectrum analyser is introduced to acquire spectrum diagram that is helpful to visualise the communication traffic. The experiment topology is shown in Fig. 4.13. The gateway has an equal distance to both the LR-WPAN node and Wi-Fi station. A spectrum analyser is placed among them. The gateway is equipped with a Wi-Fi AP and an LR-WPAN coordinator. The AP is configured with channel 6 (2426-2488Mhz), and LR-WPAN is channel 17 (central frequency 2435Mhz). Thus these channels are overlapped. The UDP/IP protocol stack module is installed on the Wi-Fi AP and station. Base on UDP, an application is designed to generate UDP traffic at a given speed. Following, network performance is evaluated by generating Wi-Fi at various desired speeds. Because Wi-Fi traffic tends to flow from an AP to stations in the real case, the UDP traffic is generated by the gateway and sent to the Wi-Fi station. As for LR-WPAN, two types of packets are evaluated. The first type is broadcast packets; this type of packets does

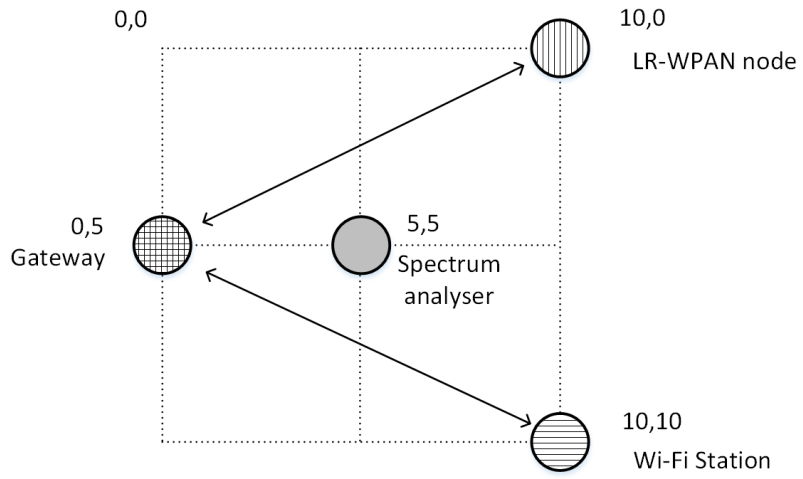

Fig. 4.13 Experiment topology (coordinate unit: meter)

not have an ACK after transmission. The other one is unicast packets, which is sent from LR-WPAN node to the gateway, because the gateway is often a collector and LR-WPAN node, as a sensor, sends data to the gateway in the real case.

The HWN module is installed on the gateway to schedule underlying two wireless technologies as well as provide service interface allow upper applications to design scheduling algorithms. In this section, static algorithms with different slot length configuration are implemented and evaluated.

The spectrum analyser in the centre senses the radio spectrum and helps understand how the time-slot based scheduling mechanism works. For example, as shown in Fig. 4.14, Wi-Fi and LR-WPAN slot is scheduling every 30 ms. The spectrum graph shows the effectiveness of the scheduling algorithm and demonstrates three common cases under a static scheduling.

- **LR-WPAN only** LR-WPAN nodes transmit packets in their allocated tiem slots. They will not send any packet if the slot is not belong to LR-WPAN, even if there is no Wi-Fi traffic.

- **Wi-Fi and LR-WPAN coexistence** LR-WPAN and Wi-Fi nodes transmit packets in their allocated time slots without harmful CTI.

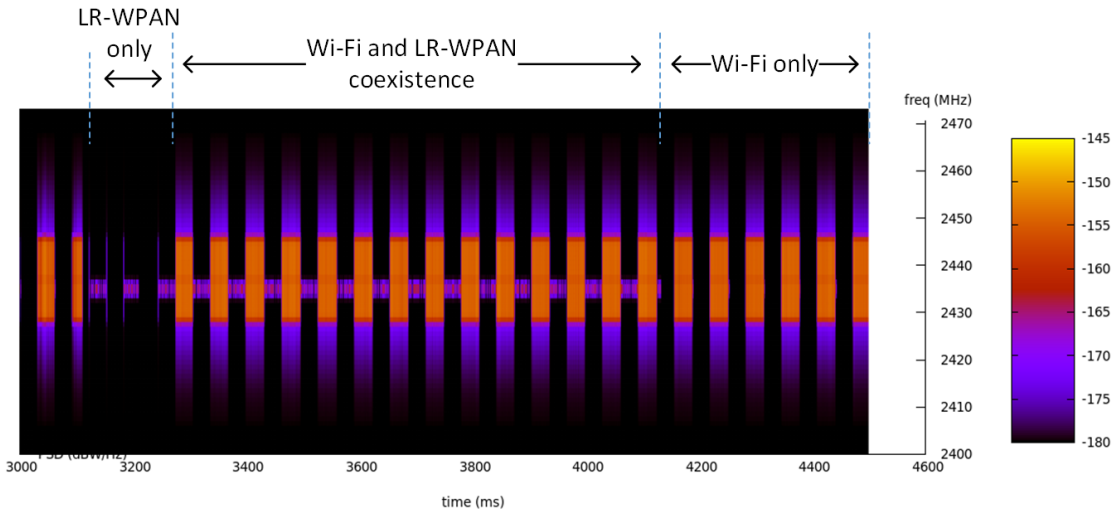

Fig. 4.14 Static scheduling spectrum

- **Wi-Fi only** Wi-Fi nodes transmit packets in their allocated tiem slots. They will not send any packet in LR-WPAN time slot, even if there is no LR-WPAN use the time slot.

4.2.3 Evaluation

LR-WPAN Broadcast vs Wi-Fi UDP

In this simulation, the LR-WPAN end node broadcasts packets to the gateway. Each packet has 20-byte dummy data as the payload of the MAC layer. According to IEEE802.15.4, broadcast packets do not require an ACK after a packet has transmitted. Therefore, there is no retransmission mechanism for this type of packets, and it is ideal to evaluate the PLR. The end node broadcasts a packet every 300ms. As for Wi-Fi, the gateway runs a UDP application and sending data to the Wi-Fi station. The simulation employs Minstrel as the Wi-Fi rate control algorithm because it is widely implemented in popular in Linux-based wireless drivers such as MadWiFi, Ath5k and Ath9k [129, 130].

We carry out simulation by sending Wi-Fi data at different desired Wi-Fi speeds, as shown in Fig.4.15. The diagram legend indicates the type of scheduling algorithm that is

used to acquire a curve. The *original* indicates the data is collected with the default MAC and without proposed scheduling algorithm. The *Scheduling* $Z : W$ indicates static scheduling parameters, where Z and W implies LR-WPAN and Wi-Fi time slot length in millisecond respectively. For instance, *Scheduling* $5 : 30$ means that LR-WPAN time slot is 5ms while Wi-Fi time slot is 30ms.

It is important to know that the desired Wi-Fi speed is not always the same as the real Wi-Fi speed. Once the Wi-Fi network is saturated and reaches its maximum capacity, the real Wi-Fi speed will stop increasing and tends to be lower than desired Wi-Fi speed. Fig. 4.15a depict the relation of the real Wi-Fi speed versus the desired Wi-Fi speed. According to the red line with the legend of *original*, we observed that the real Wi-Fi speed stopped increasing when reaching about 28 Mbps in the simulated network. However, if the static scheduling algorithm is introduced, the maximum Wi-Fi speed is reduced. The reason for this is that the static scheduling algorithm needs to reserve some Wi-Fi channel time and allocates the reserved time to LR-WPAN network. As expected, a big ratio of LR-WPAN and Wi-Fi time slot results in a large impact on Wi-Fi network capacity. The Wi-Fi maximum speed reduces to about 50% when LR-WPAN and Wi-Fi get a same time slot length at 30ms.

When it comes to LR-WPAN PLR diagram in Fig. 4.15b, the PLR performance is significantly improved when introducing static scheduling algorithm. The LR-WPAN PLR increases dramatically with the increase of Wi-Fi traffic. A PLR at 100% is observed when Wi-Fi speed is more than 14 Mbps, meaning that the LR-WPAN cannot survive under the interfere of Wi-Fi, even if the Wi-Fi network is not saturated when there is not a scheduling algorithm. The simulation shows that the static scheduling algorithm reduces PLR to less than 15%. In the case of non-saturated Wi-Fi traffic, the static scheduling algorithm performs even better, and PLR drops to near 0%. For a scheduling algorithm where LR-WPAN and Wi-Fi are configured with the same time slot at 30ms, the PLR keeps at near zero until the Wi-Fi network starts being saturated at about 15 Mbps. In consideration of CSMA/CA MAC

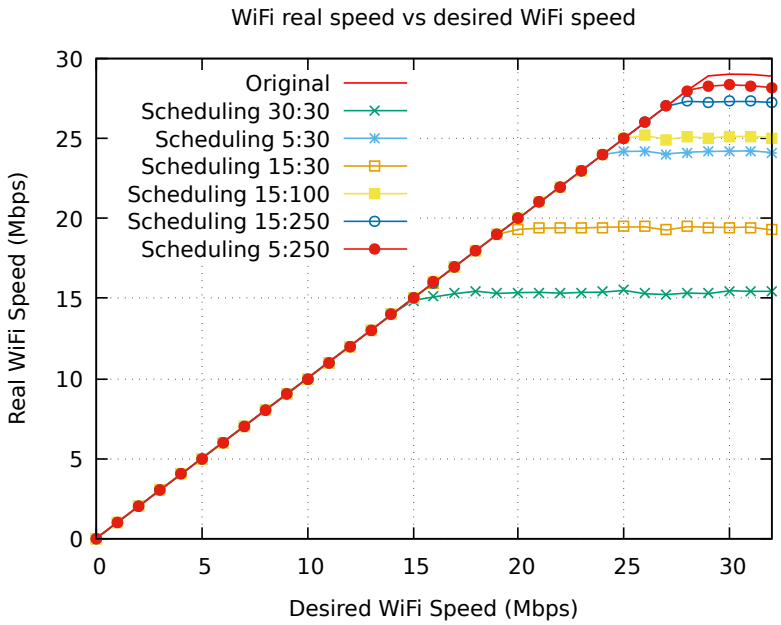

(a) Wi-Fi UDP throughput

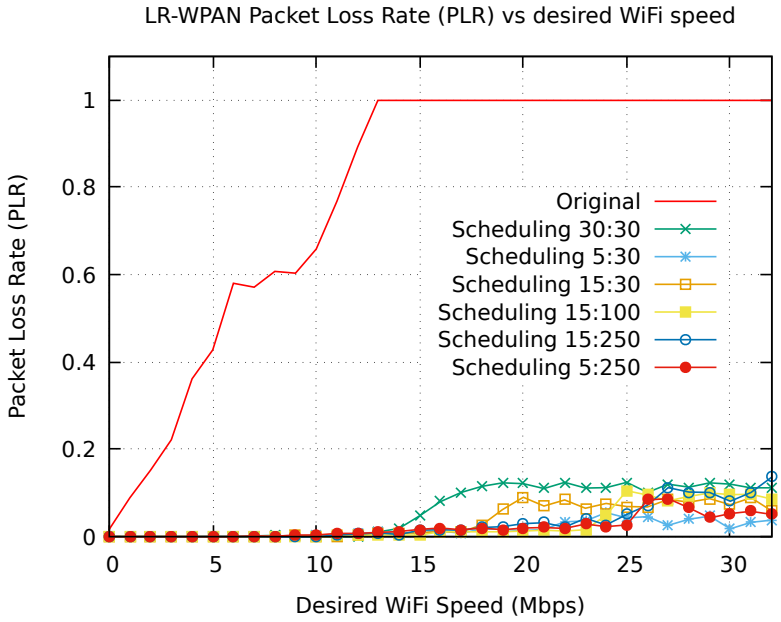

(b) LR-WPAN PLR

Fig. 4.15 Wi-Fi throughput vs LR-WPAN PLR

features that CTS/AN command frame may conflict with ongoing wireless packets, there is a small chance that a scheduling may fail and the chance becomes larger for the busy network. This explains why an increase of PLR is observed when Wi-Fi network is busy.

Comparing Fig. 4.15a and Fig. 4.15b, we found that the static scheduling algorithm decreases PLR substantially at the cost of reduced Wi-Fi network capacity. Nevertheless, if the LR-WPAN time slot is small enough, the impact on Wi-Fi network capacity is negligible.

In addition to the evaluation of the Wi-Fi throughput and LR-WPAN PLR, the packet delay in both networks is also analysed as depicted in Fig. 4.16. In a Wi-Fi network, Fig. 4.16a reveals that the packet delay tends to grow with the increase of Wi-Fi traffic. In other words, the delay is more server in a busy Wi-Fi network. This can be explained by the CSMA/CA working mechanism, in which the random backoff tends to take more time to wait for a clear channel for data transmission. In result, the network experience larger latency in a heavy loaded CSMA/CA-based network. Moreover, the packet delay time soars to an unbelievable value when the Wi-Fi network starts saturating. We investigated the Wi-Fi MAC and found that the network saturated delay is mainly caused by the queuing mechanism in the MAC layer. A packet is put into a queue before transmission in a First-In-First-Out (FIFO) policy. Therefore, a packet can wait for a long before sending out. Because each queue gets a size limitation, some packets are dropped when the queue is full. That is why waiting time in the queue tends to be fixed once the network saturated. As indicated by the curves in the diagram, the packet delay time reaches a maximum delay once the network is saturated. Thus, we mainly consider the time delay before the network is saturated.

On the other side, the default Wi-Fi MAC gives the least network latency and introducing static scheduling algorithm increases packet delay time. According to the diagram, the delay mainly depends on the length of the LR-WPAN time slot. The longer the LR-WPAN time slot is, the more the Wi-Fi packet delay time is. For instance, a long LR-WPAN time slot at 30ms has the longest Wi-Fi delay of 10ms to 20ms. The Wi-Fi network latency is also

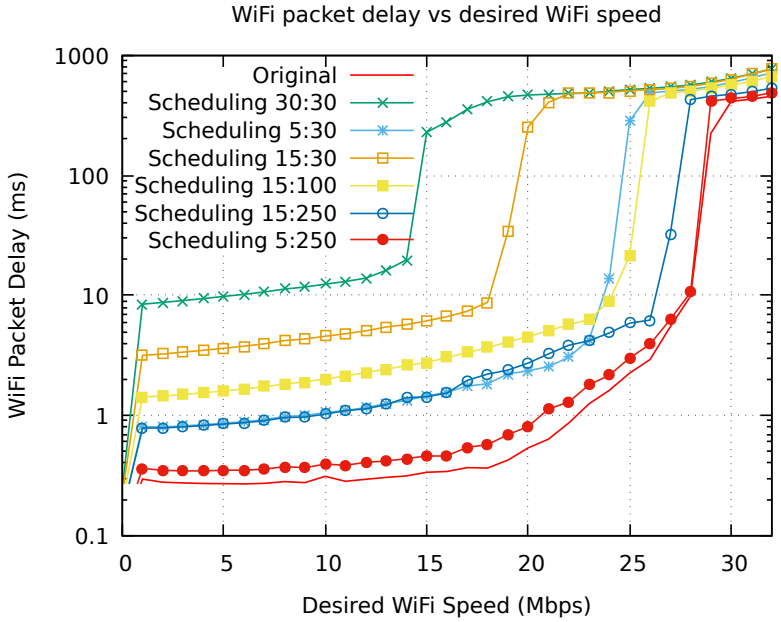

(a) WiFi packet delay

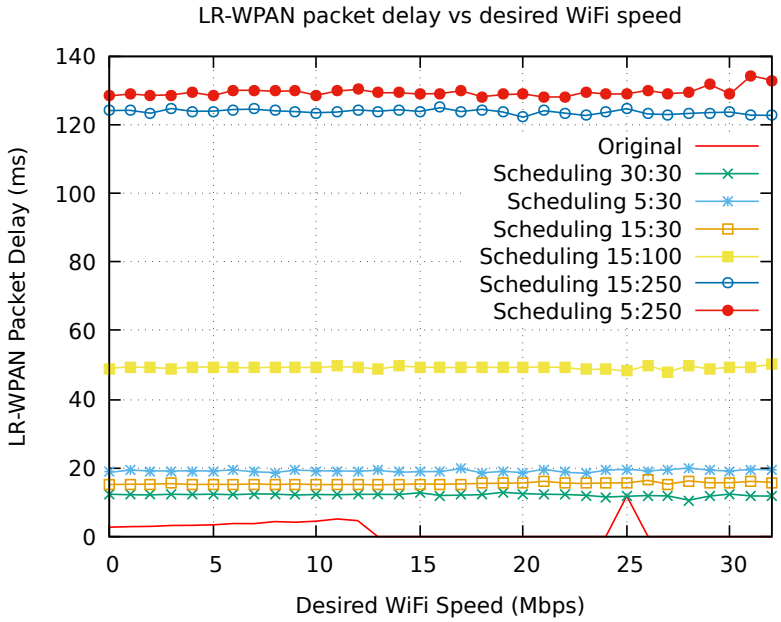

(b) LR-WPAN packet delay

Fig. 4.16 Wi-Fi and LR-WPAN packet delay

affected by the length of Wi-Fi time slot. Generally, the long Wi-Fi time slot gives short packet delay. When it comes to LR-WPAN network, the graph in Fig. 4.16b shows Wi-Fi load does not have a noticeable influence on packet delay. Nevertheless, the scheduling algorithm has a significant effect on network delay. Similar to Wi-Fi, the default LR-WPAN MAC without scheduling has the shortest delay, and the delay tends to grow if with a long Wi-Fi time slot. In the real case, LR-WPAN has rather high tolerance on packet delay, and it normally would not be a problem for such a delay. However, it is another story for Wi-Fi, because long network delay can lead to some applications unusable, i.e. the maximum delay for a VoIP application is 150ms. Therefore, a short LR-WPAN and longer Wi-Fi time slots are recommended. The static algorithm offers an acceptable packet delay on both networks. If the scheduling algorithm is properly configured, the effectuation on packet delay caused by the scheduling algorithm is marginal in a Wi-Fi network.

We also collect the Slot Usage Ratio (SUR) of the simulation. Fig. 4.17a shows SUR of Wi-Fi grows with the increase of desired Wi-Fi speed. All the curves stop increasing when the SUR reaches around 75%, which indicates Wi-Fi network is saturated. In other words, different time slot configurations do not affect the SUR for a saturated Wi-Fi networks. It also confirms that CSMA/CA cannot utilise all channel time for data transmission, because it requires a contention period to avoid conflation which is achieved by random backoffs. However, the time slot configuration determines the slopes of curves and the inflexion point when Wi-Fi network is saturated. Together with Wi-Fi throughput in Fig. 4.15a, for a given time slot configuration, both diagrams show the infection points happen at the same desired Wi-Fi speed.

Fig. 4.17b reveals that the Wi-Fi load does not have obviously influence on LR-WPAN SUR. The reason for this includes:

- Wi-Fi and LR-WPAN traffic are separated in different time slot with an effective scheduling algorithm and they do not affect each other.

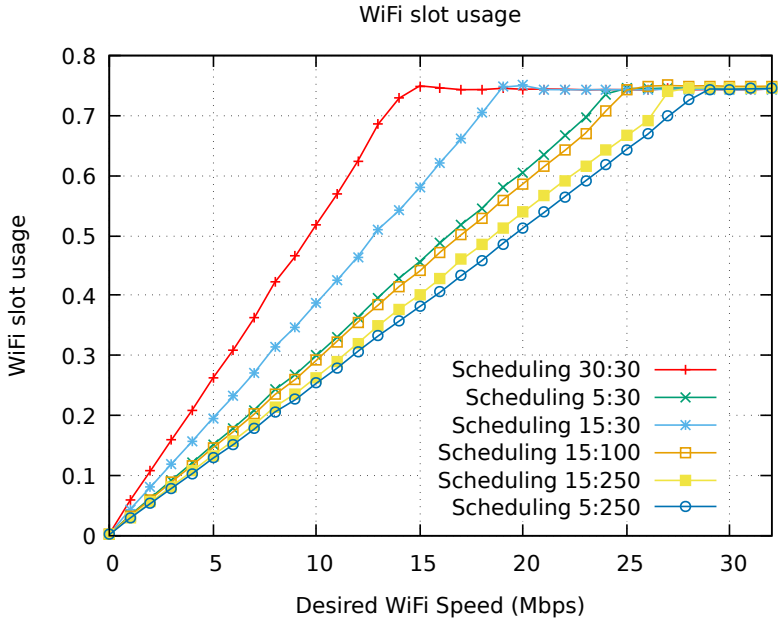

(a) Wi-Fi slot usage

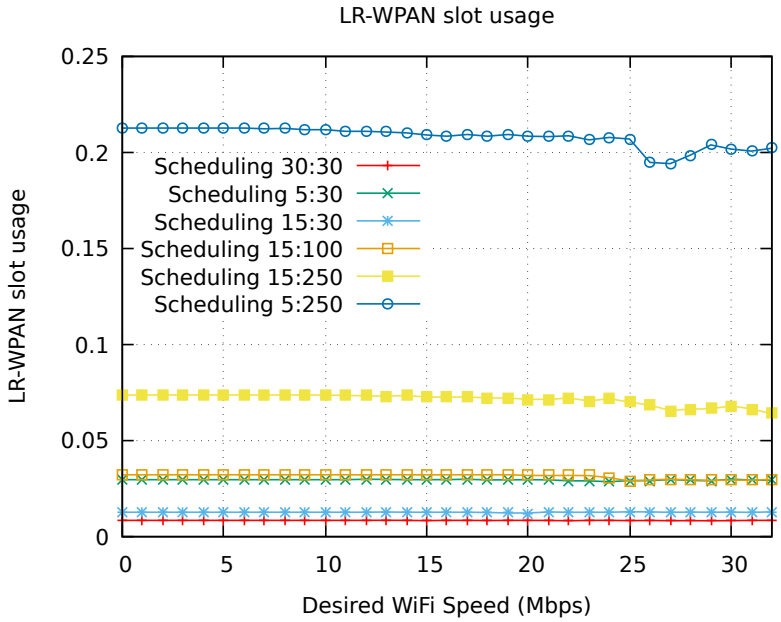

(b) LR-WPAN slot usage

Fig. 4.17 Wi-Fi and LR-WPAN slot usage

- LR-WPAN transmission packet at a fixed interval of 300ms and the length of packets are the same, indicating the LR-WPAN network has fixed load.

We could define time slot ratio (R_{WZ}) as below:

$$R_{WZ} = \frac{T_W}{T_Z} \tag{4.1}$$

Where T_Z and T_W are LR-WPAN and Wi-Fi time slot lengths. We observe that SUR of LR-WPAN mainly depends on R_{WZ}. A small R_{WZ} value helps reduce LR-WPAN SUR, because more channel time is allocated to LR-WPAN network for data transmission. However, A small R_{WZ} results in large slopes of Wi-Fi SUR curves and smaller Wi-Fi network capacity because less channel time is left for Wi-Fi network.

As mentioned before, the proposed time-slot based scheduling algorithm does have some overhead, because the algorithm is achieved by periodically sending CTS/AN command frames that occupy additional channel time. Fig. 4.18a shows that the desired Wi-Fi speed has no observable impact on the scheduling overhead, while it is determined by the scheduling cycle time. It shows the SUR decreases with the increase of scheduling cycle time. For example, the *Schdeling* $5:30$ with the shortest cycle time of six curves has the highest scheduling overhead at 2.8%, which is still rather a small portion.

Because the time-slot based scheduling mechanism sits on top of CSMA/CA MAC layer and CSMA/CA get a random delay when sending a packet, the scheduling command frames unavoidable encounter delay, too. Fig. 4.18b gives the simulation results on the scheduling delay. The graph looks similar to Wi-Fi data packet delay in 4.16a at first glance because they both increase over desired Wi-Fi speed and reaches a maximum once Wi-Fi network saturated. However, they have a large difference. The maximum delay for Wi-Fi data is up to 800ms, while this value for scheduling delay is less than 0.8 ms. The reason is that the scheduling command frames are designed to have higher priority over data packets as described in the section of time-slot design.

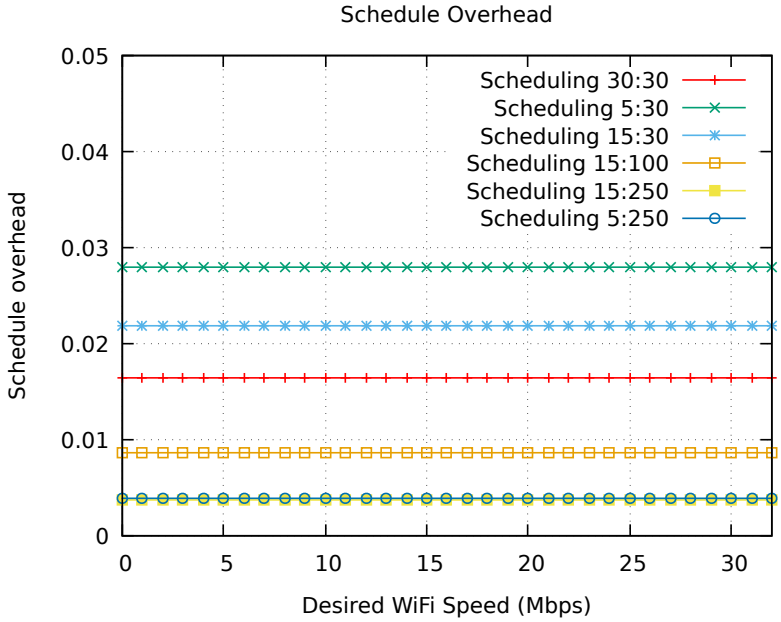

(a) HWN scheduling overhead

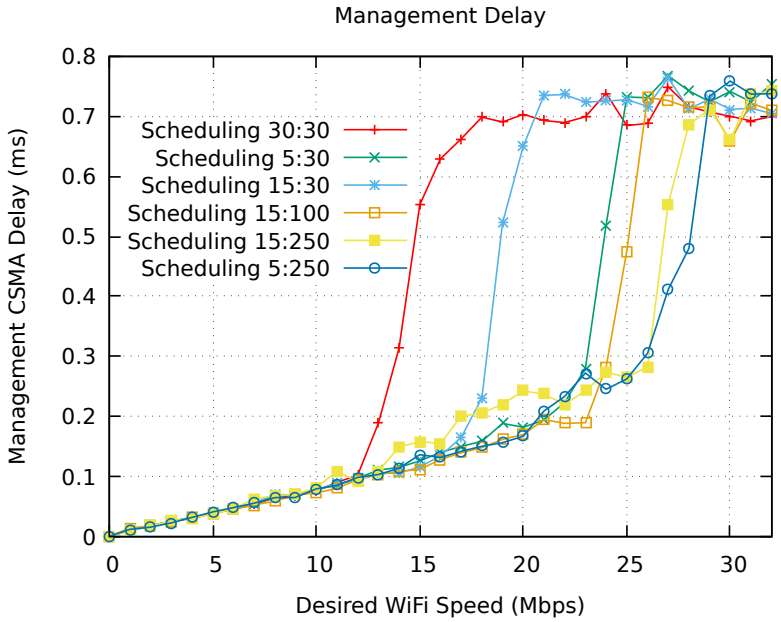

(b) HWN scheduling delay

Fig. 4.18 HWN scheduling delay and overhead

LR-WPAN Unicast vs WiFi UDP

This simulation evaluates the static time-slot based scheduling algorithm by sending LR-WPAN data to the gateway by unicast at fastest speed within given time slots. The unicast would apply ACK mechanism and retransmission if no ACK received in order to guarantee reliable sending. In comparison with the previous simulation, this section has differences as below:

- This section uses LR-WPAN unicast instead of broadcast. LR-WPAN unicast packets require an ACK reply to confirm a successful data transmission. If no ACK is received, the sender needs to perform a retransmission process. In the previous simulation, the LR-WPAN node just broadcasts packets out without ACK confirmation
- This section sends LR-WPAN packets at the maximum data rate to evaluate LR-WPAN throughput in PTR. However, the previous simulation does not assess LR-WPAN throughput and packets is sent with a fixed interval of 300ms.

Fig. 4.19 shows the simulation results. Fig. 4.19a and Fig. 4.19b are plotted from the same data source, but in different scales. The linear scale diagram give clear view on the curves with a high PTR, while the logarithmic enables to have a detail view for curves with small PTR.

The diagrams show a significant improvement in LR-WPAN throughput with static time-slot based scheduling algorithm when there is moderate or heavy Wi-Fi traffic. When there is no Wi-Fi interference, the default LR-WPAN MAC has the highest throughput of the seven curves. However, the PTR drops dramatically once Wi-Fi traffic is introduced. For example, the PTR drops by 50% percent with less than 3 Mbps Wi-Fi traffic and the PTR drops to an unusable value once Wi-Fi traffic beyond 6 Mbps. Introducing static scheduling algorithm can guarantee LR-WAPN throughput. Different time-slot configuration in the algorithm results in a large difference in LR-WPAN through. For example, *Scheduling* 30 : 30 can guarantee

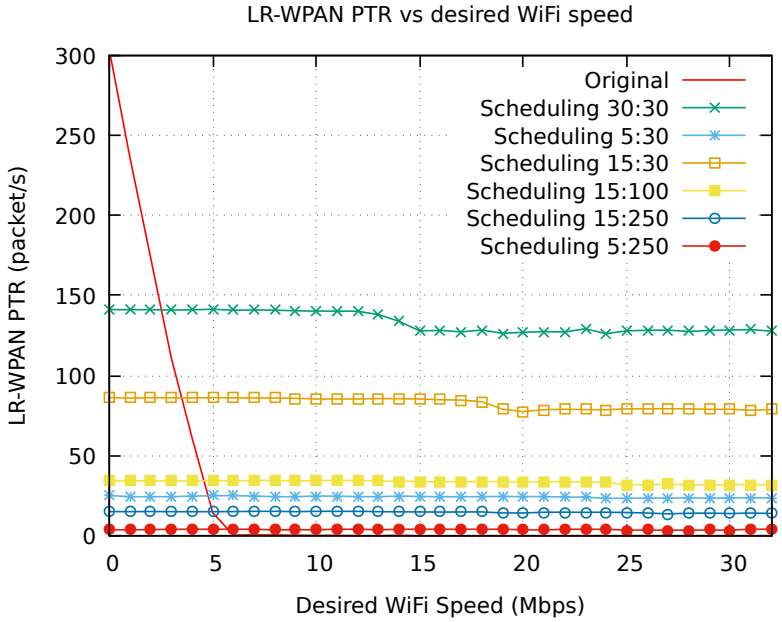

(a) Linear scale

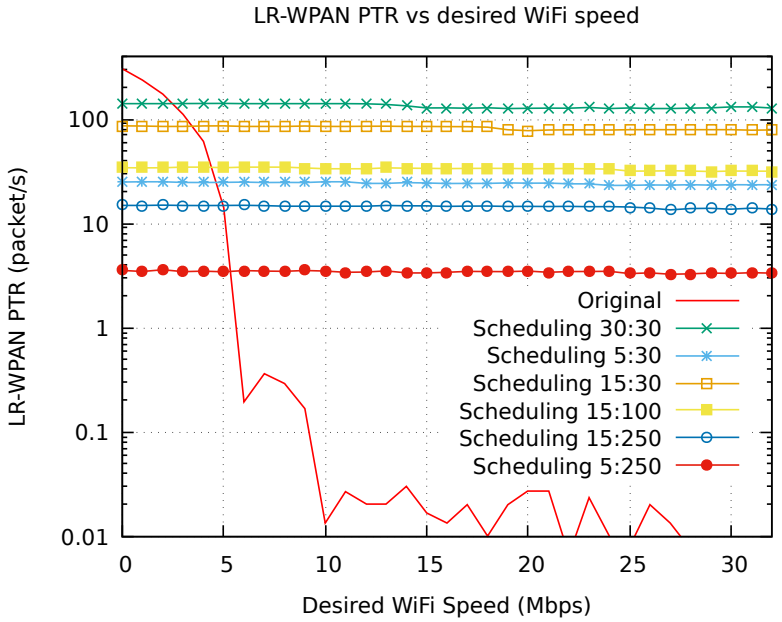

(b) Logarithmic scale

Fig. 4.19 LR-WPAN PTR vs desired Wi-Fi speed

throughput of more than 130 packets/s, while *Scheduling* 5 : 250 only gives throughput around four packets/s. The throughput is mainly determined by the Wi-Fi time slot (T_W) and the LR-WPAN time slot (T_Z). Piratically, the PTR with the scheduling algorithm in this simulation can be estimated by the below equation:

$$PTR_e = \frac{PTR_s \cdot T_Z}{T_Z + T_W} \tag{4.2}$$

Where PTR_e is the estimated LR-WPAN PTR and PTR_s is the PTR when LR-WPAN is saturated with standard MAC without interference from Wi-Fi. The PTR_s is about 300 packets/s in this simulation. For example, we could estimate the PTR for *Scheduling* 30 : 30 at 150 packets/s. Table 4.1 gives the comparison estimated PTR and real PTR. The estimation works well for a longer LR-WPAN time slot, but it tends to get an error when LR-WPAN time slot as short as 5ms. This reason may be that the time slot is too short that only one LR-WPAN can be transmitted and leave some unusable time fragment at the end of the slot. For instance, for a given slot time of 5ms, we assume that it takes 3ms to transmit a packet. We could infer that only one packet can be transmitted in such a time slot because transmitting two packets need at least 6ms. In result, remained 2ms became an unusable time fragment and is waste, which causes estimation error.

Table 4.1 LR-WPAN PTR estimation

LR-WPAN slot (ms)	Wi-Fi (ms)	Estimated PTR (packets/s)	Measured PTR (packets/s)
30	30	150	145
5	30	42.9	25
15	30	100	82
15	100	39.1	34
15	250	17	14
5	250	5.9	3.5

Besides the study on LR-WPAN and Wi-Fi throughput, this simulation also collects similar statistics as in the previous simulation for evaluation. Most of them confirm the results in the previous simulation, and some get a minor difference. For instance, Fig. 4.20 depicts the packet delay of LR-WPAN and Wi-Fi. In comparison with Fig. 4.16a, the Wi-Fi packet delay becomes larger for default MAC without scheduling algorithm. The Wi-Fi packet delay can be even shorter by using *Scheduling* 5 : 250 where LR-WPAN and Wi-Fi have a time slot of 5ms and 250ms respectively. This can be explained by CTI where LR-WPAN node tries to send packets at its maximum rate, and this can result in harmful interference to Wi-Fi, thus the Wi-Fi packet delay increases. Similarly, as shown in Fig. 4.20b, the packet delay for LR-WPAN without scheduling can be longer than that with the scheduling algorithm.

In addition, the LR-WPAN slot usage in Fig. 4.21 increases comparing with previous simulation results, because the LR-WPAN data is sent at the fastest speed and use more channel time. The results also indicate that the LR-WPAN time slot length is the main factor to determine the SUR in this simulation and the curves with the same LR-WPAN slot length tends to have the similar SUR.

4.3 Summary

This chapter designs a simple static time-slot based scheduling algorithm. Then the algorithm is analysed and evaluated by both hardware-based experiment and NS-3 based simulation.

In consideration of the limitation of the hardware radio modules, only a reduced version of the scheduling mechanism is implemented. The experiment shows a significant improvement on LR-WPAN PLR and PTR when there is moderate or heavy Wi-Fi interference, which confirms the effectiveness of the time-slot based scheduling mechanism. Nevertheless, the static scheduling algorithm reduces maximum Wi-Fi throughput by about 50% in our

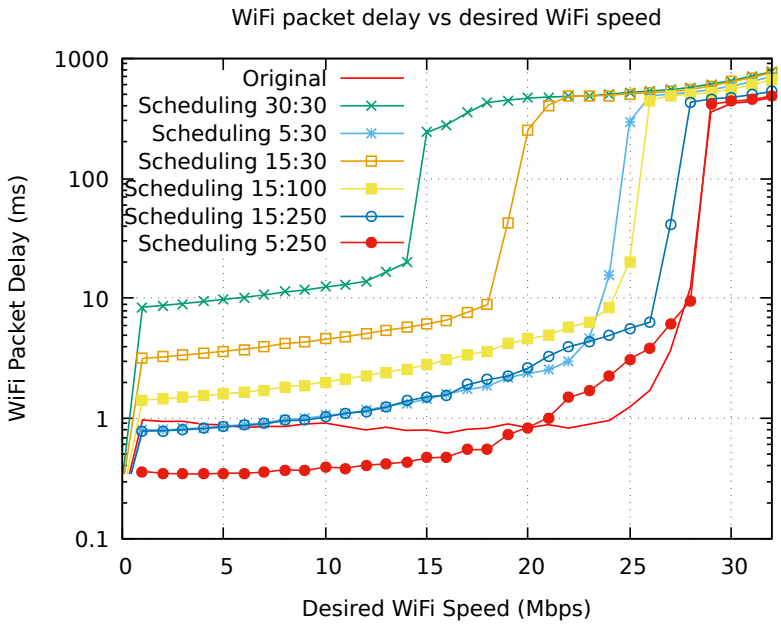

(a) WiFi delay

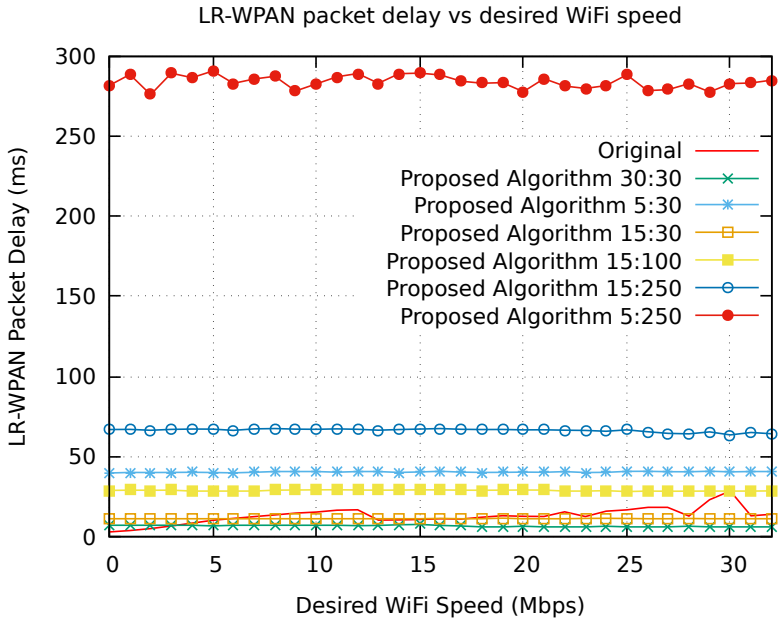

(b) LR-WPAN packet delay

Fig. 4.20 LR-WPAN and LR-WPAN packet delay

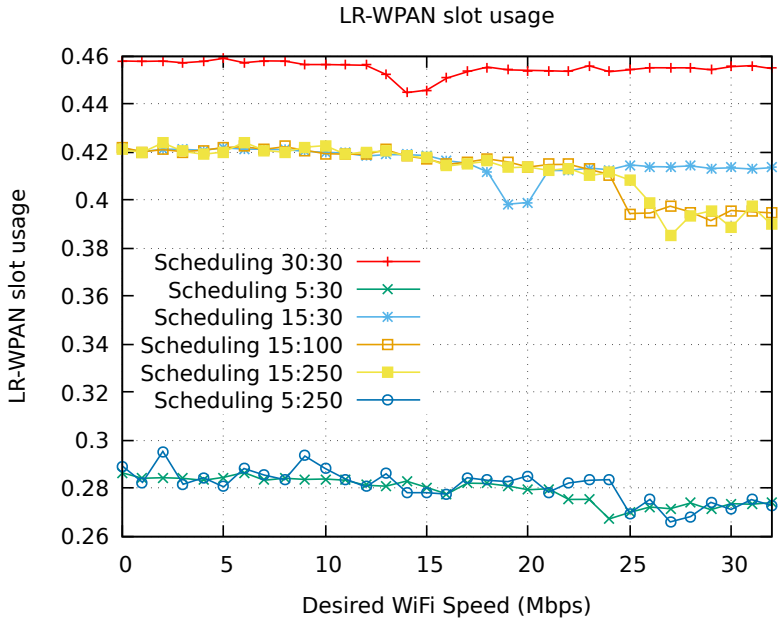

Fig. 4.21 Lr-wpan slot usage

experiment, because the algorithm schedules fixed 32ms for each network, which means that half of the channel time is allocated to LR-WPAN.

Thanks to spectrum-Aware simulation, we design an HWN module for NS-3, which implements a full version of the scheduling mechanism. Based on this, the static scheduling algorithm is evaluated in more aspects. The simulation shows that the standard LR-WPAN network can be blocked by heavy Wi-Fi interference. However, the proposed static scheduling algorithm reduces LR-WPAN PLR to less than 15% when there is heavy Wi-Fi traffic, while this value is 100% without scheduling algorithm. For the light and moderate Wi-Fi traffic, the algorithm reduces LR-WPAN PLR to almost zero. The proposed algorithm also improved LR-WPAN PTR when Wi-Fi traffic presents. Similar to hardware-based experiment, the simulation reveals that the scheduling reduces Wi-Fi throughput and the level of the reduction depends on the Wi-Fi and LR-WPAN time slot ratio. Specifically, a high ratio gives high Wi-Fi throughput but low LR-WPAN PTR, while a low ratio gives low Wi-Fi throughput but high LR-WPAN PTR. Moreover, the simulation assesses packet delay for both networks.

The scheduling algorithm can introduce an extra delay for packet transmissions but at an acceptable level. A proper time-slot configuration for the algorithm shortens the packet delay caused by the algorithm. Finally, because the scheduling algorithm does have some overhead, the simulation evaluates scheduling overhead by applying algorithms, and the result shows that the overhead is small with a range from 0.5% to 2.8% for six time-slot configurations.

What is more, the experiment and simulation reveal some limitation of the static algorithm. For example, the scheduling algorithm decreases Wi-Fi throughput, which depends on the Wi-Fi and LR-WPAN time slot ratio. The principle behind the time-slot mechanism is to design a TDMA layer on top of the CSMA layer, which allocates channel time to a network periodically and enables CTI free channel access. Allocating more channel time to one network unavoidably decrease the performance of the other. Thus, it is important to keep the allocation fair. Another limitation is the packet delay. Prior to sending a packet, a wireless node need to take extra time to wait for a time slot that belongs to itself. Thus, longer scheduling cycle time can result in larger packet delay time. The scheduling algorithm can be further optimised by scheduling the time slot length in an adaptive way that will be discussed following chapter.

Chapter 5

Adaptive Time-Slot Based Resource Scheduling Algorithm

As discussed in the previous chapter, the static scheduling algorithm mitigates CTI effectively and improve LR-WPAN PLR significantly when there is moderate or heavy Wi-Fi interference. However, the time-slot length configuration can be tricky, because allocating more channel time to one network unavoidably decreases the performance of the other. For example, if half channel time is allocated to LR-WPAN, the Wi-Fi throughput can drop by about 50%.

This chapter proposes an adaptive time-slot based scheduling algorithm to address this problem. The basic idea is to allocate a time-slot length dynamically according to the network crowdedness. For instance, if LR-WPAN is with only light traffic and Wi-Fi network gets saturated, the adaptive algorithm can increase Wi-Fi slot time and borrow some channel time from LR-WPAN. In order to achieve adaptive scheduling, the concept of congestion indicator is proposed to assess network crowdedness, and then the adaptive algorithm is designed to allocate slot time dynamically by using a crowdedness-based fair scheme.

5.1 Challenges

In the static scheduling algorithm, the channel time is allocated at a fixed ratio without considering the real demand of the networks. The fixed time slot allocation is not reasonable sometime. For example, the time slot allocated to a Wi-Fi network may not be adequate, and it may require more channel time to download a big file, while the LR-WPAN is almost idle in its time slot at the same time. If the time-slot is fixed, the LR-WPAN time slot is wasted. It can be better if shortening the LR-WPAN slot and increasing Wi-Fi slot in this case.

The basic idea to design an adaptive time-slot based scheduling algorithm is to allocate time slot length for LR-WPAN and Wi-Fi network in real-time according to the historical time slot crowdedness. The scheduling should meet below requirements:

- **High overall performance**: the algorithm needs to "borrow" channel time from the idle network and allocate to the busy network when it is necessary.
- **Fairness**: the algorithm needs to guarantee fairness between LR-WPAN and Wi-Fi network if both networks are busy. In other words, the time slot allocation needs to reach a balance point if both networks are busy.
- **Low scheduling overhead**: When the networks are in high load, the algorithm can increase the scheduling cycle time to reduce scheduling overhead.
- **Low network latency**: the algorithm can decrease scheduling cycle time to reduce packet transmission delay if both networks are with light traffic. Moreover, the maximum packet delay caused by the scheduling algorithm should be limited. Especially for Wi-Fi, excessively network latency can lead to the failure of some time-critical application (e.g., VoIP).

In order to achieve adaptive scheduling, it is critical to assess the time slot crowdedness. Slot Usage Ratio(SUR) reflects whether the current slot is crowded or not to some extent.

This section investigation on Slot Usage Ratio(SUR) and explain why it is not a good option to assess the time slot crowdedness.

5.1.1 Slot Usage Ratio (SUR)

A stable indicator is required to show the crowdedness of Wi-Fi and LR-WPAN slots. One possible selection is to use Slot Usage Ratio(SUR), which can be simply defined as below:

$$SUR = \frac{Transmition\ time\ of\ all\ the\ frames\ in\ a\ slot}{Cooresponding\ slot\ duration} \tag{5.1}$$

In a slot, if N frames are received and sent. We can get IEEE 802.15.4 Slot Usage Ratio (SUR_Z) and Wi-Fi Slot Usage Ratio (SUR_W)

$$SUR_Z = \frac{\sum_{n=1}^{N} T_{Z,n}}{T_{Z,slot}} \tag{5.2}$$

$$SUR_W = \frac{\sum_{n=1}^{N} T_{W,n}}{T_{W,slot}} \tag{5.3}$$

$T_{Z,n}$ and $T_{W,n}$ denote the transmission of nth frame for IEEE 802.15.4 and WiFi. Due to IEEE 802.15.4 devices tend to be a low performance, the slot usage equation can be simplified. Together with equation 3.3

$$SUR_Z = \frac{\sum_{n=1}^{N} T_{Z,MPDU,n} + \sum_{n=1}^{N} \left(T_{Z,BF,n} + T_{Z,CCA,n} + T_{Z,Rx2Tx,n} + T_{Z,SHR,n} + T_{Z,PHR,n}\right)}{T_{Z,slot}} \tag{5.4}$$

In an IEEE 802.15.4 network, $T_{Z,BF,n}$, $T_{Z,CCA,n}$, $T_{Z,Rx2Tx,n}$, $T_{Z,SHR,n}$, and $T_{Z,PHR,n}$ are constants, and the sum of them (T_{const}) is 832 microseconds according to the specification. IEEE 802.15.4 define only one channel rate (R_Z) in 2.4GHz band and the MPDU is exactly the PHY payload, the sizes of which ($S_{Z,MPDU}$) is indicate in PHR. It is obviously that

$$T_{Z,MPDU} = \frac{8 \cdot S_{Z,MPDU}}{R_Z} \tag{5.5}$$

Simplify equation 5.4, we have

$$SUR_Z = \frac{\frac{8}{R_Z} \cdot \sum_{n=1}^{N} S_{Z,MPDU} + N \cdot T_{const}}{T_{Z,slot}} \tag{5.6}$$

Thus, IEEE 802.15.4 slot usage is acquired by two simple statistics: (a) the number of frames transmitted and received in the slot, (b) the quantity of MAC layer data send and received in bytes. These data can be collected in the MAC layer.

5.1.2 SUR Evaluation

In order to evaluate if SUR is a stable indicator to reflect crowdedness, NS-3 based simulation is conducted on LR-WAPN and Wi-Fi network. The simulation adopts the same network setup as in section 4.2.3. The LR-WPAN end node sends unicast packets to the gateway, and Wi-Fi AP sends UDP packets Wi-Fi station. Differently, the simulation assesses SUR against different packet sizes and time slot length.

If the data are sent at the maximum rate, the network reaches its maximum capacity, namely the network is saturated and the most crowded. At such a crowdedness level, a reasonable indicator should give the same result. Thus, the algorithm can know a network is saturated, and more channel time is required to further increase network performance. Based on this, this section presents two simulations to evaluate if SUR can give a stable/fixed output when the network is saturated.

The first simulation is designed for Wi-Fi SUR. As shown in Fig. 5.1, each data point is acquired by setting a Wi-Fi slot and packet size. In detail, the simulation is conducted in many rounds. In each round, we set a specific Wi-Fi packet size and adopt a static scheduling algorithm with a given Wi-Fi slot time; and then Wi-Fi AP sends data at maximum speed.

The simulation lasts for 300s in each round. A curve is acquired by configuring Wi-Fi slot time from 5ms to 245ms with a step of 5ms. Repeating simulation by setting packet size from 200 to 1472 bytes, seven curves are plotted.

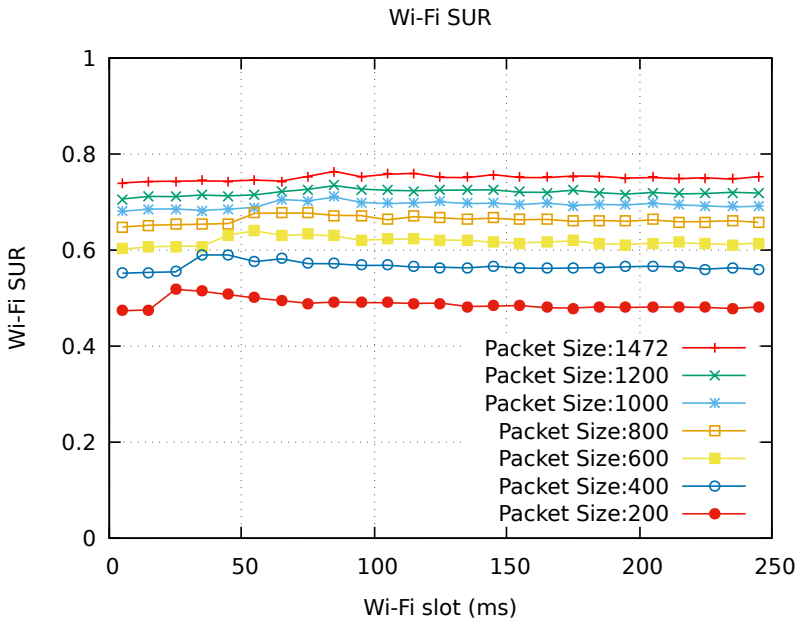

Fig. 5.1 WiFi slot usage

The result shows that the SUR can give a stable output with the same packet size over different Wi-Fi slot settings. For instance, when the packet size is 200, the SUR is around 0.48. This value is quite stable with a small fluctuation when Wi-Fi slot length is configured from 5ms to 245ms. However, the SUR can be excessively affected by the transmission packet size. If the packet size increases from 200 to 1472 bytes, the SUR can grow from 0.48 to 0.75, or the SUR increases by around 56%. Therefore, Wi-Fi SUR is not a good indicator for Wi-Fi crowdedness, because this value highly depends on the packet size, and it gives different outputs when the network is saturated. In other words, it is no way to determine if the allocated slot is adequate for Wi-Fi data transmission even the Wi-Fi SUR is known, because the same SUR value may imply a different level of crowdedness. For example, a SUR at 0.48 may indicate the Wi-Fi network reaches its maximum capacity with a packet

size of 200 bytes, and the algorithm may need to increase the Wi-Fi slot time to enable a higher Wi-Fi throughput. However, it may also indicate the network has not saturated yet when the packet size is 1472 bytes, and there is no need to increase Wi-Fi slot time.

Similarly, the second simulation is carried out to evaluate LR-WPAN SUR, in which the LR-WPAN packets at different sizes are sent from the LR-WPAN end node to the gateway at maximum speed. As shown in the Fig. 5.2, in consideration of differences between Wi-Fi and LR-WAPN, a curve is acquired by configuring LR-WPAN slot time with a short range from 1ms to 30ms, because long LR-WPAN may result in Wi-Fi packet excessively delayed that some time-critical Wi-Fi application can fail. Another difference is that the seven curves are plotted by setting packet size from 12 to 100 bytes because the LR-WPAN have much shorter MAC payload than Wi-Fi.

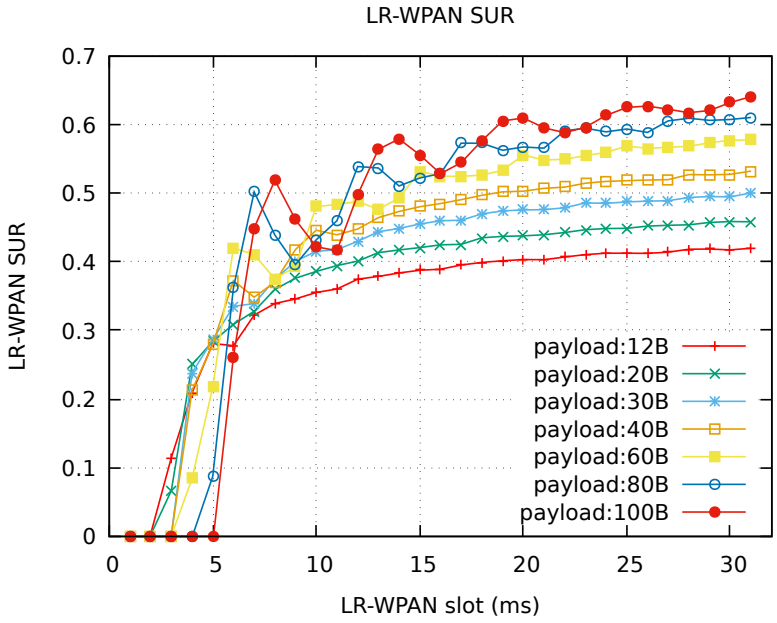

Fig. 5.2 Lr-wpan slot usage

The diagram can be explained by dividing the slot time into two ranges. One range is when the slot time is less than 6ms, in which the LR-WPAN slot is to short that an LR-WPAN packet is hard to fit into the slot. For example, for the successful transmission of a 100-byte

packet, it requires about 5ms to 7ms, including data frame transmission, ACK transmission, turnaround time and random CSMA/CA backoff time. Thus, a long packet is not likely transmitted within a short time slot. Fig. 5.2 confirms this point and the SUR is zero when the packet size is 100 bytes with a slot time less than 6ms. Therefore, the minimum time slot setting in an adaptive scheduling algorithm should not be less than 6ms to allow a long LR-WPAN packet to be transmitted. The other range is when the slot time is equal or more than 6ms, in which the LR-WPAN slot is long enough to fit at least one packet into a slot. The simulation shows that SUR in this range highly depends on the LR-WPAN slot and the packet payload size. Generally, a larger packet size gives a higher SUR. Different from Wi-Fi SUR that has stable value over different slot time, the LR-WPAN SUR grows with the increase of time slot length. Combining the factors of time slot and packet payload, a saturated LR-WPAN network can have SUR range from 0.3 to 0.65. Therefore, LR-WPAN SUR is not a good indicator for LR-WPAN network crowdedness, because the same LR-WPAN SUR may indicate either the network is saturated to require more channel time or the network is still with light traffic and no more channel time required. For example, a SUR at 0.3 may indicate the LR-WPAN has reached its maximum capacity with a payload of 20 bytes and slot time of 6ms, while this value only reaches a half capacity of a time slot with a payload of 80 bytes and slot time of 31ms. Therefore, the algorithm can not make a decision if an allocated time slot is adequate or not for data transmission and a new indicator is required to get an accurate assessment on time slot crowdedness.

5.1.3 Conclusion

One of the crucial challenges for an adaptive time-slot based scheduling algorithm is to tell whether an allocated time slot is adequate for data transmission or not for a specific network. It is obvious that the number of transmitted packets is not a proper answer. An idea to decide if a time slot is adequate for data transmission is by distinguishing whether the network is

saturated or not. If the data transmission reaches the maximum speed in a given time slot, we say that the network is saturated and have a high crowdedness level. Then, simulation on SUR is conducted. The result shows that SUR is not a stable indicator to reflect the crowdedness of a network. In Wi-Fi, a saturated Wi-Fi network can have various SUR value which highly depends on packet size. As for an LR-WPAN network, the SUR value can be affected by more factors, which is not only determined by packet size but also the allocated time slot length.

Without an indicator for the network crowdedness in a given slot, the adaptive algorithm cannot tell if a time slot is properly allocated. However, there is not such an indicator available in the CSMA/CA-based network. In the following section, the thesis proposes a slot-based Congestion Indicator (CI) to assess the network crowdedness, enabling a crowdedness-aware adaptive scheduling algorithm.

5.2 Time-slot Congestion Indicator

As discussed on the previous section, a crucial challenge for an adaptive time-slot based scheduling algorithm is to tell whether an allocated time slot is adequate for data transmission or not for a specific network. This section proposes a slot-based Congestion Indicator (CI) to assess the network congestion level and crowdedness in this section. Generally, a low CI value indicates the network is with light traffic and suggests the allocated slot may be more than a network required. However, a high CI value indicates that a network is about to be saturated and it can be better to allocate more channel to the network.

5.2.1 Definition of a Congestion Indicator

The CSMA/CA-based wireless nodes access medium randomly. In result, there is always random white space between frame transmissions. The experiment is conducted in a two-

node LR-WPAN network in a simulation way. One node is for receiving the packet and one for sending. The packet size is randomly set and transmitted at the fastest rate. As depicted in Fig. 5.3, the spectrum diagram shows that there are many white spaces between packet transmission. Thus the SUR can never reach 100%. There are mainly two kinds of white spaces in the diagram, including, the white space caused by random backoff mechanism of CSMA/CA and by ACK frame delay during waiting for an ACK frame to confirm the packet is sent.

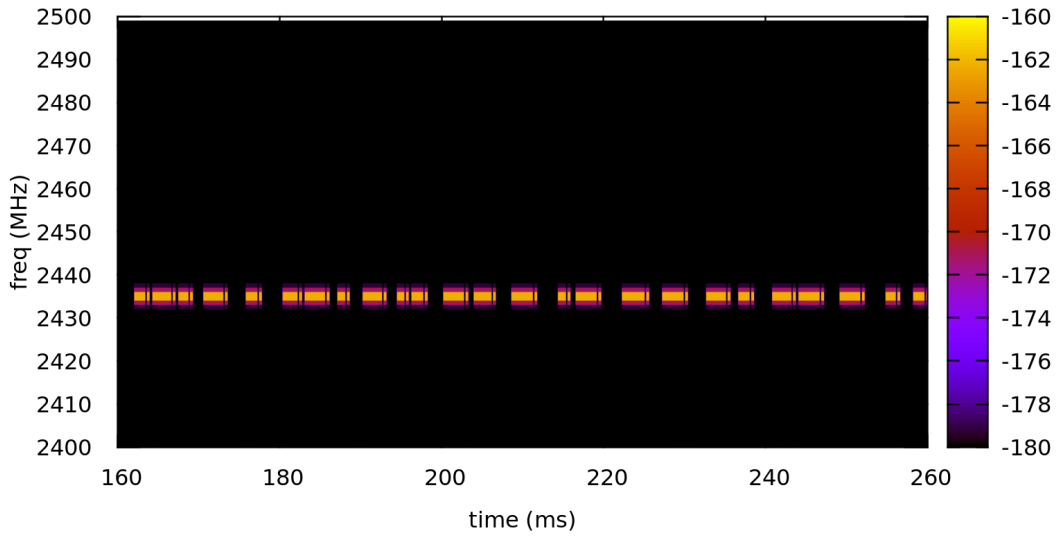

Fig. 5.3 Spectrum diagram: LR-WPAN packet sending at maximum speed

The other curves in Fig. 5.1 shows that SUR of Wi-Fi varies from 0.48 to 0.8, even if the data is sent at the fastest rate. In other words, Wi-Fi is not able to use up all the allocated medium in an efficient way due to random backoff of sending. SUR may depend on the size of the packet, slot length and number of nodes. Similarly, SUR of LR-WPAN is not able to reflect crowdedness of the allocated slots as well, as shown in Fig. 5.2. Thus, it is important to find a way to measure the level of slot congestion, which enable adaptive scheduling according to the indicator. This indicator should include the features:

- giving a numerical indicator. The value should be 0 (idle) if no traffic in a slot and be 1 (the busiest) if the all the nodes sending data at the fastest rate
- Be independent of packet size
- Be independent of the number of nodes
- Be independent of allocated slot length

Due to the existence of white space between data transmissions, it can be tricky to determine the crowdedness of a network. To make things clear, in an allocated time slot, the system can collect every detail of the real transmitted packets in that slot, such as the number of frames, the length of each packet, packet types. Then, slot-based CI for this slot is defined as below:

1. T_c: The calculated time slot length required to transmit these packets. T_c is a calculated time based on the real packets sent in this time slot if the network were saturated. Basically, T_c can be calculated by estimate white space length in a saturated network according to probability theory. If no packet is transmitted in a slot, we have $T_c = 0$. A model is proposed in the following sections to perform such an estimation on LR-WPAN and Wi-Fi network.
2. T_r: The real allocated time slot length.
3. CI: Congestion indicator for the slot, which is defined by below equation:

$$CI = \frac{T_c}{T_r} \tag{5.7}$$

According to the definition, $CI = 1$ indicates that a slot is saturated and the network has reached its maximum capacities in a given time slot. If $CI < 1$, it suggests the allocated slot is not fully utilized, and there is still room to increase the throughput if wireless nodes try to

send more packets. It is important to note that *CI* can be greater than one; it is called slot overload. The reason is that T_c is a calculated value in probability theory, and it is possible that $CI > 1$ occurs in a specific time slot. However, in the long run, the averaged *CI* should not be more than one. The *CI* can never be negative, and *CI* at zero indicates no traffic in the scheduled slot.

5.2.2 Congestion Indicator Estimation in LR-WPAN network

One way to estimate CI is to use probability theory and deduce CI statistically analyse white space probability distribution. In a normal CSMA/CA network, there are two types of white spaces. They are the white space caused by random backoff mechanism of CSMA/CA and by ACK frame delay during waiting for an ACK frame to confirm the packet has been successfully sent. When taking time slots into consideration, another kind of white space is introduced. This kind of white space happens just before the end of a slot. Due to the fact that remaining slot length may not be long enough to complete transmission of a packet, the sender has to give up the transmission according to the AN mechanism. Therefore, a slot-margin white space is observed.

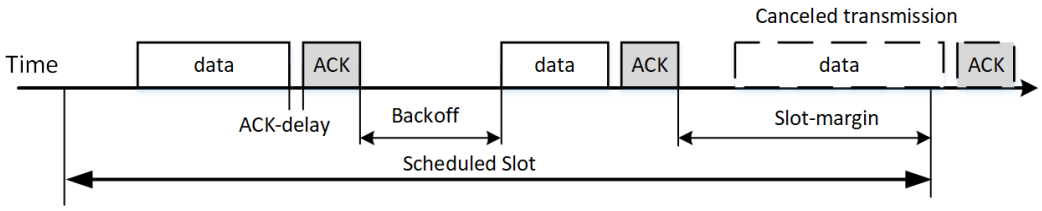

Fig. 5.4 Three major kinds of white spaces

In summary, there are three major categories of white space for a given slot.

- Backoff white space, caused by random backoffs before sending
- ACK-delay white space, happening when waiting for an ACK after the frame has sent

- slot-margin white space, happening when a sender gives up transmission before the end of a slot because of not enough slot time remaining

This section analyses these three types of white space in detail and present a model to estimate the *CI* of given LR-WPAN slot.

Backoff white space model for greedy nodes

According to CSMA standard in IEEE802.15.4 [113], as depicted in Fig. 3.20a in section 3.3.1, one frame is sent out adopting a listen-before-talk method. The algorithm starts by setting the variable *BE* to $macMinBE$, and this value will increase by one for each attempt of sending until reaching $macMaxBE$. Before, sending CCA is performed to identify if the channel is idle or not. If the channel is idle, the sender starts sending. Otherwise, it back off for a random number of $aUnitBackoffPeriod$ and start next round of attempt, until the frame is sent or reach maximum attempts of $macMaxCSMABackoffs$. How the number of backoff period is chosen is the key to infer expectation of backoff white space. The MAC sub-layer shall delay for a random number of complete backoff periods in the range 0 to $2^{BE}-1$.

IEEE802.15.4 specify that one symbol duration is 16 microseconds and one byte is two symbols for the 2.4Ghz frequency band. The constants and attributes used in the LR-WPAN CSMA-CA algorithm as in table :

Let N denote the number of nodes and η is SUR. Assuming that all the nodes is greedy and attempt to send as many as packets they can, we have the probability of channel is busy (P_b) and clear (P_c) :

$$\begin{cases} P_b &= \frac{N-1}{N} \cdot \eta \\ P_c &= 1 - P_b \end{cases} \tag{5.8}$$

Table 5.1 LR-WPAN MAC attribute and constants

Attribute/Constant	Description	value
macMinBE	The minimum value of the backoff exponent value range $0-3$	3
macMaxCSMABackoffs	The maximum number of backoffs will attempt before declaring a channel access failure. value range $0-5$	4
aMaxBE	The maximum value of the backoff exponent	5
aTurnaroundTime	RX-to-TX or TX-to-RX maximum turnaround time (symbol periods)	12
aCCADuration	Clear Channel Assessment duration in 2.4Ghz Frequency band (symbol periods)	8
macLIFSPeriod	The minimum time forming a LIFS period (symbol periods)	40
macSIFSPeriod	The minimum time forming a SIFS period (symbol periods)	12
aMaxSIFSFrameSize	The maximum size of an MPDU, in octets, that can be followed by a SIFS period.	18
aUnitBackoffPeriod	The number of symbols forming the basic time period used by the CSMA-CA algorithm.	20

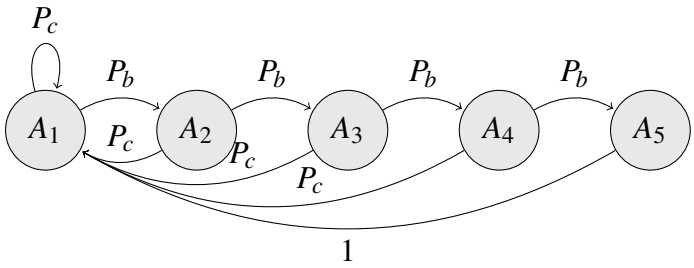

Fig. 5.5 Markov chain of CSMA/CA default attempt in LR-WPAN

Specifically, the default retransmission times is four as provided in Table 5.1. In this case, the Markov Chains of the CSMA/CA attempt can be depicted as in Fig. 5.5. A_i is the ith attempt state.

The corresponding transition matrix is:

$$\mathbf{P} = \begin{bmatrix} P_c & P_b & 0 & \cdots & 0 \\ P_c & 0 & P_b & \cdots & 0 \\ \vdots & \vdots & \vdots & \ddots & 0 \\ P_c & 0 & 0 & \cdots & P_b \\ 1 & 0 & 0 & \cdots & 0 \end{bmatrix} \tag{5.9}$$

The stationary state vector $\mathbf{v}$ of the stochastic matrix is given by:

$$\begin{cases} (\mathbf{v}-\mathbf{I})\mathbf{P} & = 0 \\ \|\mathbf{v}\| & = 1 \end{cases}$$

where $\mathbf{I}$ is the identity matrix. Solve the equation, we get:

$$\mathbf{v} = \begin{bmatrix} \frac{P_b^0}{\sum_{m=0}^{M-1} P_b^m} & \frac{P_b^1}{\sum_{m=0}^{M-1} P_b^m} & \cdots & \frac{P_b^{M-2}}{\sum_{m=0}^{M-1} P_b^m} & \frac{P_b^{M-1}}{\sum_{m=0}^{M-1} P_b^m} \end{bmatrix} \tag{5.10}$$

Where M is the dimension of the transition matrix. While in the case of default retransmission times as shown in Fig. 5.5, the transition matrix is:

$$P = \begin{bmatrix} P_c & P_b & 0 & 0 & 0 \\ P_c & 0 & P_b & 0 & 0 \\ P_c & 0 & 0 & P_b & 0 \\ P_c & 0 & 0 & 0 & P_b \\ 1 & 0 & 0 & 0 & 0 \end{bmatrix}$$

And coresponding stable-state vector is:

$$\mathbf{v} = \begin{bmatrix} \frac{P_b^0}{\sum_{m=0}^{4} P_b^m} & \frac{P_b^1}{\sum_{m=0}^{4} P_b^m} & \frac{P_b^2}{\sum_{m=0}^{4} P_b^m} & \frac{P_b^3}{\sum_{m=0}^{4} P_b^m} & \frac{P_b^4}{\sum_{m=0}^{4} P_b^m} \end{bmatrix}$$

Let P_{Ai} stands for ith sending attempt for a particular frame and $P_{Ai} = \mathbf{V}_i$. Let $P\{BE = k\}$ denotes the probability of the sender when BE equal k. P{BE=k} should be sum of all the attempt probability ($P_A i$) where $BE = k$ for the attempt. Particularly, the default MAC attribute and constant is listed in Table 5.1 We have:

$$\begin{cases} P\{BE = 3\} & = \mathbf{v}_1 = \frac{P_b^0}{\sum_{m=0}^{4} P_b^m} \\ P\{BE = 4\} & = \mathbf{v}_2 = \frac{P_b^1}{\sum_{m=0}^{4} P_b^m} \\ P\{BE = 5\} & = \mathbf{v}_3 + \mathbf{v}_4 + \mathbf{v}_5 = \frac{\sum_{m=2}^{4} P_b^m}{\sum_{m=0}^{4} P_b^m} \end{cases} \tag{5.11}$$

Due to the MAC sublayer shall delay for a random number of complete backoff periods in the range 0 to $2^{BE} - 1$, which is total 2^{BE} choices. Let BN denotes the number of backoff periods for each node. The probability is given by equation as below:

$$\begin{cases} P\{BN = 8\} & = P\{BE = 3\} \\ P\{BN = 16\} & = P\{BE = 4\} \\ P\{BN = 32\} & = P\{BE = 5\} \end{cases} \tag{5.12}$$

According to equation 5.8, 5.11 and 5.12, we have:

$$\begin{cases} P\{BN=8\} & = \frac{1}{\sum_{m=0}^{4}(\frac{N-1}{N}\cdot\eta)^m} \\ P\{BN=16\} & = \frac{\frac{N-1}{N}\cdot\eta}{\sum_{m=0}^{4}(\frac{N-1}{N}\cdot\eta)^m} \\ P\{BN=32\} & = \frac{\sum_{m=2}^{4}(\frac{N-1}{N}\cdot\eta)^m}{\sum_{m=0}^{4}(\frac{N-1}{N}\cdot\eta)^m} \end{cases} \tag{5.13}$$

As illustrated in Fig. 5.6a, Assuming η is 0.5, the probability of $BN = 32$ and $BN = 16$ increase with more transmission nodes introduced. For example, BN has the only value of eight when there is one node sending data only. It's reasonable because there is no conflict and channel always idle and all the frame is sent without retrial. Fig 5.6b indicates that the expectation of BN increases with an increase of η and the number of sending node.

Let RB denote random backoff choice for each node. RB is randomly chosen, in default. Thus we have:

$$P\{RB=x\} = \begin{cases} \frac{P\{BN=8\}}{8} + \frac{P\{BN=16\}}{16} + \frac{P\{BN=32\}}{32} & 0 \le x < 8 \\ \frac{P\{BN=16\}}{16} + \frac{P\{BN=32\}}{32} & 8 \le x < 16 \\ \frac{P\{BN=32\}}{32} & 16 \le x < 32 \end{cases} \tag{5.14}$$

The Fig. 5.7 shows the probability for the random backoff choice, where is one, three or six nodes in the LR-WPAN and η is 0.5.

CSMA/CA allows the node which has the minimum RB value can access the medium. If multiple nodes choose the same backoff unit, conflict happens. The probability of white space caused by backoff (WB) for one channel can be considered as an independent random

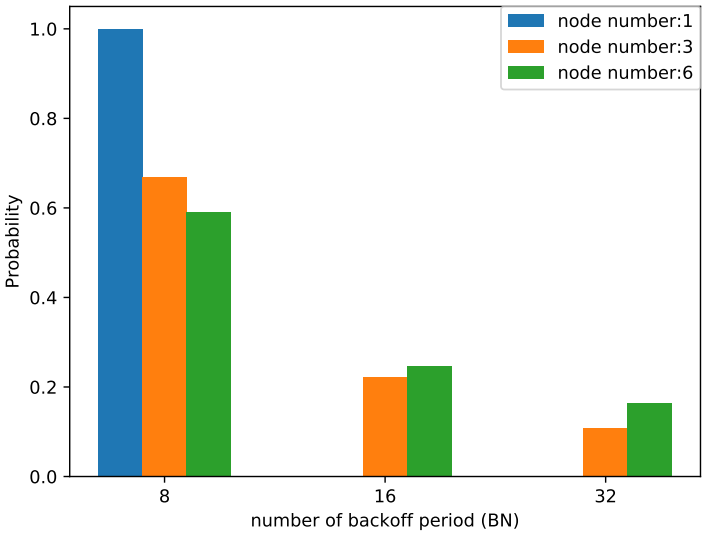

(a) PDF of BN, η=0.5

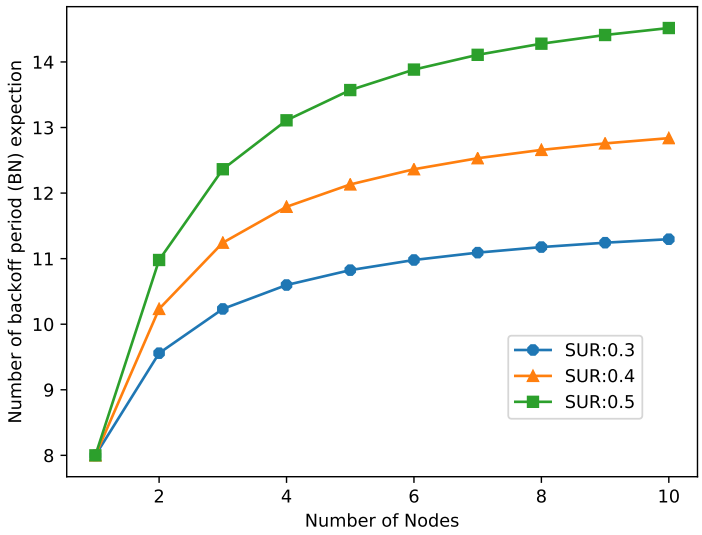

(b) Expectation of BN

Fig. 5.6 Lr-Wpan number of backoff period

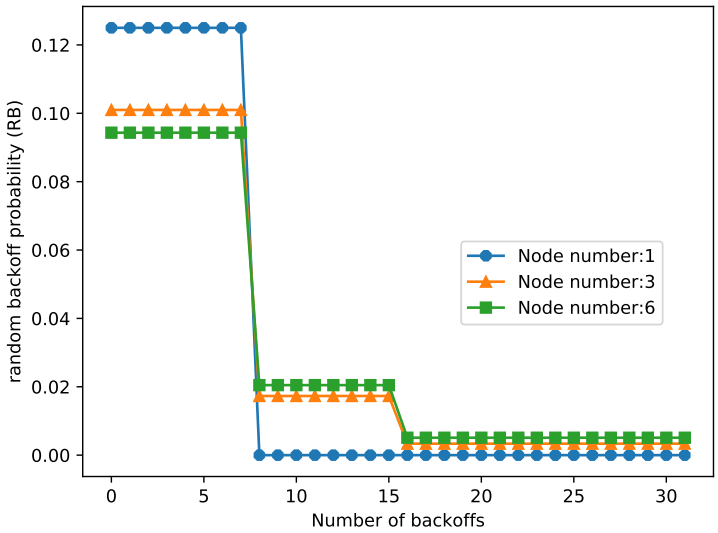

(a) PDF of RB, η=0.5

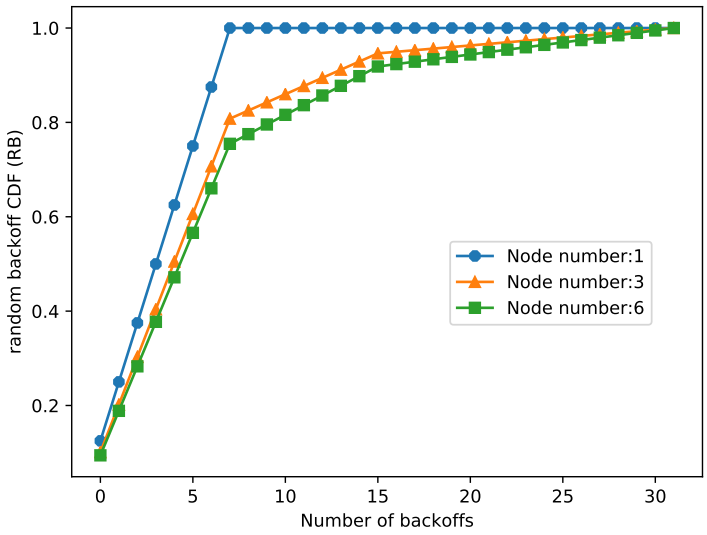

(b) PDF of RB, η=0.5

Fig. 5.7 Lr-Wpan number of random backoff probability for each node

event. Thus, probability $P\{WB = 0\}$ is equal to $1 - P\{all\ the\ node : RB > 0\}$, in other word

$$P\{WB = 0\} = 1 - (P\{RB > 0\})^N$$

. In the case of $WB \neq 0$, this can be calculate by formula:

$$P\{WB = x\} = (P\{RB > x-1\})^N - (P\{RB > x\})^N$$

To recap, the formula is as Equation 5.15:

$$P\{WB = x\} = \begin{cases} 1 - (P\{RB > 0\})^N & x = 0 \\ \\ (P\{RB > x-1\})^N - (P\{RB > x\})^N & x > 0 \end{cases} \tag{5.15}$$

where $P\{RB > x\}$ is the complementary cumulative distribution function.

By using Formula 5.14 and 5.15, white space caused by backoff is calculated as in Table 5.2 and Fig. 5.8.

Table 5.2 LR-WPAN white space backoff expection

η	$N=1$	$N=2$	$N=3$	$N=4$	$N=5$	$N=6$	$N=7$	$N=8$
0.5	3.5	2.68	2.02	1.58	1.28	1.06	0.89	0.76
0.4	3.5	2.55	1.89	1.47	1.18	0.97	0.81	0.68
0.3	3.5	2.44	1.78	1.36	1.08	0.88	0.73	0.61
0.2	3.5	2.34	1.68	1.29	1.00	0.81	0.67	0.56

Fig. 5.8c shows that the expected number of backoffs drops with the increase of node number.

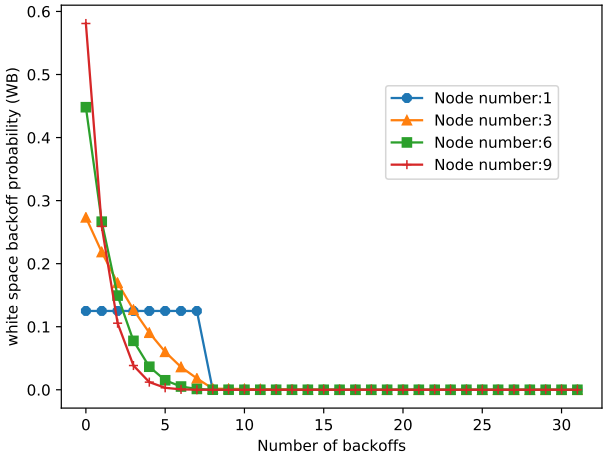

(a) PDF of WB, η=0.5

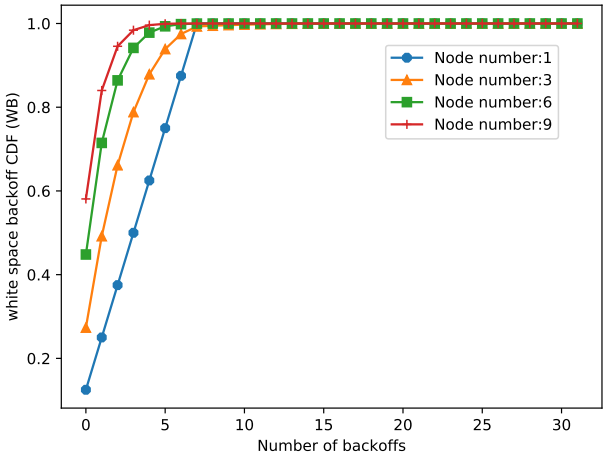

(b) CDF of WB, η=0.5

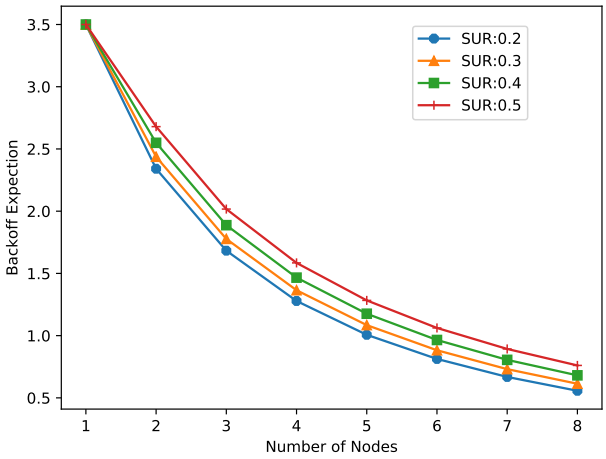

(c) Expection of WB

Fig. 5.8 LR-WPAN white space backoff for a channel

Backoff white space model for normal nodes

If the nodes are not greedy, the busy level of each node is reflected by SUR. Let η denote SUR and η_n is the SUR of nth node, and they have to satisfy the equation as below:

$$\eta = \sum_{n=1}^{N} \eta_n$$

And the Equation 5.8 can be extended for node n:

$$\begin{cases} P_{bn} & = \eta - \eta_n \\ P_{cn} & = 1 - P_{bn} \end{cases} \tag{5.16}$$

P_{bn} is the channel busy probability for the nth node that tries to sense the channel, and P_{cn} is the channel clear probability. From Equation 5.10 and 5.16, we have probability of BE. In the case of default CSMA/CA attribute, the formula is as below:

$$\begin{cases} P_n\{BE=3\} & = \frac{P_{bn}^0}{\sum_{m=0}^{4} P_{bn}^m} \\ P_n\{BE=4\} & = \frac{P_{bn}^1}{\sum_{m=0}^{4} P_{bn}^m} \\ P_n\{BE=5\} & = \frac{\sum_{m=2}^{4} P_{bn}^m}{\sum_{m=0}^{4} P_{bn}^m} \end{cases} \tag{5.17}$$

According to equation 5.16, 5.17 and 5.12, we have:

$$\begin{cases} P_n\{BN=8\} & = \frac{1}{\sum_{m=0}^{4}(\eta-\eta_n)^m} \\ P_n\{BN=16\} & = \frac{\eta-\eta_n}{\sum_{m=0}^{4}(\eta-\eta_n)^m} \\ P_n\{BN=32\} & = \frac{\sum_{m=2}^{4}(\eta-\eta_n)^m}{\sum_{m=0}^{4}(\eta-\eta_n)^m} \end{cases} \tag{5.18}$$

Let *RB* denote random backoff choice for each node. *RB* is randomly chosen, in default, thus we have:

$$P_n\{RB=x\} = \begin{cases} \frac{P_n\{BN=8\}}{8} + \frac{P_n\{BN=16\}}{16} + \frac{P_n\{BN=32\}}{32} & 0 \le x < 8 \\ \frac{P_n\{BN=16\}}{16} + \frac{P_n\{BN=32\}}{32} & 8 \le x < 16 \\ \frac{P_n\{BN=32\}}{32} & 16 \le x < 32 \end{cases} \tag{5.19}$$

In the Equation 5.15, the probability $P\{WB=x\}$ is treated as a problem in which independent events happen in the same time. Here, it cannot be dealt with by using the same method, because each node has different SURs; in other words, the nodes have different weights when access medium. For example, if one node accounts 95% of SUR, while the other one only accesses channel at a low rate. In this case, the backoff white space is more like when there is only one node access channel, rather than two nodes compete the medium. It is not reasonable if treating them as independent and fair events.

The problem can be resolved by introducing Participation Probability (PR), which imply the ratio for a node to participate in competing medium and has a value range between zero

and one. The definition of PR is as below:

$$PR_n = \frac{\eta_n}{\max\limits_{1 \le n \le N} \eta_n} \tag{5.20}$$

where PR_n is the participation ratio for nth node. The PR has a trend that larger SUR has larger PR, while the node with maximum SUR has PR value one. The PR value is one for all nodes when they have the same SUR with each other.

The probability $P\{WB = 0\}$ is equal to $P\{at\ least\ one\ node\ RB = 0\}$, namely probability of $1 - P\{all\ the\ node\ RB > 0\}$. If PR is not considered, we have:

$$P\{all\ the\ node\ RB > 0\} = \prod_{n=1}^{N} P_n\{RB > 0\} \tag{5.21}$$

If a node does not participate medium competition, it acts like a node with large RB, namely the probability of $RB > 0$ is one. If it participates the competition, the probability is $P_n\{RB > 0\}$. Thus, the total probability is $PR_n \cdot P_n\{RB > 0\} + (1 - PR_n) \cdot 1$. Put it into Formula 5.21, we get the extended equation with PR considered:

$$P\{all\ the\ node\ RB > 0\} = \prod_{n=1}^{N} (PR_n \cdot (P_n\{RB > 0\} - 1) + 1)$$

Replace PR_n by Equation 5.20:

$$P\{all\ the\ node\ RB > 0\} = \prod_{n=1}^{N} (\frac{\eta_n \cdot (P_n\{RB > 0\} - 1)}{\max\limits_{1 \le n \le N} \eta_n} + 1)$$

Thus:

$$P\{WB = 0\} = 1 - \prod_{n=1}^{N} (\frac{\eta_n \cdot (P_n\{RB > 0\} - 1)}{\max\limits_{1 \le n \le N} \eta_n} + 1)$$

In the same way, When WB is not 0:

$$P\{WB=x\}=\prod_{n=1}^{N}(\frac{\eta_n\cdot(P_n\{RB>x-1\}-1)}{\max\limits_{1\le n\le N}\eta_n}+1)-\prod_{n=1}^{N}(\frac{\eta_n\cdot(P_n\{RB>x\}-1)}{\max\limits_{1\le n\le N}\eta_n}+1)$$

In summary, the formula for white space caused by backoff is as below:

$$P\{WB=x\}=\begin{cases}1-\prod_{n=1}^{N}(\frac{\eta_n\cdot(P_n\{RB>0\}-1)}{\max\limits_{1\le n\le N}\eta_n}+1) & x=0\\ \prod_{n=1}^{N}(\frac{\eta_n\cdot(P_n\{RB>x-1\}-1)}{\max\limits_{1\le n\le N}\eta_n}+1)-\prod_{n=1}^{N}(\frac{\eta_n\cdot(P_n\{RB>x\}-1)}{\max\limits_{1\le n\le N}\eta_n}+1) & x>0\end{cases} \tag{5.22}$$

The Equation 5.22 regresses to Equation 5.15 when η_i is same for all the nodes.

Assuming a given network with four nodes, the SUR for nth node is as in the Table 5.3 and the backoff expectation is calculated according to formula 5.19 and 5.22. Case one in the table shows that only one of four nodes sends data, and the exportation backoffs are 3.50, which is constant with the Formula 5.15. Likewise, case two and three also suggest this point. Case four gives reasonable expectation at 3.18.

Table 5.3 LR-WPAN white space backoff in various SUR condition

Condition	η_1	η_2	η_3	η_4	η	Expection
case 1	0.50	0	0	0	0.50	3.50
case 2	0.167	0.167	0.166	0	0.50	2.02
case 3	0.125	0.125	0.125	0,125	0.50	1.58
case 4	0.25	0.15	0.09	0.01	0.50	3.18

Due to there are mandatory CCA and Rx-to-Tx time added on the backoff. Let t_{bw} denotes expectation of backoff white space time. We have:

$$t_{bw}=E[WB]\cdot aUnitBackoffPeriod+aCCADuration+aTurnaroundTime \tag{5.23}$$

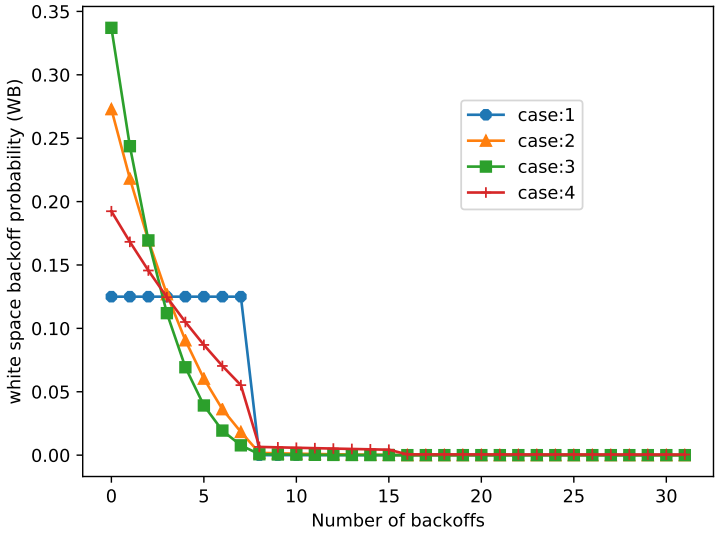

(a) PDF of WB, η=0.5

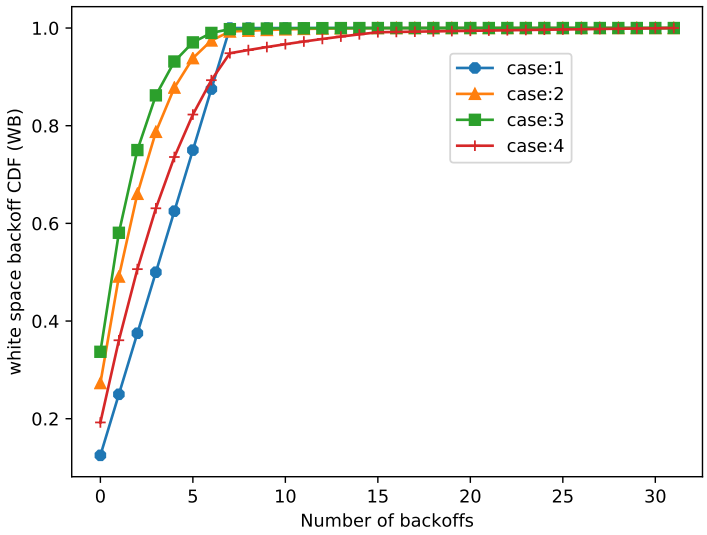

(b) CDF of WB, η=0.5

Fig. 5.9 LR-WPAN white space backoff for a channel

where $E[WB]$ is Expectation of backoffs.

ACK-delay white space

As depicted in Fig. 5.4, there is ACK-delay white space when sending out a normal data frame. According to IEEE 802.15.4, the ACK need to start replying with a duration t_{ack}after the sender completes sending a frame:

$$aTurnaroundTime \leq t_{ack} \leq (aTurnaroundTime + aUnitBackoffPeriod)$$

where $aTurnaroundTime$ and $aUnitBackoffPeriod$ is listed in the Table 5.1. Thus:

$$12\ symbols \leq t_{ack} \leq 32\ symbols$$

It is reasonable to pick the average value, 22 symbol duration, as the ACK-delay white space.

IFS white space

Not the major one. Especially, there is already CCA and Rx-to-Tx turnaround time (20 symbol period). Generally, there is no need to consider IFS white space.

slot-margin white space

This type of white space is caused by giving up sending a packet before the end of a slot because of not enough slot time left. As shown in Fig. 5.4, the slot-margin is the unused slot time following the last frame until the end of a slot.

As shown in Fig 5.10, three cases can happen in a slot. Case 1 illustrates the worst case where the transmission has to be cancelled because the rest slot is only a little less than required. Case 2 indicates the normal situation, while case 3 shows the best case in which

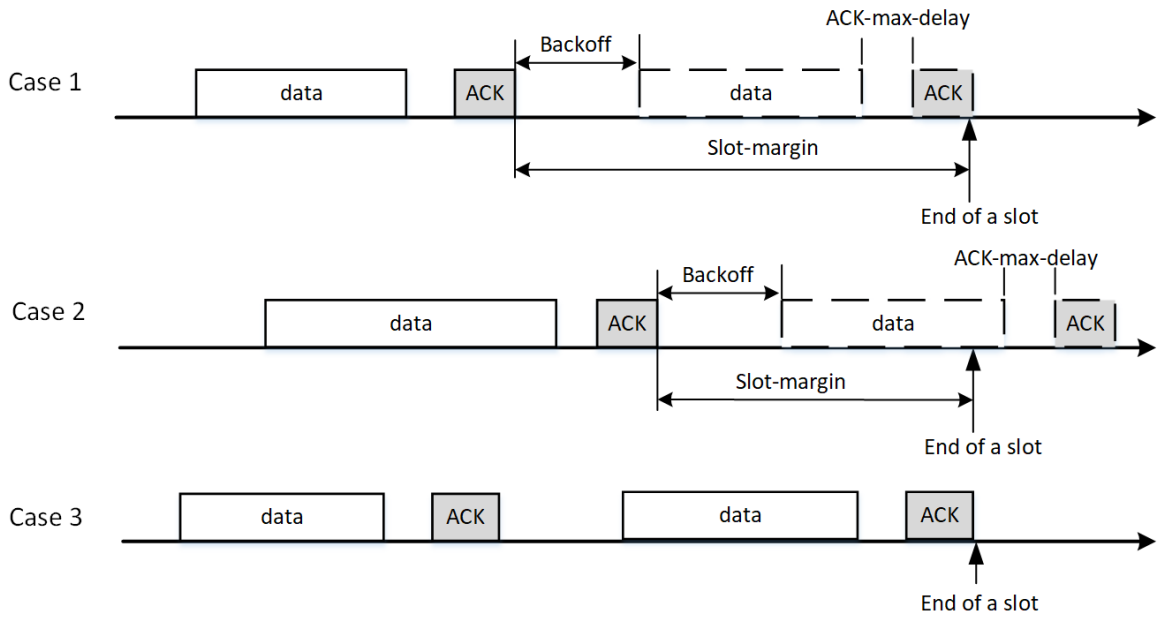

Fig. 5.10 Slot-margin white space in three cases

the last frame is just sending out and use up all the slot without any margin. Therefore, we have the slot-margin white space:

$$0 \leq slot\ margin < t_{bw} + t_{df} + t_{ackMax} + t_{af}$$

where t_{ackMax} is the maximum ACK delay duration (32 symbols duration), t_{df} is the data frame duration and t_{af} is the ACK frame duration.

If a slot is long engough comparing with the frame length, the length of slot-margin can be treated as random distributed. Based on this assumption,

$$t_{smw} = \frac{t_{bw} + t_{df} + t_{ackMax} + t_{af}}{2} \tag{5.24}$$

where t_{smw} is the expectation of slot-margin white space duration. One the limitation of Formula 5.24 is that the slot-margin length may not be evenly distributed when the slot length is close to packet length.

CI estimation of a given slot

CI is an indicator for channel crowdedness and reflects how busy the channel is. The indicator should be one statistically for a channel at its busiest state and zero if it is idle. The busiest state means the allocated channel resource is inadequate for nodes' usage, and they compete for the resource and send a packet at the maximum rate. As a result, over a given busy time slot T, the slot duration should be statistically equal to the duration of which the channel is occupied plus the duration of three kinds of white space analyzed before, as explained by the formula below:

$$T = \eta \cdot T + T_{ws}$$

where T_{ws} is the white spaces including backoff white space, ACK delay and slot-margin white space. However, when the channel is idle or has only a few data flow:

$$T \gg \eta \cdot T + T_{ws}$$

Therefore, according to the definition of CI in equation 5.7 (CI is represented by φ):

$$\varphi = \frac{\eta \cdot T + T_{ws}}{T}$$

Let C denote the frame count in the slot, including data and ACK frames. Practically, data and ACK frames have a ratio of 1:1. Thus,

$$T_{ws} = \frac{C \cdot (t_{bw} + t_{ack})}{2} + t_{smw}$$

and

$$t_{df} + t_{af} = \frac{2\eta \cdot T}{C}$$

Put it into Equation 5.24:

$$t_{smw} = \frac{t_{bw} + t_{ackMax} + \frac{2\eta \cdot T}{C}}{2}$$

By considering the formulas above:

$$\varphi = \eta + \frac{\eta}{C} + \frac{C \cdot (t_{bw} + t_{ack}) + t_{bw} + t_{ackMax}}{2T} \tag{5.25}$$

In Equation 5.25, η, C and T are collected statistic in a time slot, while other parameters have type value or are calculated as in Table 5.4.

Table 5.4 LR-WPAN congestion indicator formula parameters

name	symbol durations	microseconds
t_{ack}	22	352
t_{ackMax}	32	512
t_{bw}	Formula 5.23, 5.22 and Table 5.1	various

Algorithm of CI Estimation

In order to design the algorithm of CI estimation in NS-3 simulator, some data in the MAC layer needs to be collected, including:

- Packet count, counting the frame number during a slot.
- allocated time slot length.
- channel busy time for whole packets in a slot, which can be collected by recording all the frames in-air duration, include command frames, beacon frames, data frames ACK frames.
- channel busy time for each node in a slot, which can be collected by recording frames with the source address and categorized by the short network address.

Equation 5.25 is derived from probability. Therefore, the reliability of confidence Level of φ can be improved by using an average over multiple slots. One common method is to introduce EMA (Exponential Moving Average), which means η C and T is the average value over past slots. The algorithm is as below.

Algorithm 5.1 CI (φ) algorithm for LR-WPAN

S - number of slots in EMA

E_T - EMA of slot length

E_C - EMA of packet count

E_B - EMA of channel busy time

$E_B[address, time]$ - EMA of channel busy time map for each node

T - current slot length

C - packet count in current slot

B - channel busy time in current slot

$B[address, time]$ - channel busy time map for each node in current slot

1: $k \leftarrow \frac{2}{S+1}$
2: **if** is initial slot and EMA is not set **then**
3: $E_T \leftarrow T$; $E_C \leftarrow C$; $E_B \leftarrow B$
4: $E_B[address, time] \leftarrow B[address, time]$
5: **else**
6: $E_T \leftarrow k \times T + (1-k) \times E_T$
7: $E_C \leftarrow k \times C + (1-k) \times E_C$
8: $E_B \leftarrow k \times B + (1-k) \times E_B$
9: **for all** $(addr1, time1) \in E_B[address, time]$ **do**
10: **if** $B[address, time]$ contain key $addr1$ **then**
11: $time2 \leftarrow B[addr1]$
12: Remove item $addr$ from B[address,time]
13: **else**
14: $time2 \leftarrow 0$
15: **end if**
16: $E_B[addr1] \leftarrow k \times time2 + (1-k) \times time1$
17: **end for**
18: **for all** $(addr, time) \in B[address, time]$ **do**
19: put $(addr, time)$ into $E_B[address, time]$
20: **end for**
21: **end if**

22: $\eta \leftarrow \frac{E_B}{E_T}$
23: $i \leftarrow 0$
24: **for all** $(addr, time) \in E_B[address, time]$ **do**
25: $\quad \eta_i \leftarrow \frac{time}{E_T}$
26: $\quad i \leftarrow i+1$
27: **end for**
28: compute t_{bw} by Equation 5.22 and 5.23
29: $\varphi \leftarrow \eta + \frac{\eta}{E_C} + \frac{E_C \cdot (t_{bw}+t_{ack})+t_{bw}+t_{ackMax}}{2E_T}$

5.2.3 Congestion Indicator Estimation in Wi-Fi network

According to AN in Section 3.3.1, the slot length for Wi-Fi is up to about 250 milliseconds. Because of the high throughput, there is a great number of packets sent during a slot and the slot-margin white space is negligible. Moreover, different from LR-WPAN, Wi-Fi support virtual carrier-sensing mechanism, namely NAV (network allocation vector), which enables Wi-Fi access medium with high efficiency. Practically, Wi-Fi has a SUR of up to 75%, while LR-WPAN hardly reaches 50%. This indicates the White space caused by CSMA/CA backoffs in Wi-Fi is not as significant as that in LR-WPAN.

Table 5.5 IEEE802.11g/n MAC attribute and constants

Attribute/Constant	Description	time (us)
$SIFS$	Short Interframe Space	10
$aSlotTime$	The backoff slot time	9 or 20
$DIFS$	DCF Interframe Space ($SIFS + 2 \times aSlotTime$)	28 or 50
$PIFS$	PCF Interframe Space ($SIFS + aSlotTime$)	19 or 30

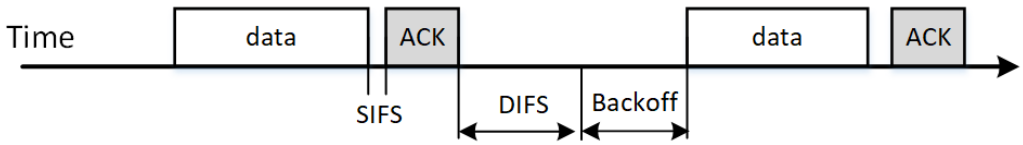

Fig. 5.11 Wi-Fi white space

As shown in Fig. 5.11, Wi-Fi white spaces mainly consist of SIFS, DIFS and backoff. Due to the high efficiency of Wi-Fi MAC, average number of backoff is assumed to be one when the network is busy.For one data transmission frame with ACK enabled, We have:

$$t_{ws} = SIFS + DIFS + aSlotTime$$

where t_{ws} is the time duration of white space. Let C denotes the frame count in the MAC layer and assume that data and ack have a ratio 1:1; we have CI

$$\varphi = \eta + \frac{t_{ws} \cdot C}{2T}$$

In summary:

$$\varphi = \eta + \frac{C \cdot (SIFS + DIFS + aSlotTime)}{2T} \tag{5.26}$$

In the case of $aSlotTime$ is 20 microseconds, the formula is:

$$\varphi = \eta + \frac{C \cdot 40us}{T}$$

5.2.4 Evaluation of CI Estimation model

According to the definition of CI in equation 5.7, CI should be equal to one for a saturated network regardless of packet size, the number of nodes and allocated slot length. Based on this rule, a saturated network can be created by sending data at maximum speed, and then the CI estimation model can be evaluated by applying diverse configurations on packet size, the number of nodes and allocated slot length. If the proposed CI estimation model is a successful model, it should give a stable output of one.

Simulation Result Evaluation

First, simulation is designed to evaluate how the proposed CI estimation model is effected by allocated time slot length and packet size, as shown in Fig. 5.12.

Fig. 5.12a is acquired by using one Wi-Fi station send UDP packets at maximum speed under the different time slot and packet size configuration. The result shows that Wi-Fi *CI* get range from 0.88 to 0.97, which is a little below expected value one. The maximum error of estimated Wi-Fi *CI* in this simulation is 12% when the Wi-Fi slot is 5ms and packet size is 200 bytes. As for LR-WPAN *CI*, the analysis needs to be divided into two ranges at mentioned in section 5.1.2. The first range is when the LR-WPAN slot less than 6ms, where some long packet may not be able to fit into the slot. For example, when the LR-WPAN payload size is 100 bytes, the CI is zero in this range, which indicates no data is sent in the allocated time slot because a 100-bytes LR-WPAN packet requires more than 5ms to transmit. Therefore, the LR-WPAN slot should never be set less than 6ms, because it is necessary to make sure LR-WPAN packets at any size can be transmitted in the allocated time slot. The other range is when slot time not less than 6ms, which shows general *CI* values fluctuate around one with a range from 0.83 to 1.18. The LR-WPAN *CI* gets the maximum error of 18% in this range when the packet payload is 80 bytes and slot time is 7ms. *CI* error tends to be big when the slot is short, and packet payload is large, which is mainly caused by slot-margin white space. *CI* estimation for a short time slot tends to be more easily affected slot-margin white space while Big packets lead to a long slot-margin white space.

Then this thesis evaluates how the proposed CI estimation model is effected by allocated time slot length and sender numbers, as shown in Fig. 5.12. In this simulation, Wi-Fi UDP packets and LR-WPAN unicast packets have fixed sizes of 400 bytes and 20 bytes respectively. Differently, multiple senders are introduced to send data at maximum speed.

Fig. 5.13a depicts Wi-Fi CI when there are multiple Wi-Fi stations sending data at a time slot. It shows the estimated *CI* has a range from 0.9 to 1.01, and the maximum error is 10%

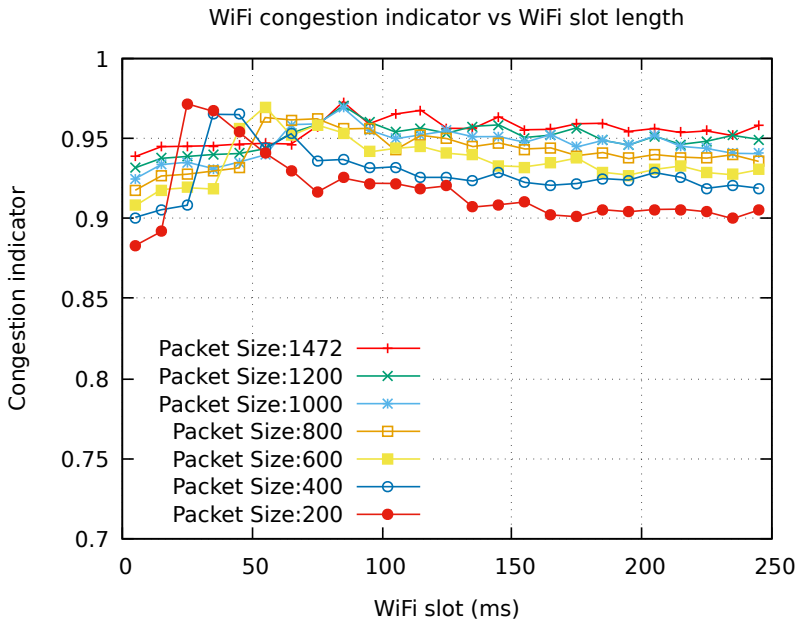

(a) WiFi congestion indicator

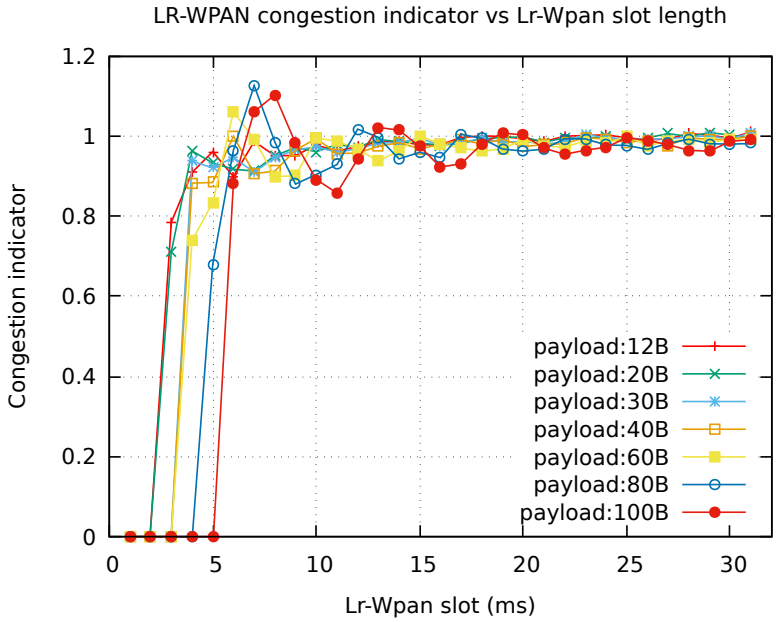

(b) Lr-wpan congestion indicator

Fig. 5.12 Congestion indicator over allocated time slot length and packet size

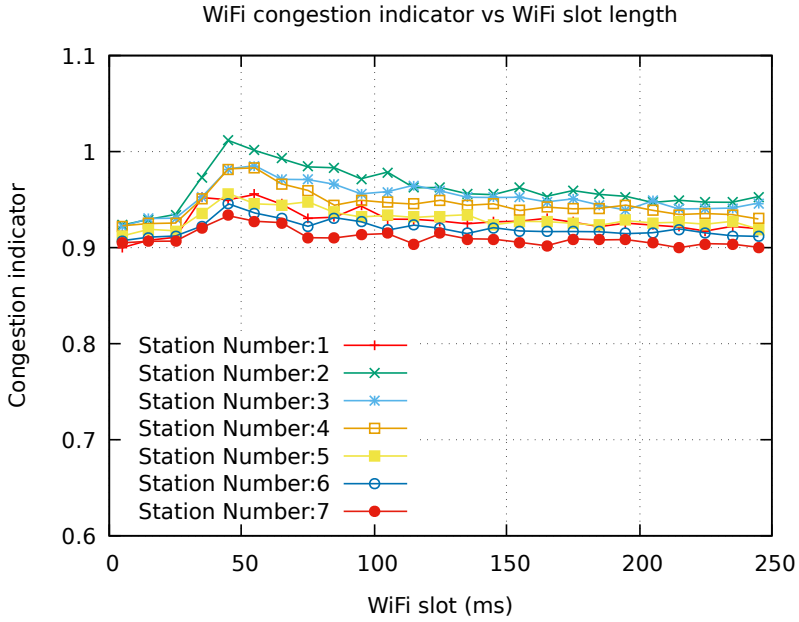

(a) WiFi congestion indicator with packet size of 400 bytes

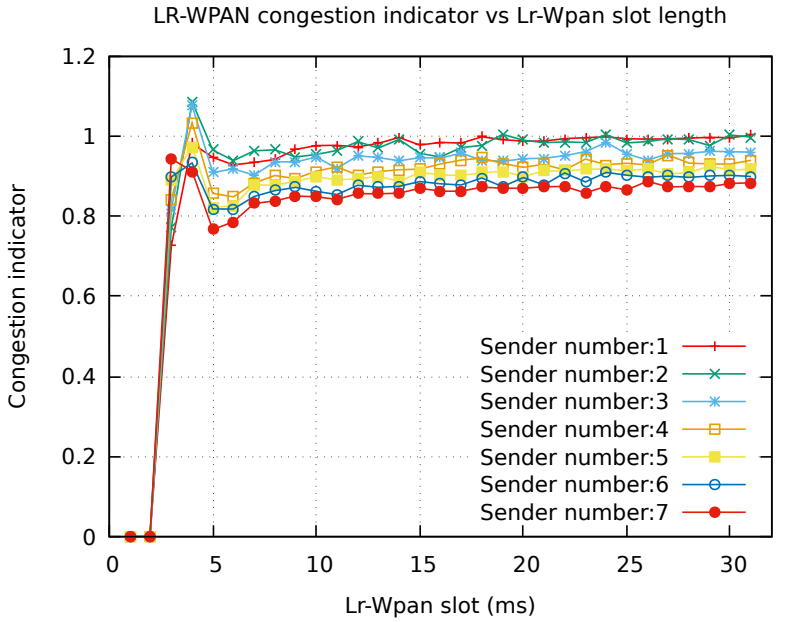

(b) LR-WPAN congestion indicator with MAC payload size of 20 bytes

Fig. 5.13 Congestion indicator over allocated time slot length and sender numbers

when there are seven nodes sending data at the same time slot. When it comes to LR-WPAN in Fig. 5.13b, the LR-WPAN *CI* varies from 0.8 to 1.0 when slot time is equal or more than 6ms. The estimated *CI* reaches maximum error when the LR-WPAN sender number is seven. This diagram also reveals a trend that the estimated *CI* have a larger error when more nodes try to send data at a time slot, but the error is still within the acceptable level.

In order to confirm the stability of the CI estimation model, more simulation is conducted by testing it in different packet size, as shown in Fig. 5.14. Fig. 5.14a shows the Wi-Fi *CI* when the packet size is 1472 bytes. Compared with Fig. 5.13a, the error of estimated CI in this diagram has a small increase, and the maximum error is 12% when there are seven Wi-Fi senders. In a LR-WPAN network, Fig. 5.14b and Fig. 5.14c by configuring the MAC payload to 50 and 80 bytes respective. Both diagrams give the same maximum error of 20% when the slot time is not less than 6ms. They also suggest that long slot time is good for reducing CI estimation error.

Conclusion

In a saturated network where the nodes try to send data at maximum speed, it is expected to have $CI = 1$ according to its definition. However, it is complicated and impractical to get a precise *CI* value. Therefore, a *CI* estimation model is proposed to reduce network statistic requirement and simplify the calculation to give an estimated *CI*. For a saturated time slot, the simulation results show that the estimated Wi-Fi *CI* has an error of less than 12%. LR-WAPN *CI* is investigated by dividing the slot time into two ranges with a threshold at 6ms. Because a slot time less than 6ms is not long enough to allow a long packet transmission, this thesis mainly considers the case where slot time is equal or more than 6ms and a maximum 20% error observed for the estimated LR-WPAN *CI* in the simulation.

Although the proposed *CI* estimation model can have an error up to 20% for a saturated time slot, it is good enough to assess if a time slot is busy. For example, If the estimated

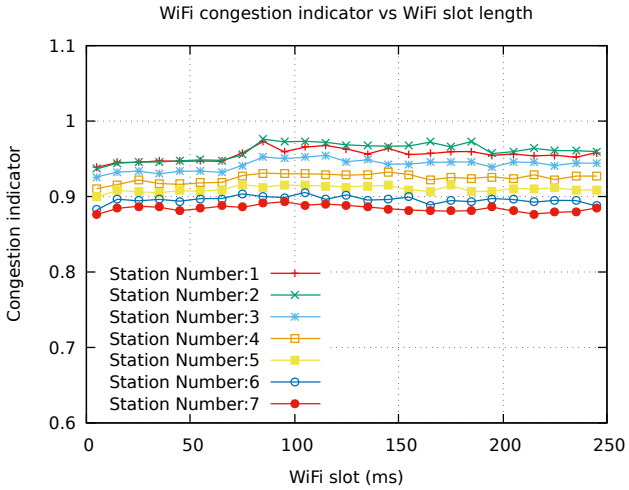

(a) WiFi congestion indicator with packet size of 1472 bytes

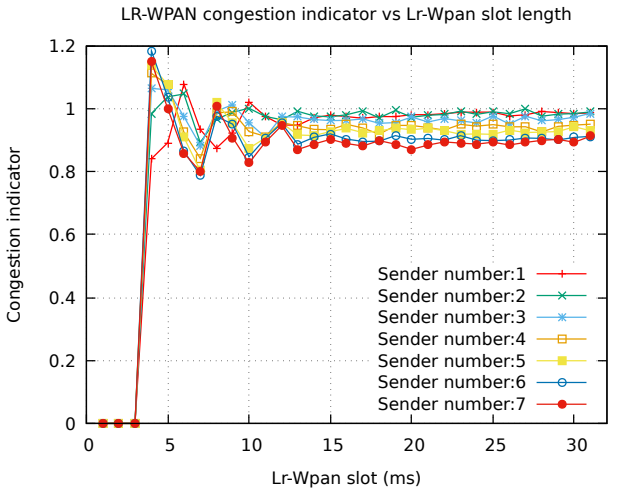

(b) LR-WPAN congestion indicator with MAC payload size of 50 bytes

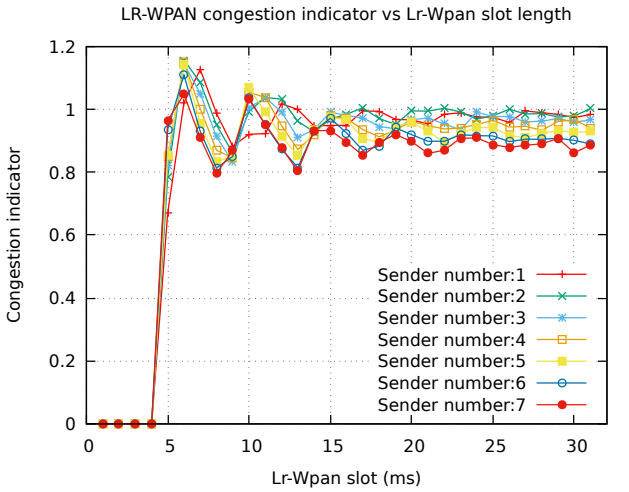

(c) LR-WPAN congestion indicator with MAC payload size of 80 bytes

Fig. 5.14 Congestion indicator over allocated time slot length and sender numbers

CI is more than 0.8, it is confident to infer that the allocated slot is almost saturated and at high congestion level. If calculated *CI* is less than 0.3, it indicates that the allocated slot is with light traffic. Therefore, The estimated CI error can be good enough for an adaptive scheduling algorithm.

5.3 Scheduling Algorithm Design

This section design adaptive time-slot based scheduling algorithm based on the concept of CI, namely crowdedness-aware time-slot scheduling. As shown in Fig. 5.15, the proposed time-slot mechanism in section 3.3.2 enables networks to be scheduled in periodical time slot. As discussed in section 5.1, a fixed time slot setting can waste allocated channel time significantly. The idea for an adaptive scheduling algorithm is to schedule the time slot for LR-WPAN and Wi-Fi dynamically in real-time. At the end of a scheduling cycle, the LR-WPAN slot and Wi-Fi slot of the next scheduling cycle is scheduled in consideration of the network congestion level and other network information. For example, some data are collected in the period of T_n. With these data, the algorithm decides the length of $T_{z,n+1}$ and $T_{w,n+1}$ at the end of T_n.

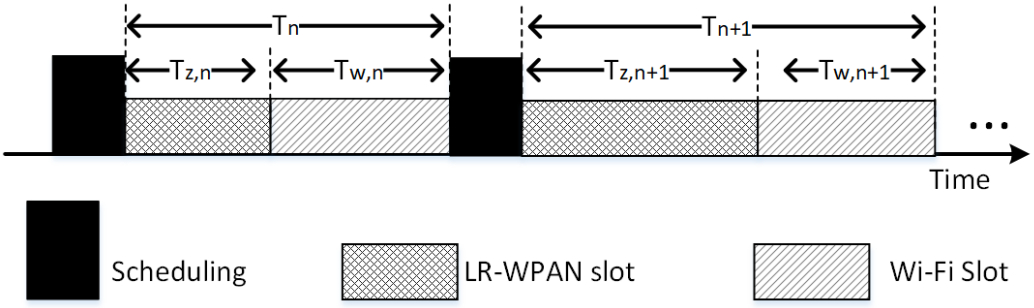

Fig. 5.15 Adaptive scheduling time line

Because LR-WPAN and Wi-Fi are wireless technologies that designed for completely different purpose. Thus, the scheduling algorithm needs to considering the differences between them. The constants are different for these network work:

- $T_{z,min}$ **and** $T_{z,max}$: LR-WPAN slot should be allocated within the range of $[T_{z,min}, T_{z,max}]$. As discussed in previous section, the $T_{z,max}$ cannot be too big, or Wi-Fi packets can be severely delay which result some time-critical application fail. Moreover, the $T_{z,min}$ cannot be too small, or some long LR-WPAN packets cannot fit into the time slot and result in these packets never transmitted. In combination of above fators, $T_{z,min}$ and $T_{z,max}$ is suggested to have a value of 6ms and 30ms respectively.

- $T_{w,min}$ **and** $T_{w,max}$: Wi-Fi slot should be allocated within the range of $[T_{w,min}, T_{w,max}]$. LR-WPAN is normally have a high network latency, thus $T_{w,max}$ is longer than $T_{z,max}$. A typical section for $T_{w,min}$ and $T_{w,max}$ are 5ms and 145ms respectively.

The time slot scheduling can be repented in vector. Letting

$$\mathbf{S_n} = \begin{pmatrix} T_{w,n} \\ T_{z,n} \end{pmatrix}$$

The scheduling in Fig. 5.15 can be express as in Fig. 5.16. The scheduling from cycle n to

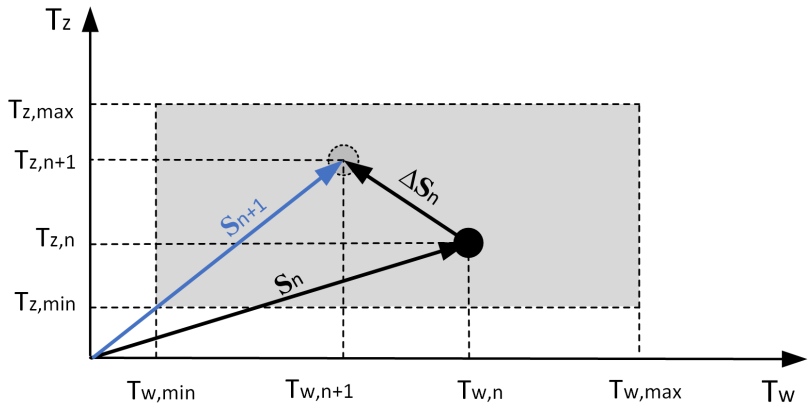

Fig. 5.16 Time slot as a vector

cycle $n+1$ can be represented as vector $\mathbf{S_n}$ changes to vector $\mathbf{S_{n+1}}$, while the $\Delta\mathbf{S_n}$ denotes the change of Wi-Fi and LR-WPAN time slots. In addition to Fig. 5.15, Fig. 5.16 also shows a grey area that describes the minimum and maximum values that LR-WAPN and Wi-Fi slot

can take. Therefore, the scheduling problem is translated to how to select a reasonable $\mathbf{S_{n+1}}$. Because $\mathbf{S_{n+1}} = \mathbf{S_n} + \Delta\mathbf{S_n}$, we can have $\mathbf{S_{n+1}}$ once we know $\Delta\mathbf{S_n}$.

$\Delta\mathbf{S_n}$ has direction and magnitude. The direction can be implied by CI, which is denoted by φ. In order to analyse CI, we can introduce a threshold constant of β for φ. If $\varphi > \beta$, it indicates the allocated time slot is crowded with high traffic; otherwise, the time slot is with low traffic. In combination with Wi-Fi and LR-WPAN, we get four cases:

1. Both Wi-Fi and LR-WPAN network have high traffic. In this case, both networks want to get more network capacity. However, there is no more channel time available to allocate. Thus the algorithm needs to guarantee the network fairness and guides the time slot allocation toward a compromised point where LR-WPAN and Wi-Fi time slots are $T_{z,c}$ and $T_{w,c}$. For example, the algorithm can try to allocate each network the same channel time to ensure fairness in the time domain. The compromised point should be constant for the algorithm. In the following experiment, Wi-Fi and LR-WPAN slots are set to the same at 30ms as a compromised point.

2. Wi-Fi has high traffic while LR-WPAN has low traffic. In this case, the LR-WPAN network can lend unused channel time slot to Wi-Fi which enables a high converged network performance. Thus the algorithm should direct the slot allocation toward a High-Wi-Fi point where Wi-Fi gets the longest time slot, and LR-WPAN is shortest, namely Wi-Fi and LR-WPAN time slots are $T_{w,max}$ and $T_{z,min}$.

3. Wi-Fi has low traffic while LR-WPAN has high traffic. Similar to above point 2, the slot allocation should be guided toward a High-LR-WPAN point, where Wi-Fi and LR-WPAN time slots are $T_{w,min}$ and $T_{z,max}$.

4. Both Wi-Fi and LR-WPAN network have low traffic. Both of the two networks was allocated adequate time slot, no need to change the allocation. Thus, the time slots just keep as the original value.

In the above four cases, the algorithm should guide the slot allocation to different points, such as compromised point, High-Wi-Fi point and High-LR-WPAN point. These points is named as scheduling anchors. If a scheduling anchor is selected according to the CI in a scheduling cycle, it becames an active anchors, which acts as a direction point that the slot allocation will go toward. Table 5.6 is a summary of the scheduling anchors. $\varphi_{w,n}$ and $\varphi_{z,n}$ are the CI of n^{th} scheduling cycle for Wi-Fi and LR-WPAN.

Table 5.6 Mapping of congestion indicators and scheduling anchors

$\varphi_{w,n}$	$\varphi_{z,n}$	$T_{w,sa}$	$T_{z,sa}$	Anchor name
High	High	$T_{w,c}$	$T_{z,c}$	Compromised
High	Low	$T_{w,max}$	$T_{z,min}$	High-Wi-Fi
Low	High	$T_{w,min}$	$T_{z,max}$	High-LR-WPAN
Low	Low	$T_{w,n}$	$T_{z,n}$	original

If letting $\mathbf{A_n}$ denotes the anchor vector inferred from n^{th} scheduling cycle. Table 5.6 can be represented as below:

$$\mathbf{A_n} = \begin{cases} \begin{pmatrix} T_{w,c} & T_{z,c} \end{pmatrix}^{\mathsf{T}} & \text{if } \varphi_{w,n} > \beta \text{ and } \varphi_{z,n} > \beta \\ \begin{pmatrix} T_{w,max} & T_{z,min} \end{pmatrix}^{\mathsf{T}} & \text{if } \varphi_{w,n} > \beta \text{ and } \varphi_{z,n} \leq \beta \\ \begin{pmatrix} T_{w,min} & T_{z,max} \end{pmatrix}^{\mathsf{T}} & \text{if } \varphi_{w,n} \leq \beta \text{ and } \varphi_{z,n} > \beta \\ \mathbf{S_n} & \text{if } \varphi_{w,n} \leq \beta \text{ and } \varphi_{z,n} \leq \beta \end{cases} \tag{5.27}$$

Adding scheduling anchors to the coordinate, we get Fig. 5.17. The three red dots are the anchor points mentioned above. As mentioned above, the black dot moves towards the active anchor. In the graph, the High-LR-WPAN is the active anchor, and the direction of

vector $\Delta\mathbf{S_n}$ straightly points to it. By connecting these three points, a triangle area is acquired. Because the black dot is always attracted by one the three anchor point, it will stay in this area during adaptive scheduling. As for the magnitude of the $\Delta\mathbf{S_n}$, we can apply diverse

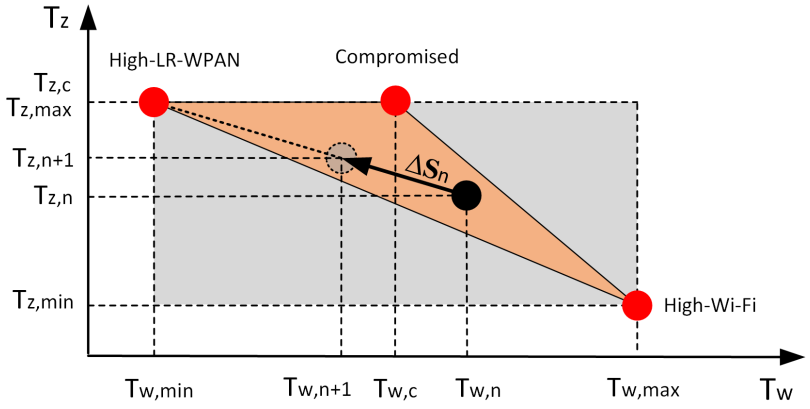

Fig. 5.17 Adaptive scheduling 2D view

algorithms to smooth the movement. One popular way is to employ Exponential Moving Average (EMA). EMA introduces a coefficient α as constant smoothing factor between 0 and 1. By applying EMA, we have:

$$\mathbf{S_{n+1}} = \alpha\mathbf{A_n} + (1-\alpha)\mathbf{S_n} \tag{5.28}$$

$\mathbf{S_{n+1}}$ is the calculated scheduling vector for the next scheduling cycle. Fig. 5.17 illustrates how the adaptive algorithm works. In following a fair long time, we assume that there is no Wi-Fi traffics while LR-WPAN nodes transmit data at maximum speed. Thus High-LR-WPAN anchor is activated according to Table 5.6. Therefore, in each scheduling cycle, the black dot ($\mathbf{S_n}$) will move forward to High-LR-WPAN anchor by a distance depending on the coefficient α. A higher α results in a faster speed for the black dot moving forward to the target anchor. After a few cycles, the black dot can be close to High-LR-WPAN anchor, where Wi-Fi is allocated with the shortest time slot while LR-WPAN gets maximum time slot. In other words, the LR-WPAN network almost dominates the channel time because

Wi-Fi has no data to transmit. If the Wi-Fi has lots of data that need to transmit suddenly, the compromised anchor point will be activated, and then the black dot starts to move to the compromised anchor which give a fair use of the channel in the time domain.

In summary, the adaptive scheduling algorithm includes two major steps:

1. to calculate active anchor point $\mathbf{A_n}$, acording to the equation 5.27
2. to calculate scheduling vector $\mathbf{S_{n+1}}$ by applying EMA algorithm according to equation 5.28

Putting everything together, we design an adaptive time-slot based scheduling algorithm as below Algorithm 5.2.

Algorithm 5.2 Adaptive Time-Slot Based Resource Scheduling Algorithm

Parameters:

α – EMA coefficient as a constant smoothing factor between 0 and 1

β – Congestion indicator threshold to distinguish high or low traffic

$\mathbf{A_c}$ - Compromised scheduling anchor vector

$T_{Z,min}$, $T_{Z,max}$ – LR-WPAN time slot range

$T_{W,min}$, $T_{W,max}$ – Wi-Fi time slot range

1: $\varphi_{w,n} \leftarrow 0$

2: $\varphi_{z,n} \leftarrow 0$

3: $\mathbf{S_n} \leftarrow \mathbf{A_c}$

4: **while** true **do**

5: Perform scheduling by using scheduling vector $\mathbf{S_n}$

6: Wait until the end of current scheduling cycle

7: Derive LR-WPAN conogestion indicator $\varphi_{z,n}$ according to Algorithm 5.1

8: Derive Wi-Fi congestion indicator $\varphi_{w,n}$ according to Equation 5.26

9: Derive scheduling anchor vector $\mathbf{A_n}$ according to Equation 5.27

10: Calculate next scheduling vector $\mathbf{S_{n+1}}$ according to Equation 5.27

11: $\mathbf{S_n} \leftarrow \mathbf{S_{n+1}}$

12: **end while**

5.4 Evaluation

The evaluation of the adaptive time-slot based algorithm includes two parts. First, it is evaluated by using a hardware-based system. However, due to the limitation of the hardware, only the basic version is implemented. The result of the hardware experiment confirms the effectiveness of the scheduling mechanism. Then, the algorithm is implemented in NS-3

simulator and evaluate performance by simulating to transmit Wi-Fi and LR-WPAN data over a period of time to see how the adaptive algorithm response.

5.4.1 Hardware-based Evaluation

The major challenge for a hardware-based evaluation is that the information in Wi-Fi lower-level MAC and PHY layer cannot be collected by the upper application. More than six Wi-Fi card were tested. Unfortunately, all of them adopt a design that low-level MAC is fully processed in the Wi-Fi chip itself to offload the PC's load. The proposed CI estimation cannot be performed in this case because of lack of information. Moreover, as mentioned in the previous section 4.1, the time-slot mechanism is implemented in a reduced version.

In order to perform a hardware-based evaluation, the algorithm is evaluated by configuring LR-WPAN as greedy nodes which send data at the maximum data. Thus, the CI is not calculated by using Algorithm 5.1. According to CI definition in Equation 5.7, the CI should be one because greedy LR-WPAN nodes send data at maximum data rate and the allocated time slot is always saturated. What is more, the CI in Wi-Fi is estimated by observing the data rate of the saturated network and use it as a parameter to estimate CI directly, rather than estimated dynamically. For example, the previous experiment reveals the saturated Wi-Fi network is about 20Mbps when both Wi-Fi and LR-WPAN have a time slot of 32ms. If the Wi-Fi network drops to 10Mpbs, the CI should be about 0.5 according to Equation 5.7.

After the above simplification, the adaptive scheduling algorithm is implemented on hardware, and the result is as shown in Fig. 5.18. The experiment is performed by using a greedy LR-WPAN node that sends unicast packets with 20 bytes MAC payload at maximum speed. Wi-Fi network traffic is sent at different desired speeds. At each desired Wi-Fi speed, three rounds of experiments are conducted, and each round lasts for five minutes. The curve for the adaptive algorithm in the diagram is the averaged value of the three rounds, with the

error bar showing the maximum and minimum value of three rounds. The curves for *No algorithm* and *Static algorithm* are from previous experiment data in Section 4.1.

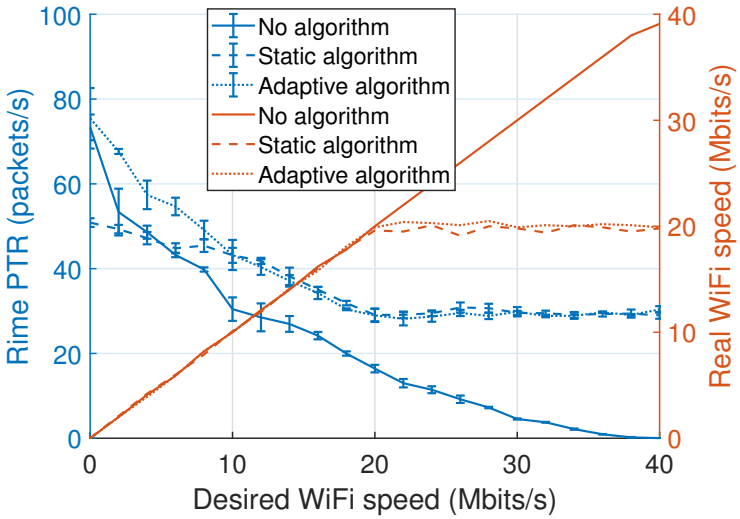

Fig. 5.18 Static vs basic adaptive scheduling

According to the graph, when Desired Wi-Fi speed more than 10 Mbits/s, the adaptive algorithm keeps nearly the same performance with the static algorithm. Nevertheless, the adaptive algorithm covers the shortage of the static algorithm when Wi-Fi traffic less than 10 Mbits/s. The graph shows that the adaptive algorithm even shows higher performance than no algorithm when desired Wi-Fi traffic is zero. This is because zero desired Wi-Fi speed does not mean no Wi-Fi traffic at all; there still may be Wi-Fi management frame, e.g. beacon frames or other nearby unexpected Wi-Fi network interference that cannot be controlled during experiments. The scheduling algorithm guaranteed there is almost no interruption during the time slot of IEEE 802.15.4. That is why the adaptive algorithm performs better than no algorithm even there is zero desired Wi-Fi traffic.

5.4.2 Simulation-based Evaluation

The simulation is achieved on top of proposed HWN layer explained in Section 4.2.1, which provides scheduling interface to upper application and allows upper layer get related

notification of HWN scheduling. It also enables a upper layer to schedule over LR-WPAN and Wi-Fi dynamically. The costants in the algorithm 5.2 are selected as following. The simulation uses EMA coefficient $\alpha = 0.2$ and CI threshold $\beta = 0.6$. The maximum and minimum value for the time slot in Wi-Fi and LR-WPAN is selected as below:

$$T_{z,min} = 6ms \qquad T_{z,max} = 30ms \qquad T_{w,min} = 5ms \qquad T_{w,max} = 250ms$$

Compromised point for LR-WPAN ($T_{z,c}$) and Wi-Fi ($T_{w,c}$) is set to 30ms to ensure the fairness in time domain. In other words, the compromised scheduling anchor vector is:

$$\mathbf{A_c} = \begin{pmatrix} 30ms \\ 30ms \end{pmatrix}$$

In the simulation, the LR-WPAN nodes and Wi-Fi nodes are programmed to send a high amount of data at the given time period. At the beginning 20s, the LR-WPAN and Wi-Fi get enough to form networks, but neither Wi-Fi nor LR-WPAN sends any data. Then, at the 20s, the LR-WPAN nodes start to transmit a high amount of dummy data with a MAC payload of 20 bytes, which simulates a busy LR-WPAN network. Wi-Fi nodes are not programmed to transmit any data until 100s. After 100s, Wi-Fi nodes start transmitting the high amount of UDP data to simulate a busy Wi-Fi network. Such a busy Wi-Fi network may be caused by downloading a big file or buffering a video through Wi-Fi. At this time, both Wi-Fi and LR-WAPN are sending data at high speed. At 160s, LR-WPAN stops sending data and Wi-Fi nodes still trying to sending at high speed until the end of the simulation at 230s. Duration the simulation, Wi-Fi throughput and LR-WPAN PTR is collected every 10s. Fig. 5.19 is acquired by repeating the above process in three cases:

- **No algorithm**: the simulation is conducted by using standard LR-WPAN and Wi-Fi MAC, no proposed algorithm introduced.

- **Static algorithm**: the simulation is conducted by the proposed static time-slot based scheduling algorithm designed in Chapter 4. The time slots for both Wi-Fi and LR-WPAN are set to 30ms.

- **Adaptive algorithm**: the simulation is conducted by using an adaptive time-slot based scheduling algorithm proposed in Section 5.3 and with scheduling constants as described at the beginning of this section.

Fig. 5.19a and Fig. 5.19b show the result of Wi-Fi throughput and LR-WPAN PTR over a period of 230s simulation. Comparing these two diagrams side by side, the Wi-Fi network without the proposed algorithm has the highest throughput. However, as many previous studies stated that heavy Wi-Fi load could block LR-WPAN communication, LR-WPAN cannot even successfully transmit packets after 100s when Wi-Fi starts transmitting at a high data rate. When the static scheduling algorithm applied, LR-WPAN communication is protected to achieve a PTR at about 130 packets/s. Nevertheless, because the static algorithm has a fixed time slot length that is not adaptive to real communication traffic, the LR-WPAN PTR keeps at such value even there is no Wi-Fi traffic. Moreover, the Wi-Fi communicate is significantly suppressed and drops to its half network capacity over the whole simulation period. Therefore, a considerable amount of channel time is wasted. In comparison to the static algorithm, the network performance can be substantially improved by applying the adaptive scheduling algorithm. In the duration of LR-WPAN only communication, the LR-WPAN PTR is about 17% less than that of *No Algorithm*, but it increases about 78% when comparing to the static scheduling algorithm. In addition, the adaptive algorithm nearly double the Wi-Fi throughput in the Wi-Fi only duration after 160s. The simulation shows that the adaptive algorithm cannot achieve a high PTR as *No Algorithm* when there is no Wi-Fi interference. The reason for this is that the adaptive algorithm needs to reserve some channel time for Wi-Fi network. When analysing adaptive algorithm in a combination of these two graphs, a process is summarized as below:

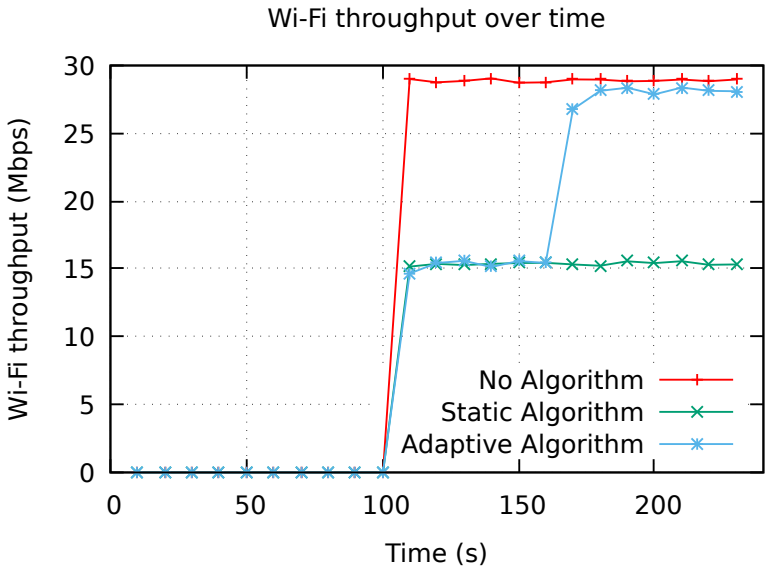

(a) Wi-Fi throughput

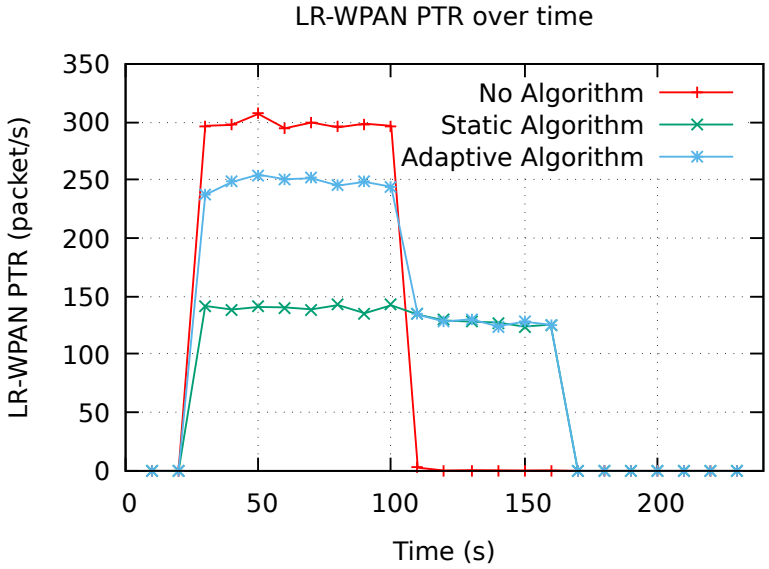

(b) LR-WPAN PTR

Fig. 5.19 Wi-Fi and LR-WPAN adaptive scheduling algorithm

- At the begin of the simulation, there is no Wi-Fi traffic. The adaptive algorithm scheduling at High-LR-WPAN anchor point to achieve a high performance than the static algorithm.

- In the middle of simulation, both networks want more channels time, but channel time is limited. Thus, they need to compromise. The adaptive algorithm keeps the fairness of two networks according to a pre-set compromised point.

- In the last duration, LR-WPAN stops transmitting. The adaptive algorithm detects that LR-WPAN network has a low CI and allocates most of the channel time to Wi-Fi, enabling Wi-Fi to have a high throughput.

Talbe 5.7 summarizes the total amount of data sent over the whole simulation period. In the LR-WPAN network, the highest number of packets is observed by using the adaptive scheduling algorithm. The adaptive algorithm does not achieve the highest Wi-Fi data transmission because it needs to allocate some channel time to LR-WPAN to guarantee the fairness of the network. The tables show that the adaptive algorithm shows a distinct improvement over the static scheduling algorithm.

Table 5.7 Total data transmitted over the simulation period

Algorithm	Wi-Fi (MB)	LR-WPAN (number of packets)
No Algorithm	469.2	23880
Static Algorithm	249.5	11879
Adaptive Algorithm	359.2	27499

5.5 Summary

This chapter defines the time-slot congestion indicator (CI) to indicate the crowdedness level of given slots and designs adaptive time-slot based scheduling algorithm.

One of the crucial challenges for an adaptive time-slot based scheduling algorithm is to tell whether an allocated time slot is adequate for data transmission or not for a specific network. Without an indicator for the network crowdedness in a given slot, the adaptive algorithm cannot tell if a time slot is properly allocated. It is obvious that the number of transmitted packets is not a proper answer, and our simulation result shows that SUR is not a stable indicator to reflect the crowdedness of a network. To the best of our knowledge, there is not such an indicator available for this purpose in a CSMA/CA-based network.

This chapter proposes and defines a slot-based congestion indicator (CI) to assess the network congestion level and crowdedness, enabling a crowdedness-aware adaptive scheduling algorithm. However, it is complicated and impractical to get a precise CI value. Therefore, a CI estimation model is designed to reduce the network statistic requirement and simplify the calculation to give an estimated CI. The CI is evaluated in NS-3 simulator, and the result shows that proposed CI estimation model and algorithm have an error less than 20% for a saturated time slot, regardless of network types, packet sizes, the number of nodes and allocated slot length, which indicates that they are good enough for an adaptive scheduling algorithm.

The adaptive time-slot based scheduling algorithm is designed based on CI. A reduced version of the algorithm is implemented on the hardware-based platform with some special assumptions and limitations. The experiment shows that the adaptive algorithm covers the shortage of the static algorithm when WiFi traffic less than 10 Mbits/s. The full implementation in the NS-3 simulator confirms the algorithm effectiveness that the adaptive algorithm shows a distinct improvement over the static scheduling algorithm. If both networks want more channels time for data transmission, but channel time is limited, the adaptive algorithm makes compromise and guarantees the fairness of two networks according to a pre-set compromised point.

Chapter 6

Conclusion and Future Work

6.1 Conclusion

With the development of IoT, Wi-Fi and LR-WPAN are two types of widely adopted Wireless technologies. They offer different features to meet various requirements for wireless networks. Wi-Fi is a simple and universal way to connect wireless devices that require high throughput, while LR-WPAN is designed for low-power sensors. Thus, it is necessary to have both IEEE 802.15.4 and Wi-Fi available in IoT. Due to they operate in the same ISM frequency band at 2.4Ghz and no coordination mechanism is available to guarantee communications. This unavoidably causes interference among them. Wi-Fi and LR-WPAN both employ CSMA/CA mechanism in their MAC layer. However, the CSMA/CA mechanism is powerless when facing CTI between Wi-Fi and LR-WPAN, because of asymmetric transmission power, incompatible CCA and different timing parameters. Plenty of studies have shown that Wi-Fi always has higher priority to access the wireless medium and even block LR-WPAN transmission in the worst case. Our experiments confirm this point and conclude that Wi-Fi can interrupt LR-WPAN severely even block LR-WPAN traffic, while the interference from LR-WPAN to Wi-Fi is negligible.

Although overlapping channel interference is excessively investigated by a great amount of literature, the non-overlapping channel interference should be taken into consideration as well, especially when Wi-Fi and LR-WPAN nodes are close to each other. Therefore, this thesis conducts hardware-based experiments about the coexistence of Wi-Fi and LR-WPAN. The main difference from others is that the experiment in this thesis is based on a heterogeneous gateway where Wi-Fi and LR-WPAN radio modules are integrated into the small box. In consideration of the small size of the gateway and the fact that LR-WPAN and Wi-Fi antennas are at an extremely short distance, the out-of-band emission can be a considerable factor that contributes to harmful CTI. Besides, the experiments also show some interference phenomenon that is not intuitive. For example, the ZigBee PLR unexpectedly goes up as AP transmission power reduces, indicating that lowering AP power is not good for ZigBee packet transmission. In result, common interference mitigation methods, e.g. LR-WPAN channel switching and AP radio power adjusting, can not work in such a heterogeneous gateway scenario.

Then, this thesis presents a novel centralized scheduling mechanism in the time domain to harmonize coexistence of Wi-Fi and LR-WPAN. In a Wi-Fi network, there is an RTS/CTS command frame that can be used for scheduling active and blocked periods, but the LR-WPAN network does not provide a proper way for this purpose. Thus, a new command frame, named AN, is introduced into IEEE 802.15.4 MAC. The AN command frame is designed with the consideration of different network features. With the CTS and AN command frames, a time-slot based scheduling mechanism is presented with the features of low scheduling overhead, optimized synchronization of scheduling and low Wi-Fi latency. In order to evaluate the mechanism, this thesis builds a CIM-HetNet system, where the Wi-Fi module and LR-WPAN coordinator module are integrated into one box (CIM-HetNet gateway). The gateway, as the central point of the network, does not only provide data service for LR-WPAN and Wi-Fi but also schedules both network channel time and mitigate harmful CTI.

A static time-slot based scheduling algorithm is designed and evaluated on both real hardware-based system and NS-3 simulator. Because of the limitation of the hardware radio modules, only a reduced version of the scheduling mechanism is implemented. The experiment shows a significant improvement on LR-WPAN PLR and PTR when there is moderate or heavy Wi-Fi interference, which confirms the effectiveness of the time-slot based scheduling mechanism. Thanks to spectrum-Aware simulation, an HWN module for NS-3 is designed. It implements a full version of time-slot scheduling mechanism and the algorithm performance is evaluated in more aspects, in terms of PLR, PTR, packet delay and scheduling overhead. Specifically, the proposed static scheduling algorithm reduces LR-WPAN PLR to less than 15% when there is heavy Wi-Fi traffic, while this value is 100% without scheduling algorithm. If Wi-Fi traffic is light, the algorithm reduces LR-WPAN PLR to almost zero. In all the six simulation configuration, the scheduling overhead is small with a range from 0.5% to 2.8%. Nevertheless, the static scheduling algorithm reduces maximum Wi-Fi throughput by about 50% in our simulation, because the principle behind the time-slot mechanism is to design TDMA layer on top of CSMA layer, which allocates channel time to a network periodically and enables CTI free channel access. Allocating more channel time to one network unavoidably decrease the performance of the other.

The static scheduling algorithm is further optimized by scheduling the time slot length adaptively. One of the challenges for an adaptive time-slot based scheduling algorithm is to tell whether an allocated time slot is adequate for data transmission or not for a specific network. A slot-based congestion indicator (CI) is proposed and defined for this purpose. More importantly, CI estimation models are proposed to reduce the network statistic requirement and simplify the calculation complexity of getting an estimated CI. The simulation shows that the model has an error less than 20% for a saturated time slot, regardless of network types, packet sizes, the number of nodes and allocated slot length, which suggests that they are good enough for an adaptive scheduling algorithm. Based

on CI, an adaptive time-slot based scheduling algorithm is designed. The hardware-based evaluation shows that the adaptive algorithm covers the shortage of the static algorithm when Wi-Fi traffic less than 10 Mbits/s. Further evaluation in the NS-3 simulator confirms the algorithm effectiveness by observing a distinct improvement in comparison with static scheduling algorithm. Moreover, if both LR-WPAN and Wi-Fi want more channels time for data transmission than a channel can provide, the adaptive algorithm makes compromise and guarantees the fairness of two networks according to a pre-set compromised point.

6.2 Future Work

Time-slot based scheduling mechanism proposed in the thesis offers a new approach to address the wireless coexistence problem. We did many fundamental works, such as proposing a scheduling mechanism and refining the concept of the time-slot congestion indicator. The research in this thesis involves one gateway with one-hop networks only. In the future, the research can be developed in following directions.

The research can be extended by increasing the number of gateways and LR-WPAN coordinators in an area. Multiple heterogeneous gateways and sensor networks may coexist at a location. In order to manage multiple gateways, a centralized controller may be required. The controller can be a powerful PC that connects to each gateway by a dedicated network. Nevertheless, the synchronization of these gateways can difficult. We may design an algorithm on the controller to manage and allocate time slots for a group of networks. What is more, because the Wi-Fi channel is four times wider than an LR-WPAN channel, It can be meaningful to study on scheduling multiple LR-WPAN channels against one Wi-Fi channel. The multiple LR-WPAN nodes with different channels may access medium concurrently.

The future work will introduce some sleeping LR-WPAN nodes. The sleep nodes cannot keep the radio on all the time. In some extreme case, the radio for a sleeping node only turns on when they have data to send. In most time, the radio is off. For this reason, the AN

command frame is not likely to be received by sleeping nodes. Therefore, sleeping nodes may not always be aware of the scheduled time slot. However, these nodes can still benefit from the time-slot based scheduling mechanism by changing the CSMA/CA algorithm of this node. A potential approach is that a sleeping node can use standard CSMA/CA to listen to channel status as the first step to transmit a packet. If the channel is not busy, the node can send the packet according to the standard CSMA/CA procedure. Otherwise, it may listen to the channel for a short period to receive an AN frame that includes time slot information, and then data can be sent in allocated WI-Fi interference-free time slot.

Another direction is to consider a multi-hop LR-WPAN, where LR-WPAN can cover a much larger area than Wi-Fi network. In this case, some nodes are out of the maximum range that the CIM-HetNet gateway can manage directly. In this case, we may design a network mediator that is similar to CIM-HetNet gateway but does not provide data service. The algorithm in the mediator can be specially designed to extend the management range of a CIM-HetNet gateway.

Artificial Intelligence (AI) is increasingly popular and powerful. The key step in the scheduling algorithm is to decide the length the time slot to allocate. By introducing AI, the time-slot length can be decided in a smarter way. For example, neural network in AI can make complicated decision by learning habits of the user. Moreover, a AI-based schduling algorithm can evolve over time with more training.

References

[1] ABIresearch (2012). Total cumulative wi-fi enabled device shipments reached 5 billion in 2012, set to double by 2015. [Accessed: Aug. 20, 2019].

[2] ABIresearch (2019). Wi-fi celebrates 20 years with more than 20 billion anticipated device shipments over the next six years. [Accessed: July. 12, 2020].

[3] Abusubaih, M. (2011). A combined approach for detecting hidden nodes in 802.11 wireless lans. *annals of telecommunications-annales des télécommunications*, 66(11-12):635–642.

[4] Alliance, W. (2016). Wi-fi® device shipments to surpass 15 billion by end of 2016. [Accessed: Mar. 12, 2017].

[5] Alliance, Z. (2019). Zigbee 3.0. [Accessed Jul. 25, 2019].

[6] Angelakis, V., Papadakis, S., Siris, V., and Traganitis, A. (2008). Adjacent channel interference in 802.11 a: Modeling and testbed validation. In *2008 IEEE Radio and Wireless Symposium*, pages 591–594. IEEE.

[7] Angelakis, V., Papadakis, S., Siris, V. A., and Traganitis, A. (2011). Adjacent channel interference in 802.11 a is harmful: Testbed validation of a simple quantification model. *IEEE Communications Magazine*, 49(3):160–166.

[8] Association, I. S. et al. (2012). Part 11: Wireless lan medium access control (mac) and physical layer (phy) specifications. *IEEE Std.*, 802.

[9] Atheros Communications, I. (2010). *AR9331 Highly-Integrated and Cost Effective IEEE 802.11n 1x1 2.4 GHz SoC for AP and Router Platforms*.

[10] Au, E., Cheong, M., Ngo, C., Cordeiro, C., and Zhuang, W. (2014). The future of wi-fi [guest editorial]. *IEEE Communications Magazine*, 52(11):20–21.

[11] Balasubramanian, N., Balasubramanian, A., and Venkataramani, A. (2009). Energy consumption in mobile phones: a measurement study and implications for network applications. In *Proceedings of the 9th ACM SIGCOMM Conference on Internet Measurement*, pages 280–293.

[12] Baldo, N. and Miozzo, M. (2009). Spectrum-aware channel and phy layer modeling for ns3. In *Proceedings of the Fourth International ICST Conference on Performance Evaluation Methodologies and Tools*, pages 1–8.

[13] Bertocco, M., Gamba, G., and Sona, A. (2007). Experimental optimization of cca thresholds in wireless sensor networks in the presence of interference. In *Proc. of IEEE EMC Europe 2007 Workshop on Electromagnetic Compatibility (June 2007)*.

[14] Bertocco, M., Gamba, G., and Sona, A. (2008). Is csma/ca really efficient against interference in a wireless control system? an experimental answer. In *2008 IEEE International Conference on Emerging Technologies and Factory Automation*, pages 885–892. IEEE.

[15] Boroumand, L., Khokhar, R. H., Bakhtiar, L. A., and Pourvahab, M. (2012). A review of techniques to resolve the hidden node problem in wireless networks. *SmartCR*, 2(2):95–110.

[16] Bosch, P., De Schepper, T., Zeljković, E., Famaey, J., and Latré, S. (2020). Orchestration of heterogeneous wireless networks: State of the art and remaining challenges. *Computer Communications*, 149:62–77.

[17] Bulhões, R. P., Passos, D., and Albuquerque, C. V. (2016). Collision probability estimation in wireless networks. In *2016 8th IEEE Latin-American Conference on Communications (LATINCOM)*, pages 1–6. IEEE.

[18] Chen, Q., Yu, G., Shan, H., Maaref, A., Li, G. Y., and Huang, A. (2016). Cellular meets wifi: Traffic offloading or resource sharing? *IEEE Transactions on Wireless Communications*, 15(5):3354–3367.

[19] Chen, X., Han, P., He, Q.-S., Tu, S.-l., and Chen, Z.-L. (2006). A multi-channel mac protocol for wireless sensor networks. In *The Sixth IEEE International Conference on Computer and Information Technology (CIT'06)*, pages 224–224. IEEE.

[20] Cheng, C.-H. and Ho, C.-C. (2016). Implementation of multi-channel technology in zigbee wireless sensor networks. *Computers & Electrical Engineering*, 56:498–508.

[21] Cheng, C.-M., Hsiao, P.-H., Kung, H., and Vlah, D. (2006). Wsn07-1: Adjacent channel interference in dual-radio 802.11 a nodes and its impact on multi-hop networking. In *IEEE Globecom 2006*, pages 1–6. IEEE.

[22] De Nardis, L. and Di Benedetto, M.-G. (2007). Overview of the ieee 802.15. 4/4a standards for low data rate wireless personal data networks. In *Positioning, Navigation and Communication, 2007. WPNC'07. 4th Workshop on*, pages 285–289. IEEE.

[23] Deylami, M. and Jovanov, E. (2016). A novel method for mitigating the effects of dynamic coexistence on the operation of ieee 802.15. 4-based mobile wsns. *Wireless Communications and Mobile Computing*, 16(3):362–372.

[24] Ding, N., Wagner, D., Chen, X., Pathak, A., Hu, Y. C., and Rice, A. (2013). Characterizing and modeling the impact of wireless signal strength on smartphone battery drain. *ACM SIGMETRICS Performance Evaluation Review*, 41(1):29–40.

[25] Dunkels, A. (2007). Rime-a lightweight layered communication stack for sensor networks. In *Proceedings of the European Conference on Wireless Sensor Networks (EWSN), Poster/Demo session, Delft, The Netherlands*.

[26] Dunkels, A. (2011). The contikimac radio duty cycling protocol. *SICS Report*.

[27] Eady, F. (2010). *Hands-on ZigBee: Implementing 802.15. 4 with microcontrollers*. Newnes.

[28] ElBatt, T. A., Krishnamurthy, S. V., Connors, D., and Dao, S. (2000). Power management for throughput enhancement in wireless ad-hoc networks. In *2000 IEEE International Conference on Communications. ICC 2000. Global Convergence Through Communications. Conference Record*, volume 3, pages 1506–1513. IEEE.

[29] Elias, J., Paris, S., and Krunz, M. (2014). Cross-technology interference mitigation in body area networks: An optimization approach. *IEEE Transactions on Vehicular Technology*, 64(9):4144–4157.

[30] ElSawy, H., Hossain, E., and Camorlinga, S. (2011). A distributed spectrum sharing method for improving coexistence of ieee 802.15. 4 networks. In *2011 IEEE Global Telecommunications Conference-GLOBECOM 2011*, pages 1–5. IEEE.

[31] Gollakota, S., Adib, F., Katabi, D., and Seshan, S. (2011). Clearing the rf smog: making 802.11 n robust to cross-technology interference. In *Proceedings of the ACM SIGCOMM 2011 conference*, pages 170–181.

[32] Golmie, N., Cypher, D., and Rébala, O. (2005). Performance analysis of low rate wireless technologies for medical applications. *Computer Communications*, 28(10):1266–1275.

[33] Gronemeyer, S. and McBride, A. (1976). Msk and offset qpsk modulation. *IEEE Transactions on Communications*, 24(8):809–820.

[34] Group, I. . W. et al. (2003). Stardard for part 15.4: wireless medium access control (mac) and physical layer (phy) specifications for low-rate wireless personal area networks (lr-wpans). *IEEE Std.*, 4.

[35] Group, T. (2019). Waht is thread. [Accessed: Mar. 20, 2019].

[36] Gummadi, R., Wetherall, D., Greenstein, B., and Seshan, S. (2007). Understanding and mitigating the impact of rf interference on 802.11 networks. *ACM SIGCOMM Computer Communication Review*, 37(4):385–396.

[37] Ha, T. T. (2010). *Theory and design of digital communication systems*. Cambridge University Press.

[38] Han, J. S. and Kim, M. J. (2013). Offset quadrature-quadrature phase shift keying with half-sine pulse shaping. In *2013 International Conference on ICT Convergence (ICTC)*, pages 931–935. IEEE.

[39] Haron, M. A., Syed-Yusof, S. K., Fisal, N., Syed-Ariffin, S. H., and Abdallah, A. (2008). Performance study of the coexistence of wireless sensor networks (wsn) and wireless local area networks (wlan). In *2008 Second Asia International Conference on Modelling & Simulation (AMS)*, pages 475–479. IEEE.

[40] Hauer, J.-H., Handziski, V., and Wolisz, A. (2009). Experimental study of the impact of wlan interference on ieee 802.15. 4 body area networks. In *European Conference on Wireless Sensor Networks*, pages 17–32. Springer.

[41] Henderson, T. R., Lacage, M., Riley, G. F., Dowell, C., and Kopena, J. (2008). Network simulations with the ns-3 simulator. *SIGCOMM demonstration*, 14(14):527.

[42] Hou, J., Chang, B., Cho, D.-K., and Gerla, M. (2009). Minimizing 802.11 interference on zigbee medical sensors. In *Proceedings of the Fourth International Conference on Body Area Networks*, page 5. ICST (Institute for Computer Sciences, Social-Informatics and Telecommunications Engineering).

[43] Howitt, I. and Gutierrez, J. A. (2003). Ieee 802.15. 4 low rate-wireless personal area network coexistence issues. In *Wireless Communications and Networking, 2003. WCNC 2003. 2003 IEEE*, volume 3, pages 1481–1486. IEEE.

[44] Hu, J., Qin, Z., Sun, Y., Shu, L., Lu, B., and Wang, L. (2016). Cii: A light-weight mechanism for zigbee performance assurance under wifi interference. In *Computer Communication and Networks (ICCCN), 2016 25th International Conference on*, pages 1–9. IEEE.

[45] Huang, J., Xing, G., Zhou, G., and Zhou, R. (2010). Beyond co-existence: Exploiting wifi white space for zigbee performance assurance. In *Network Protocols (ICNP), 2010 18th IEEE International Conference on*, pages 305–314. IEEE.

[46] Huang, X., Zhang, J. A., and Guo, Y. J. (2015). Out-of-band emission reduction and a unified framework for precoded ofdm. *IEEE Communications Magazine*, 53(6):151–159.

[47] Hung, F.-Y. and Marsic, I. (2010). Performance analysis of the ieee 802.11 dcf in the presence of the hidden stations. *Computer Networks*, 54(15):2674–2687.

[48] Hwang, L.-J., Sheu, S.-T., Shih, Y.-Y., and Cheng, Y.-C. (2005). Grouping strategy for solving hidden node problem in ieee 802.15. 4 lr-wpan. In *First International Conference on Wireless Internet (WICON'05)*, pages 26–32. IEEE.

[49] Inc., T. I. (2009). *A True System-on-Chip Solution for 2.4-GHz IEEE 802.15.4 and ZigBee Applications*.

[50] Inc., T. I. (2015). *CC2538 Powerful Wireless Microcontroller System-On-Chip for 2.4-GHz IEEE 802.15.4, 6LoWPAN and ZigBee Application*. Texas Instruments Inc.

[51] Ishida, S., Tagashira, S., and Fukuda, A. (2015). Ap-assisted cts-blocking for wifi-zigbee coexistence. In *Computing and Networking (CANDAR), 2015 Third International Symposium on*, pages 110–114. IEEE.

[52] Ismail, D., Rahman, M., and Saifullah, A. (2018). Low-power wide-area networks: opportunities, challenges, and directions. In *Proceedings of the Workshop Program of the 19th International Conference on Distributed Computing and Networking*, pages 1–6.

[53] Jamal, A., Tham, C.-K., and Wong, W.-C. (2015). Dynamic packet size optimization and channel selection for cognitive radio sensor networks. *IEEE Transactions on Cognitive Communications and Networking*, 1(4):394–405.

[54] Jiang, H., Liu, B., and Chen, C. W. (2017). Performance analysis for zigbee under wifi interference in smart home. In *2017 IEEE International Conference on Communications (ICC)*, pages 1–6. IEEE.

[55] Jung, B. H., Chong, J. W., Jeong, S. H., Hwang, H. Y., Kim, S. M., Kang, M. S., and Sung, D. K. (2007). Ubiquitous wearable computer (uwc)-aided coexistence algorithm in an overlaid network environment of wlan and zigbee networks. In *2007 2nd International Symposium on Wireless Pervasive Computing*. IEEE.

[56] Jung, B. H., Chong, J. W., Jung, C. Y., Kim, S. M., and Sung, D. K. (2008). Interference mediation for coexistence of wlan and zigbee networks. In *2008 IEEE 19th International Symposium on Personal, Indoor and Mobile Radio Communications*, pages 1–5. IEEE.

[57] Kapadia, V. V., Patel, S. N., and Jhaveri, R. H. (2010). Comparative study of hidden node problem and solution using different techniques and protocols. *arXiv preprint arXiv:1003.4070*.

[58] Kim, J.-W., Kim, J., and Eom, D.-S. (2008). Multi-dimensional channel management scheme to avoid beacon collision in lr-wpan. *IEEE Transactions on Consumer Electronics*, 54(2):396–404.

[59] Kim, S. M. and He, T. (2015). Freebee: Cross-technology communication via free side-channel. In *Proceedings of the 21st Annual International Conference on Mobile Computing and Networking*, pages 317–330.

[60] Koubâa, A., Severino, R., Alves, M., and Tovar, E. (2009). Improving quality-of-service in wireless sensor networks by mitigating "hidden-node collisions". *IEEE Transactions on Industrial Informatics*, 5(3):299–313.

[61] Krishnan, M. N., Haghani, E., and Zakhor, A. (2011). Packet length adaptation in wlans with hidden nodes and time-varying channels. In *2011 IEEE Global Telecommunications Conference-GLOBECOM 2011*, pages 1–6. IEEE.

[62] Lan, Y.-Y., Lai, I.-W., Lee, C.-H., and Chiueh, T.-D. (2015). Efficient active precoder identification for receivers with inter-cell interference in heterogeneous networks. *IEEE Transactions on Wireless Communications*, 14(9):5009–5021.

[63] LaSorte, N. J., Rajab, S. A., and Refai, H. H. (2012). Experimental assessment of wireless coexistence for 802.15. 4 in the presence of 802.11 g/n. In *2012 IEEE International Symposium on Electromagnetic Compatibility*, pages 473–479. IEEE.

[64] Leão, E., Montez, C., Moraes, R., Portugal, P., and Vasques, F. (2017). Superframe duration allocation schemes to improve the throughput of cluster-tree wireless sensor networks. *Sensors*, 17(2):249.

[65] Lee, Y., Kim, K., and Choi, Y. (2002). Optimization of ap placement and channel assignment in wireless lans. In *27th Annual IEEE Conference on Local Computer Networks, 2002. Proceedings. LCN 2002.*, pages 831–836. IEEE.

[66] Liang, C.-J. M., Priyantha, N. B., Liu, J., and Terzis, A. (2010). Surviving wi-fi interference in low power zigbee networks. In *Proceedings of the 8th ACM Conference on Embedded Networked Sensor Systems*, pages 309–322. ACM.

[67] Lim, A. O. and Kado, Y. (2011). Deployment and experimental verification for data communication in heterogeneous wireless networks. In *2011 7th International Conference on Information Technology in Asia*, pages 1–7. IEEE.

[68] Lin, S., Miao, F., Zhang, J., Zhou, G., Gu, L., He, T., Stankovic, J. A., Son, S., and Pappas, G. J. (2016). Atpc: adaptive transmission power control for wireless sensor networks. *ACM Transactions on Sensor Networks (TOSN)*, 12(1):1–31.

[69] Liu, Q., Li, X., Xu, W., and Zhang, D. (2014). Empirical analysis of zigbee and wifi coexistence. In *Proceedings of the 2014 International Conference on Innovative Design and Manufacturing (ICIDM)*, pages 117–122. IEEE.

[70] Masud, M., Latif, S., and Alam, F. A. M. (2014). A scheduling algorithm for bandwidth aggregation in heterogeneous wireless network. In *2014 International Conference on Informatics, Electronics & Vision (ICIEV)*, pages 1–4. IEEE.

[71] Miao, J., Hu, Z., Yang, K., Wang, C., and Tian, H. (2012). Joint power and bandwidth allocation algorithm with qos support in heterogeneous wireless networks. *IEEE Communications Letters*, 16(4):479–481.

[72] Mishra, A., Banerjee, S., and Arbaugh, W. (2005a). Weighted coloring based channel assignment for wlans. *ACM SIGMOBILE Mobile Computing and Communications Review*, 9(3):19–31.

[73] Mishra, A., Rozner, E., Banerjee, S., and Arbaugh, W. (2005b). Using partially overlapped channels in wireless meshes. *Wimesh, Santa Clara*, 26.

[74] Mohammad, M., Guo, X., and Chan, M. C. (2016). Oppcast: Exploiting spatial and channel diversity for robust data collection in urban environments. In *2016 15th ACM/IEEE International Conference on Information Processing in Sensor Networks (IPSN)*, pages 1–12. IEEE.

[75] Musaloiu-E, R. and Terzis, A. (2008). Minimising the effect of wifi interference in 802.15. 4 wireless sensor networks. *International Journal of Sensor Networks*, 3(1):43–54.

[76] Mvulla, J., Kim, Y., and Park, E.-C. (2018). Probe/preack: A joint solution for mitigating hidden and exposed node problems and enhancing spatial reuse in dense wlans. *IEEE Access*, 6:55171–55185.

[77] Myers, S., Megerian, S., Banerjee, S., and Potkonjak, M. (2007). Experimental investigation of ieee 802.15. 4 transmission power control and interference minimization. In *2007 4th Annual IEEE Communications Society Conference on Sensor, Mesh and Ad Hoc Communications and Networks*, pages 294–303. IEEE.

[78] Myoung, K.-J., Soo-Young, S., Hong-Seong, P., and Wook-Hyun, K. (2007). Ieee 802.11 b performance analysis in the presence of ieee 802.15. 4 interference. *IEICE Transactions on Communications*, 90(1):176–179.

[79] Nachtigall, J., Zubow, A., and Redlich, J.-P. (2008). The impact of adjacent channel interference in multi-radio systems using ieee 802.11. In *2008 International Wireless Communications and Mobile Computing Conference*, pages 874–881. IEEE.

[80] Nguyen, A.-H., Tanigawa, Y., and Tode, H. (2019). Adaptive channel access control solving compound problem of hidden nodes and continuous collisions among periodic data flows. *IEICE Transactions on Communications*, page 2018EBP3329.

[81] Nishikori, S., Kinoshita, K., Tanigawa, Y., Tode, H., and Watanabe, T. (2017). A cooperative channel control method of zigbee and wifi for iot services. In *2017 14th IEEE Annual Consumer Communications & Networking Conference (CCNC)*, pages 1–6. IEEE.

[82] NS-3 (unknown). 3gpp http applications — model library of ns-3. https://www.nsnam.org/docs/models/html/applications.html. (Accessed on 30/05/2020).

[83] NXP (2013). *Co-existence of IEEE 802.15.4 at 2.4 GHz Application Note*.

[84] NXP (2014). *Calculating 802.15.4 Data Rates*.

[85] Ock, J., Choi, Y.-J., and Bahk, S. (2014). Performance analysis of periodic busy tones protecting a zigbee network from wi-fi interruption. In *2014 IEEE 79th Vehicular Technology Conference (VTC Spring)*, pages 1–5. IEEE.

[86] open zb (2017). Opensource tool set for ieee 802.15.4 and zigbee. [Accessed: Aug. 20, 2017].

[87] OS, C. (2018). Contiki: The open source os for the internet of things. [Accessed: Mar. 20, 2018].

[88] Pasupathy, S. (1979). Minimum shift keying: A spectrally efficient modulation. *IEEE Communications Magazine*, 17(4):14–22.

[89] Peng, X., Guo, D., Song, M., and Song, J. (2008). On the study of resource scheduling in next generation heterogeneous wireless networks. In *2008 World Automation Congress*, pages 1–5. IEEE.

[90] Petrova, M. and Gutierrez, J. (2006). Ieee 802.15. 4 low rate-wireless personal area network coexistence issues. *Proc. IEEE WCNC'06*.

[91] Petrova, M., Wu, L., Mahonen, P., and Riihijarvi, J. (2007). Interference measurements on performance degradation between colocated ieee 802.11 g/n and ieee 802.15. 4 networks. In *Sixth International Conference on Networking (ICN'07)*, pages 93–93. IEEE.

[92] Phunchongharn, P., Hossain, E., and Camorlinga, S. (2011). Electromagnetic interference-aware transmission scheduling and power control for dynamic wireless access in hospital environments. *IEEE transactions on information technology in biomedicine*, 15(6):890–899.

[93] Piamrat, K., Ksentini, A., Bonnin, J.-M., and Viho, C. (2011). Radio resource management in emerging heterogeneous wireless networks. *Computer Communications*, 34(9):1066–1076.

[94] Pollin, S., Ergen, M., Timmers, M., Dejonghe, A., Van der Perre, L., Catthoor, F., Moerman, I., and Bahai, A. (2006). Distributed cognitive coexistence of 802.15. 4 with 802.11. In *2006 1st International Conference on Cognitive Radio Oriented Wireless Networks and Communications*, pages 1–5. IEEE.

[95] Pollin, S., Tan, I., Hodge, B., Chun, C., and Bahai, A. (2008). Harmful coexistence between 802.15. 4 and 802.11: A measurement-based study. In *2008 3rd International Conference on Cognitive Radio Oriented Wireless Networks and Communications (CrownCom 2008)*, pages 1–6. IEEE.

[96] Qashi, R., Bogdan, M., and Hänssgen, K. (2011). Evaluating the qos of wlans for the ieee 802.11 edcf in real-time applications. In *2011 International Conference on Communications and Information Technology (ICCIT)*, pages 32–35. IEEE.

[97] Radunović, B., Chandra, R., and Gunawardena, D. (2012). Weeble: Enabling low-power nodes to coexist with high-power nodes in white space networks. In *Proceedings of the 8th international conference on Emerging networking experiments and technologies*, pages 205–216.

[98] Rahman, A. and Gburzynski, P. (2006). Hidden problems with the hidden node problem. In *23rd Biennial Symposium on Communications, 2006*, pages 270–273. IEEE.

[99] Saeed, K., Khalil, W., Ahmed, S., Abbas, A. W., and Khattak, M. N. K. (2019). Analysis of different packet size optimization techniques for twsns. In *2019 2nd International Conference on Computing, Mathematics and Engineering Technologies (iCoMET)*, pages 1–6. IEEE.

[100] Saha, D. and Birdsall, T. G. (1989). Quadrature-quadrature phase-shift keying. *IEEE Transactions on Communications*, 37(5):437–448.

[101] Sahoo, S. K. et al. (2017). Load aware channel estimation and channel scheduling for 2.4 ghz frequency band based wireless networks for smart grid applications. *International Journal on Smart Sensing & Intelligent Systems*, 10(4).

[102] Sankarasubramaniam, Y., Akyildiz, I. F., and McLaughlin, S. (2003). Energy efficiency based packet size optimization in wireless sensor networks. In *Proceedings of the First IEEE International Workshop on Sensor Network Protocols and Applications, 2003.*, pages 1–8. IEEE.

[103] Sha, M., Hackmann, G., and Lu, C. (2013). Energy-efficient low power listening for wireless sensor networks in noisy environments. In *Proceedings of the 12th international conference on Information processing in sensor networks*, pages 277–288.

[104] Shin, S. Y., Choi, S., Park, H. S., and Kwon, W. H. (2005). Lecture notes in computer science: packet error rate analysis of ieee 802.15. 4 under ieee 802.11 b interference. In *International Conference on Wired/Wireless Internet Communications*, pages 279–288. Springer.

[105] Shin, S. Y., Park, H. S., and Kwon, W. H. (2007). Packet error rate analysis of ieee 802.15. 4 under saturated ieee 802.11 b network interference. *IEICE transactions on communications*, 90(10):2961–2963.

[106] Shuaib, K., Boulmalf, M., Sallabi, F., and Lakas, A. (2006). Co-existence of zigbee and wlan-a performance study. In *2006 IFIP International Conference on Wireless and Optical Communications Networks*, pages 5–pp. IEEE.

[107] Sikora, A. and Groza, V. F. (2005). Coexistence of ieee802. 15.4 with other systems in the 2.4 ghz-ism-band. In *Instrumentation and Measurement Technology Conference, 2005. IMTC 2005. Proceedings of the IEEE*, volume 3, pages 1786–1791. IEEE.

[108] SiliconLabs (2020). *AN709: Adjacent Channel Rejection Measurements for 802.15.4 Radios*.

[109] Sisinni, E., Saifullah, A., Han, S., Jennehag, U., and Gidlund, M. (2018). Industrial internet of things: Challenges, opportunities, and directions. *IEEE Transactions on Industrial Informatics*, 14(11):4724–4734.

[110] Sparber, T., Boano, C. A., Kanhere, S. S., and Römer, K. (2017). Mitigating radio interference in large iot networks through dynamic cca adjustment. *Open Journal of Internet Of Things (OJIOT)*, 3(1):103–113.

[111] Specification, Z. (2006). Zigbee alliance. *ZigBee Document 053474r06, Version*, 1.

[112] Srinivasan, K., Dutta, P., Tavakoli, A., and Levis, P. (2010). An empirical study of low-power wireless. *ACM Transactions on Sensor Networks (TOSN)*, 6(2):1–49.

[113] Std, I. (2006). Part 15.4: Wireless medium access control (mac) and physical layer (phy) specifications for low-rate wireless personal area networks (wpans). *IEEE Std. 802.15.4TM -2006*.

[114] Suarez, P., Renmarker, C.-G., Dunkels, A., and Voigt, T. (2008). Increasing zigbee network lifetime with x-mac. In *Proceedings of the workshop on Real-world wireless sensor networks*, pages 26–30. ACM.

[115] Sui, K., Zhao, Y., Pei, D., and Zimu, L. (2015). How bad are the rogues' impact on enterprise 802.11 network performance? In *2015 IEEE Conference on Computer Communications (INFOCOM)*, pages 361–369. IEEE.

[116] Tao, Y., Li, X.-Y., and Bo, C. (2013). Performance of coexisted wifi and zigbee networks. In *2013 IEEE 33rd International Conference on Distributed Computing Systems Workshops*, pages 315–320. IEEE.

[117] Thonet, G., Allard-Jacquin, P., and Colle, P. (2008). Zigbee-wifi coexistence. *Schneider Electric White Paper and Test Report*, 1:1–38.

[118] Tseng, Y.-C., Ni, S.-Y., and Shih, E.-Y. (2003). Adaptive approaches to relieving broadcast storms in a wireless multihop mobile ad hoc network. *IEEE transactions on computers*, 52(5):545–557.

[119] Tytgat, L., Yaron, O., Pollin, S., Moerman, I., and Demeester, P. (2012). Avoiding collisions between ieee 802.11 and ieee 802.15. 4 through coexistence aware clear channel assessment. *EURASIP Journal on Wireless Communications and Networking*, 2012(1):137.

[120] Vikram, K. and Narayana, K. V. L. (2016). Cross-layer multi channel mac protocol for wireless sensor networks in 2.4-ghz ism band. In *2016 International Conference on Computing, Analytics and Security Trends (CAST)*, pages 312–317. IEEE.

[121] Vikram, K. and Sahoo, S. K. (2017). Interference aware adaptive transmission power control algorithm for zigbee wireless networks. In *International Conference on Next Generation Computing Technologies*, pages 56–69. Springer.

[122] Vu, H. L. and Sakurai, T. (2006). Collision probability in saturated ieee 802.11 networks. In *Australian Telecommunication Networks and Applications Conference, Australia*.

[123] Wang, X. and Yang, K. (2017). A real-life experimental investigation of cross interference between wifi and zigbee in indoor environment. In *Internet of Things (iThings) and IEEE Green Computing and Communications (GreenCom) and IEEE Cyber, Physical and Social Computing (CPSCom) and IEEE Smart Data (SmartData), 2017 IEEE International Conference on*, pages 598–603. IEEE.

[124] Wikipedia (2020a). Carrier-sense multiple access with collision avoidance. [Accessed: Jul. 12, 2020].

[125] Wikipedia (2020b). Carrier-sense multiple access with collision detection. [Accessed: Jul. 12, 2020].

[126] Wikipedia (2020c). Frequency-division multiple access. [Accessed: Jul. 12, 2020].

[127] Wikipedia (2020d). Time-division multiple access. [Accessed: Jul. 12, 2020].

[128] Wu, K., Tan, H., Liu, Y., Zhang, J., Zhang, Q., and Ni, L. M. (2011). Side channel: Bits over interference. *IEEE Transactions on Mobile Computing*, 11(8):1317–1330.

[129] Xia, D., Hart, J., and Fu, Q. (2012). On the performance of rate control algorithm minstrel. In *2012 IEEE 23rd International Symposium on Personal, Indoor and Mobile Radio Communications-(PIMRC)*, pages 406–412. IEEE.

[130] Xia, D., Hart, J., and Fu, Q. (2013). Evaluation of the minstrel rate adaptation algorithm in ieee 802.11 g wlans. In *2013 IEEE International Conference on Communications (ICC)*, pages 2223–2228. IEEE.

[131] Xie, R., Yu, F. R., Ji, H., and Li, Y. (2012). Energy-efficient resource allocation for heterogeneous cognitive radio networks with femtocells. *IEEE Transactions on Wireless Communications*, 11(11):3910–3920.

[132] Xu, J., Wu, S., Xu, L., Zhang, N., and Zhang, Q. (2017). Green-oriented user-satisfaction aware wifi offloading in hetnets. *IET Communications*, 12(5):501–508.

[133] Xu, R., Shi, G., Luo, J., Zhao, Z., and Shu, Y. (2011). Muzi: Multi-channel zigbee networks for avoiding wifi interference. In *2011 International Conference on Internet of Things and 4th International Conference on Cyber, Physical and Social Computing*, pages 323–329. IEEE.

[134] Xu, W., Ma, K., Trappe, W., and Zhang, Y. (2006). Jamming sensor networks: attack and defense strategies. *IEEE network*, 20(3):41–47.

[135] Yang, D., Xu, Y., and Gidlund, M. (2010). Coexistence of ieee802. 15.4 based networks: A survey. In *IECON 2010-36th Annual Conference on IEEE Industrial Electronics Society*, pages 2107–2113. IEEE.

[136] Yang, D., Xu, Y., and Gidlund, M. (2011). Wireless coexistence between ieee 802.11- and ieee 802.15. 4-based networks: A survey. *International Journal of Distributed Sensor Networks*, 7(1):912152.

[137] Yoon, D. G., Shin, S. Y., Kwon, W. H., and Park, H. S. (2006). Packet error rate analysis of ieee 802.11 b under ieee 802.15. 4 interference. In *Vehicular Technology Conference, 2006. VTC 2006-Spring. IEEE 63rd*, volume 3, pages 1186–1190. IEEE.

[138] Yuan, W., Linnartz, J.-P. M., and Niemegeers, I. G. (2010). Adaptive cca for ieee 802.15. 4 wireless sensor networks to mitigate interference. In *2010 IEEE Wireless Communication and Networking Conference*, pages 1–5. IEEE.

[139] Yuan, W., Wang, X., and Linnartz, J.-P. M. (2007). A coexistence model of ieee 802.15. 4 and ieee 802.11 b/g. In *2007 14th IEEE Symposium on Communications and Vehicular Technology in the Benelux*, pages 1–5. IEEE.

[140] Yun, J., Lee, B., Li, J., and Han, K. (2008). A channel switching scheme for avoiding interference of between ieee 802.15. 4 and other networks. In *2008 International Multi-symposiums on Computer and Computational Sciences*, pages 136–139. IEEE.

[141] ZBOSS (2019). Zigbee® open source stack: overview. [Accessed: Aug. 28, 2019].

[142] Zhang, D., Liu, Q., Chen, L., and Xu, W. (2017). Survey on coexistence of heterogeneous wireless networks in 2.4 ghz and tv white spaces. *International Journal of Distributed Sensor Networks*, 13(4):1550147717703966.

[143] Zhang, J., Qu, S., and Zhang, H. (2016). Regularized interference alignment for heterogeneous networks. In *2016 8th IEEE international conference on communication software and networks (ICCSN)*, pages 201–205. IEEE.

[144] Zhang, S. and Yoo, S.-J. (2012). Hidden node collision recovery protocol for low rate wireless personal area networks. *Wireless Communications and Mobile Computing*, 12(15):1351–1362.

[145] Zhang, X. and Shin, K. G. (2011a). A case for the coexistence of heterogeneous wireless networks. In *Proceedings of the 3rd ACM workshop on Wireless of the students, by the students, for the students*, pages 1–4.

[146] Zhang, X. and Shin, K. G. (2011b). Enabling coexistence of heterogeneous wireless systems: Case for zigbee and wifi. In *Proceedings of the Twelfth ACM International Symposium on Mobile Ad Hoc Networking and Computing*, page 6. ACM.

[147] Zhang, X. and Shin, K. G. (2012). Cooperative carrier signaling: Harmonizing coexisting wpan and wlan devices. *IEEE/ACM Transactions On Networking*, 21(2):426–439.

[148] Zhao, Z., Wu, X., Zhang, X., Zhao, J., and Li, X.-Y. (2014). Zigbee vs wifi: Understanding issues and measuring performances of their coexistence. In *2014 IEEE 33rd International Performance Computing and Communications Conference (IPCCC)*, pages 1–8. IEEE.

[149] Zhen, B., Li, H.-B., Hara, S., and Kohno, R. (2007). Clear channel assessment in integrated medical environments. *EURASIP Journal on Wireless Communications and Networking*, 2008(1):821756.

[150] Zhou, G., Lu, L., Krishnamurthy, S., Keally, M., and Ren, Z. (2009). Sas: Self-adaptive spectrum management for wireless sensor networks. In *2009 Proceedings of 18th International Conference on Computer Communications and Networks*, pages 1–6. IEEE.

[151] Zhou, G., Stankovic, J. A., and Son, S. H. (2006). Crowded spectrum in wireless sensor networks. *IEEE EmNets*, 6.